

AMERICAN UNIVERSITY OF BEIRUT

HIC-5 DEREGLATION IN LAMIN A/C AND EMERIN –
ASSOCIATED MYOPATHIES

by
RANIM HOUSSAM DAW

A thesis
submitted in partial fulfillment of the requirements
for the degree of Master of Science
to the Department of Biology
of the Faculty of Arts and Sciences
at the American University of Beirut

Beirut, Lebanon
February, 2017

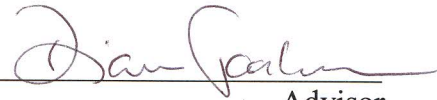
AMERICAN UNIVERSITY OF BEIRUT

HIC-5 DEREGLATION IN LAMIN A/C AND EMERIN –
ASSOCIATED MYOPATHIES

by
RANIM HOUSSAM DAW

Approved by:

Dr. Diana Jaalouk, Assistant Professor
Biology



Advisor

Dr. Georges Nemer, Professor
Biochemistry & Molecular Genetics



Member of Committee

Dr. Noël Ghanem, Assistant Professor
Biology



Member of Committee

Date of thesis defense: February 1, 2017

AMERICAN UNIVERSITY OF BEIRUT

THESIS, DISSERTATION, PROJECT RELEASE FORM

Student Name: Daw _____ Ranim _____ Houssam _____
Last First Middle

Master's Thesis Master's Project Doctoral Dissertation

I authorize the American University of Beirut to: (a) reproduce hard or electronic copies of my thesis, dissertation, or project; (b) include such copies in the archives and digital repositories of the University; and (c) make freely available such copies to third parties for research or educational purposes.

I authorize the American University of Beirut, to: (a) reproduce hard or electronic copies of it; (b) include such copies in the archives and digital repositories of the University; and (c) make freely available such copies to third parties for research or educational purposes after :
One ---- year from the date of submission of my thesis, dissertation, or project.
Two ---- years from the date of submission of my thesis, dissertation, or project.
Three years from the date of submission of my thesis, dissertation, or project.

Signature

Date

This form is signed when submitting the thesis, dissertation, or project to the University Libraries

ACKNOWLEDGMENTS

I would like to express my deepest gratitude to my advisor Dr. Diana Jaalouk, who continually and influentially conveyed a spirit of exploration in regard to research, and an enthusiasm in regard to teaching. Without her guidance, tireless help, useful comments, and engagement in this master's thesis, this dissertation would not have been possible.

I would also like to thank my committee members, Dr. George Nemer and Dr. Noel Ghanem who have willingly shared their valuable time during my thesis journey, and for their supportive comments and advice during my comprehensive exam that helped move my project towards further progress.

In addition, I would like to thank my lab members Sara Assi, Dima Diab-Harakeh, and Hind Zahr for training me on all the required lab skills. I also thank them and Elvira Dibo for making the time spent in the lab enjoyable and for showing much love, support, guidance, and patience throughout this journey. They were my family on AUB's campus.

Finally, I would like to thank my beloved father, mother, siblings, aunt, and Rafik, my partner in every step along the road, who have showed much appreciated support, motivation, and patience throughout this entire process. I will be forever grateful for your love.

AN ABSTRACT OF THE THESIS OF

Ranim Houssam Daw for Master of Science
Major: Biology

Title: Hic-5 Deregulation in Lamin A/C and Emerin – Associated Myopathies

In higher eukaryotes, the nuclear lamina – a meshwork of type V intermediate filaments – underlies and associates with the nuclear side of the inner nuclear membrane. It consists of 2 classes of proteins; (1) A-type lamins are encoded by a single *LMNA* gene that gives rise to lamin A, lamin C, lamin C2, and lamin AΔ10 by alternative splicing; (2) B-type lamins include lamin B1 and lamin B2 that are encoded by the *LMNB1* gene and lamin B3 encoded by *LMNB2* gene. Lamins associate and interact with NE proteins such as emerin. Laminopathies are a group of genetic diseases that are a consequence of mutations or anomalous post-translational modifications of the NE and/or nuclear lamina proteins. Mutations in the *LMNA* gene are the most dominant form of these diseases, and they have effects on diverse tissue types, mainly skeletal and cardiac muscle tissues. Hence, our aim is to gain a better understanding of these mechanisms that allow different mutations of the ubiquitously expressed *LMNA* gene contribute to laminopathic tissue specific phenotypes, namely Emery-Dreifuss Muscular Dystrophy (EDMD) and Dilated Cardiomyopathy (DCM). Several studies have shown that mechanical and oxidative stress are key players in the manifestation of laminopathies. In this regard, hydrogen peroxide inducible clone-5 (*Hic-5*), an adaptor protein, is oxidative stress and TGF-β sensitive and reported to have critical roles in myogenesis and muscle differentiation. It is also implicated in several vital cellular processes, such as: cell growth, proliferation, differentiation, migration, and senescence. We hereby hypothesize that there exists a deregulation in *hic-5* expression in lamin A/C and emerin – associated myopathies. In this study, we assessed the transcript and protein expression levels of *hic-5* in mouse embryo fibroblast (MEF) lines derived from mice lacking either A-type lamin (*Lmna*^{-/-}) or emerin (*Emd*^{+Y}) which have the EDMD phenotype and mice homozygous for the N195K mutant (*Lmna*^{N195K/N195K}) which have the DCM phenotype versus wild-type (WT) controls under baseline and oxidative stress conditions. Real Time PCR quantification showed that under baseline conditions, *hic-5* normalized to *18S* increases in transcript levels in *Lmna*^{-/-} and *Emd*^{+Y} MEFs with respect to WT and *Lmna*^{N195K/N195K} MEFs. Whereas, upon 0.1μM and 0.5μM treatments of H₂O₂, it significantly decreases in WT MEFs after 30min of the 0.5μM treatment with respect to the untreated controls. While, *Lmna*^{-/-} and *Lmna*^{N195K/N195K} MEFs, show direct significant increases unlike *Emd*^{+Y} MEFs that demonstrate slight insignificant fluctuations upon both treatments. On the other hand, Western Blot densitometry analysis showed that under baseline conditions, *hic-5α* is upregulated in the three mutant cell lines with respect to the WT controls. Whereas, in the latter MEFs, they

decrease upon 30min exposure to 0.5 μ M of H₂O₂ with respect to untreated controls. However, *Lmna*^{-/-} MEFs demonstrate significant increases throughout the different time points upon this treatment. While, *Lmna*^{N195K/N195K} and *Emd*^{-Y} MEFs show significant early increases upon both treatments. Immunofluorescence images show that under baseline and oxidative stress-induced conditions, hic-5 has a similar pattern of expression in *Lmna*^{+/+}, *Lmna*^{-/-}, and *Emd*^{-Y} MEFs of significantly high nuclear = cytoplasmic localization in comparison to low nuclear > cytoplasmic ones. Whereas, *Lmna*^{N195K/N195K} MEFs are significantly more localized in the nucleus rather than the nuclear = cytoplasmic distribution. Our future aims would be to test these changes and any possible altered post-translational modifications in C₂C₁₂ myoblasts and tissue sections derived from DCM mouse models. It would also be convenient to check if there exists any direct interactions between the nuclear lamina and Hic-5 through co-immunoprecipitation essays.

CONTENTS

	Page
ACKNOWLEDGEMENT	v
ABSTRACT.....	vi
LIST OF ILLUSTRATIONS	xiii
LIST OF TABLES	xv
LIST OF ABBREVIATIONS	xvi
Chapter	
I. LITERATURE REVIEW.....	1
A. Nucleus, nuclear structure, and organization.....	1
1. Overview.....	1
2. Nuclear lamins and nuclear lamina	
a. Expression of lamin isoforms.....	3
b. Structural organization and assembly of lamins.....	4
c. Important functions of lamins.....	7
i. Maintenance of nuclear architecture and cellular integrity.....	7
ii. Regulation of nuclear import/export.....	8
iii. Chromatin remodeling and organization.....	9
iv. DNA replication, repair, and transcription.....	11
v. Cell proliferation and differentiation	12
vi. Cardiac development and MKL1 signaling.....	14
B. Interactions of lamins with integral proteins of the inner nuclear membrane.....	14
1. Overview.....	14
2. Inner nuclear membrane protein Emerin.....	15
a. Overview.....	15
b. Functions of emerin	16
i. Regulation of transcription factors.....	16
ii. Maintaining nuclear structure.....	18
C. Lamins and oxidative stress.....	19

D. Laminopathies.....	20
1. Overview.....	20
2. Laminopathies affecting the muscular tissues.....	21
a. Emery-Dreifuss muscular dystrophy 2	21
b. Dilated cardiomyopathy.....	22
E. Hydrogen peroxide inducible clone-5.....	23
1. Overview.....	23
2. Hic-5 structure, isoforms, and tissue distribution.....	24
3. Hic-5 functions.....	26
a. Adaptor-like nuclear receptor coactivator.....	26
b. Response to oxidative stress signals.....	27
c. Response to TGF- β	28
d. Myogenesis and muscle differentiation.....	29
e. Downstream effector of MKL1/SRF pathway.....	29
G. Gap in knowledge, study rationale, and hypothesis.....	31
H. Objective of the study and specific aims.....	32
I. Significance of the Study.....	33
II. MATERIALS AND METHODS.....	34
A. Cell Lines.....	34
1. Cell culture.....	35
2. Cell count	36
B. RNA extraction.....	36
1. Baseline conditions.....	36
2. H ₂ O ₂ -induced oxidative stress conditions.....	37
C. Reverse transcription.....	37
D. Quantitative Real-Time PCR.....	38
E. Protein extraction, SDS-PAGE & western blot analysis.....	39
1. Protein extraction.....	39
a. Baseline conditions	39
b. H ₂ O ₂ -induced oxidative stress conditions.....	40
2. Sample protein quantification.....	40
3. SDS-PAGE.....	40

a. Casting and running the gel	40
b. Preparing and loading the samples.....	41
c. Protein transfer from gel to blot.....	42
d. Membrane blocking, washing, and antibody incubations.....	42
e. X-ray film imaging of western blots.....	43
f. Membrane stripping and re-probing.....	43
g. Western blots densitometry analysis.....	44
F. Immunofluorescence staining	45
G. Microscopic imaging.....	46
H. Statistical analysis.....	46
III. RESULTS.....	47
A. Real-time PCR	
1. Under baseline conditions, <i>hic-5</i> normalized to <i>18S</i> increases in transcript levels in the <i>Lmna</i> ^{-/-} MEFs and <i>Emd</i> ^Y MEFs with respect to their wild type controls and to <i>Lmna</i> ^{N195K/N195K} MEFs. This increase is statistically significant in the former and insignificant in the latter.....	47
2. In WT (<i>Lmna</i> ^{+/+}) MEFs, <i>hic-5</i> normalized to <i>18S</i> significantly decreases in transcript levels 15min post 0.1μM and 0.5μM treatment with H ₂ O ₂ with respect to their untreated controls.	48
3. In <i>Lmna</i> ^{-/-} MEFs, <i>hic-5</i> normalized to <i>18S</i> increases directly (statistically significant) and 1hr (statistically insignificant) after 0.5μM treatment with H ₂ O ₂ with respect to their untreated controls. Whereas, 30min post treatment with 0.1μM H ₂ O ₂ , these lamin knockout MEFs demonstrate an early-late increase in <i>hic-5</i> normalized to <i>18S</i> with respect to their untreated controls.....	50
4. In <i>Lmna</i> ^{N195K/N195K} MEFs, directly and early after 0.1μM and 0.5μM treatments with H ₂ O ₂ , <i>hic-5</i> normalized to <i>18S</i> significantly increases in transcript levels with respect to the untreated controls.....	51
5. In <i>Emd</i> ^Y MEFs, upon treatments with 0.1μM and 0.5μM of H ₂ O ₂ for different time points (5min, 15min, 30min, and 60min), <i>hic-5</i> normalized to <i>18S</i> demonstrates slight fluctuations in transcript levels that are statistically insignificant with respect to their untreated controls.	53
B. Western Blot	
1. Under baseline conditions, <i>hic-5α</i> is upregulated in the 3 laminopathic cell lines (<i>Emd</i> ^Y MEFs, <i>Lmna</i> ^{N195K/N195K} MEFs, and <i>Lmna</i> ^{-/-} MEFs) with respect to the WT (<i>Lmna</i> ^{+/+} MEFs) controls. This upregulation is highly significant in the complete lamin knockout panel (<i>Lmna</i> ^{-/-} MEFs).	55

2. Upon treatment with 0.1 μ M and 0.5 μ M of H₂O₂, the protein levels of hic-5 α are slightly altered in the WT (*Lmna*^{+/+} MEFs) at the different time points (5, 15, 30, and 60min) demonstrating a significant decrease upon 30min of their exposure to 0.5 μ M of H₂O₂ with respect to the untreated controls.....57
3. Upon treatment with 0.1 μ M of H₂O₂, the protein levels of hic-5 α in *Lmna*^{-/-} MEFs decrease insignificantly with respect to their untreated controls throughout the different time points. However, when these knockout MEFs were treated with 0.5 μ M of H₂O₂, hic-5 α demonstrates an increase which is significant only after 1hour of treatment.59
4. Upon treatment with 0.1 μ M and 0.5 μ M of H₂O₂, the protein levels of hic-5 α in *Lmna*^{N195K/N195K} MEFs show a significant increase with respect to their untreated controls directly after the treatment (5min and 15min, respectively) which then significantly decrease as more time elapses.....61
5. Upon treatment with 0.1 μ M of H₂O₂, the protein levels of hic-5 α in *Emd*^{-Y} MEFs show direct-early significant increases with respect to their untreated controls that then decrease with time. Whereas, when they are treated with 0.5 μ M of H₂O₂, hic-5 α demonstrates highly significant increases in protein levels that fluctuate as time elapses with respect to their untreated controls.....63

C. Immunofluorescence

1. Under baseline conditions, hic-5 protein has a similar pattern of expression in *Lmna*^{+/+}, *Lmna*^{-/-}, and *Emd*^{-Y} MEF cell lines of significantly high nuclear = cytoplasmic localization in comparison to low nuclear > cytoplasmic ones. Whereas, *Lmna*^{N195K/N195K} MEFs show a different pattern of hic-5 localization that is significantly higher in the nucleus in comparison with the nuclear = cytoplasmic distribution.65
2. Upon treating WT (*Lmna*^{+/+}) MEFs with 0.1 μ M and 0.5 μ M of H₂O₂ the cellular internal localization of hic-5 shows significantly higher levels of cytoplasmic = nuclear distribution in comparison with nuclear and nuclear > cytoplasmic distributions across all different time points similar to their untreated controls. Moreover, an immediate decrease in the cytoplasmic = nuclear distribution of hic-5 is observed upon treating the WT MEFs with 0.5 μ M of H₂O₂ in comparison with their untreated controls.69
3. Lamin knockout (*Lmna*^{-/-}) MEFs demonstrate a similar pattern of hic-5 distribution among the different time points post 0.1 μ M or 0.5 μ M of H₂O₂ treatments with respect to their untreated controls as those observed in the WT MEFs. In addition, hic-5's nuclear > cytoplasmic localization is higher than the nuclear one also upon both treatments and similar to the untreated controls.....72
4. *Lmna*^{N195K/N195K} MEFs show increasing and decreasing fluctuations in their nuclear hic-5 localization in comparison to the nuclear = cytoplasmic one upon treating them with 0.1 μ M and 0.5 μ M H₂O₂ and in comparison with their untreated controls. Yet, the nuclear localization significantly increases while the nuclear = cytoplasmic significantly decreases 15min post 0.1 μ M H₂O₂ treatment in comparison with the untreated controls.....74
5. *Emd*^{-Y} MEFs show similar patterns of significantly high nuclear = cytoplasmic distribution of hic-5 within the treated and untreated groups like those of WT and

lamin knockout MEFs. Yet, they are the only MEFs among the four tested samples to have a small fraction of their cells harboring hic-5 in a cytoplasmic > nuclear manner.....77

IV. DISCUSSION.....81

V. REFERENCES.....91

ILLUSTRATIONS

Figure	Page
1. Structure of the nuclear envelope.....	2
2. Structural organization of lamins.....	5
3. Post-translational modifications of lamins.....	6
4. Distribution of mutations and laminopathies along Lamin A.....	21
5. Comparison between the structures of paxillin and Hic-5.....	24
6. Pathways downstream of Hic-5 activation during EMT.....	31
7. Mean fold difference change in <i>hic-5</i> transcript expression in the mutant MEFs cell lines (<i>Lmna</i> ^{-/-} , <i>Lmna</i> ^{N195K/N195K} , and <i>Emd</i> ^{-Y}) in comparison to their WT controls at baseline conditions.....	48
8. Mean fold difference change in <i>hic-5</i> transcript expression in <i>Lmna</i> ^{+/+} MEF cells cultured at 100% confluence under 0.1 μM or 0.5 μM of H ₂ O ₂ –induced oxidative stress conditions for 5, 15, 30, and 60min.....	49
9. Mean fold difference change in <i>hic-5</i> transcript expression in <i>Lmna</i> ^{-/-} MEF cells cultured at 100% confluence under 0.1 μM or 0.5 μM of H ₂ O ₂ –induced oxidative stress conditions for 5, 15, 30, and 60min.....	51
10. Mean fold difference change in <i>hic-5</i> transcript expression in <i>Lmna</i> ^{N195K/N195K} MEF cells cultured at 100% confluence under 0.1 μM or 0.5 μM of H ₂ O ₂ –induced oxidative stress conditions for 5, 15, 30, and 60min.....	52
11. Mean fold difference change in <i>hic-5</i> transcript expression in <i>Emd</i> ^{-Y} MEF cells cultured at 100% confluence under 0.1 μM or 0.5 μM of H ₂ O ₂ –induced oxidative stress conditions for 5, 15, 30, and 60min.....	54
12. Western Blot analysis of <i>hic-5α</i> protein expression in <i>Lmna</i> ^{-/-} , <i>Lmna</i> ^{N195K/N195K} , and <i>Emd</i> ^{-Y} mutant MEFs cell lines in comparison to the control WT cells cultured at 100% confluence under baseline conditions.....	56
13. <i>hic-5α</i> protein expression in <i>Lmna</i> ^{+/+} MEF cells cultured at 100% confluence under 0.1 μM or 0.5 μM H ₂ O ₂ –induced oxidative stress conditions for 5, 15, 30 and 60min.....	58
14. <i>hic-5α</i> protein expression in <i>Lmna</i> ^{-/-} MEF cells cultured at 100% confluence under 0.1 μM or 0.5 μM H ₂ O ₂ –induced oxidative stress conditions for 5, 15, 30 and 60min...	60

15. hic-5 α protein expression in <i>Lmna</i> ^{N195K/N195K} MEF cells cultured at 100% confluence under 0.1 μ M or 0.5 μ M H ₂ O ₂ –induced oxidative stress conditions for 5, 15, 30 and 60min	62
16. hic-5 α protein expression in <i>Emd</i> ^{-Y} MEF cells cultured at 100% confluence under 0.1 μ M or 0.5 μ M H ₂ O ₂ –induced oxidative stress conditions for 5, 15, 30 and 60min.....	64
17. Immunofluorescence staining and semi-quantitative analysis of hic-5 protein cellular internal localization expression in the 4 MEFs panels (<i>Lmna</i> ^{+/+} , <i>Lmna</i> ^{-/-} , <i>Lmna</i> ^{N195K/N195K} , and <i>Emd</i> ^{-Y}) cultured at 100% confluence under baseline conditions.....	68
18. Immunofluorescence staining and semi-quantitative analysis of hic-5 protein cellular internal localization expression in <i>Lmna</i> ^{+/+} MEFs cultured at 100% confluence under 0.1 μ M or 0.5 μ M H ₂ O ₂ –induced oxidative stress conditions for 5, 15, 30 and 60min.....	71
19. Immunofluorescence staining and semi-quantitative analysis of hic-5 protein cellular internal localization expression in <i>Lmna</i> ^{-/-} MEFs cultured at 100% confluence under 0.1 μ M or 0.5 μ M H ₂ O ₂ –induced oxidative stress conditions for 5, 15, 30 and 60min.....	73
20. Immunofluorescence staining and semi-quantitative analysis of hic-5 protein cellular internal localization expression in <i>Lmna</i> ^{N195K/N195K} MEFs cultured at 100% confluence under 0.1 μ M or 0.5 μ M H ₂ O ₂ –induced oxidative stress conditions for 5, 15, 30 and 60min.....	76
21. Immunofluorescence staining and semi-quantitative analysis of hic-5 protein cellular internal localization expression in <i>Emd</i> ^{-Y} MEFs cultured at 100% confluence under 0.1 μ M or 0.5 μ M H ₂ O ₂ –induced oxidative stress conditions for 5, 15, 30 and 60min.....	78

TABLES

Table	Page
1. Comparison between the different isoforms of <i>Hic-5</i>	25
2. A list showing the sequences of the forward and the reverse primers that were used to quantify the transcriptional expression of <i>Hic-5</i> and the <i>18S</i> reference genes by Real-Time PCR.....	38
3. Summary of baseline results.....	79
4. Summary of H ₂ O ₂ -induced oxidative stress treatments results.....	80

ABBREVIATIONS

μ	micro
.tif	tag image file format
°C	degrees Celsius
3T3 cells	3-day transfer, inoculum 3x10 ⁵ cells
A	adenine
AP-1	activating protein 1
APS	ammonium persulfate
AR	androgen receptor
ARA55	androgen receptor activator
BAF	autointegration factor
Bcl-1	Bcl-2-associated transcription factor 1
BSA	bovine serum albumin
C	cytosine
<i>C. elegans</i>	<i>Caenorhabditis elegans</i>
Ca	calcium
CaaX	C: cysteine, a: aliphatic amino acid, X: any
amino acid	
CAD	coronary artery disease
CBP	CREB-binding protein
cDNA	complementary deoxyribonucleic acid
c-Fos	FBJ murine osteosarcoma viral oncogene
homolog	
CO ₂	carbon dioxide
<i>Cyp3a</i>	cytochrome P450 family 3 subfamily A
member 4	
DALP	Death associated LIM-only protein
DamID	DNA arginine methyl transferase
DAPI	4,6-diamidino-2-phenylindole
DCM	Dilated Cardiomyopathy
ddH ₂ O	deionized distilled water
DMEM-AQ	Dulbecco's Modified Eagle's Medium
DNA	deoxyribonucleic acid
E2F	e2 transcription factor
ECM	extracellular matrix
EDMD	Emery-Dreifuss Muscular Dystrophy
EMT	epithelial-mesenchymal transition
ERK	extracellular signal-regulated kinase
et al	et alli (and others)
FACE1	farnesylated proteins-converting enzyme 1
FAK	focal adhesion kinase
FG	phenylalanine-glycine
FISH	fluorescence in situ hybridization
G	guanine
G-actin	globular actin
GAPDH	glyceraldehyde 3 phosphate dehydrogenase
GCL	germ cell-less

GR	glucocorticoid receptor
H3K9me2	histone H3, dimethylated at lysine 9
HAT	histone acetyl transferase
HCl	hydrochloric acid
HDAC	histone deacetylase
HF	heart failure
Hic-5	hydrogen peroxide inducible clone-5
HRP	horseradish peroxidase
Hsp27	heat shock protein 27
Ig	immunoglobulin Ig
IHC	immunohistochemistry
INM	inner nuclear membrane
kb	kilobase pair
kD	kilodalton
LADs	lamina-associated domains
LAP	latency-associated peptide
LBR	lamin binding protein
LD	leucine-aspartate
LEM	lamina associated polypeptide-2: lap2,
emerin & man1	
LGMD	limb-girdle muscular dystrophy
LIM	lin11, isl-1, and mec-3
LINC	Linkers of nucleoskeleton and cytoskeleton
LMD	leptomycin B
Lmo7	Lim-domain-only 8
M	molar
MAN1	LEM domain-containing protein 3
MAPK	mitogen activated protein kinase
Mb	megabase pair
MEF	mouse embryo fibroblast
MET-2	histone-lysine N-methyltransferase
Mg	magnesium
min	minute
MKL1	megakaryoblastic leukaemia 1
mm	millimeter
MMTV	mouse mammary tumor virus
mol/L	mole per liter
mRNA	messenger ribonucleic acid
Myf5	myogenic factor 5
MyoD	myoblast determination protein 1
NaOH	sodium hydroxide
NCoR	nuclear receptor co-repressor 1
NE	nuclear envelope
NES	nuclear export sequence
NGPS	Nestor-Guillermo progeria syndrome
NLS	nuclear localization signal
Nox4	NADPH oxidase
NPC	Nuclear pore complexes

ONM	outer nuclear membrane
p34 ^{cdc2}	cyclin-dependent kinase 1
p53	tumor protein 53
Pax3	paired box protein 3
PBS	phosphate buffered saline
PCNA	proliferating cell nuclear antigen
PCR	polymerase chain reaction
PFA	Paraformaldehyde
pH	potential of hydrogen
PI3K	phosphoinositide 3 kinase
pK	scale of relative acid strength
PNS	perinuclear space
PPAR γ	peroxisome proliferator-activated receptor
gamma	
pRb	retinoblastoma
PVDF	polyvinylidene fluoride
Rac1	Ras-related C3 botulinum toxin substrate 1
RAC3	Ras-related C3 botulinum toxin substrate 3
RBD	Rho-binding domain
RhoC	rhodopsin-C
RIPA	radioimmunoprecipitation assay
ROCK	Rho-associated protein kinase
ROS	reactive oxygen species
Rpm	round per minute
SDS	sodium dodecyl sulfate
SEM	standard error of the mean
siRNA	short interfering ribonucleic acid
Smad	small mothers against decapentaplegic
SP-1	specificity protein 1
S-phase	synthesis phase
SRF	serum response factor
SUN1	Sad1 and UNC84 domain containing 1
T	thymine
TEMED	tetramethylethylenediamine
TF	transcription factor
TGF β 1I1	transforming growth factor β induced
transcript 1	
TIF-2	translation initiation factor 2
Tris	trisaminomethane
Tween20	polyoxyethylene sorbitol ester
V	volt
VSMC	vascular smooth muscle cells
Wnt	wingless-type MMTV integration site
family, member 1	
WT	wild-type
X	times
xg	acceleration expressed as gravity
YAP1	yes-associated protein

ZMPSTE24
 α
 β

zinc metallopeptidase ste24
alpha
beta

CHAPTER I

LITERATURE REVIEW

A. Nucleus, nuclear structure, and organization

1. Overview

The nucleus is enveloped by a phospholipid bilayer that separates the contents of its nucleoplasm from the cytoplasm. It is composed of an outer nuclear membrane (ONM) continuous with the endoplasmic reticulum (ER), an inner nuclear membrane (INM) harboring an array of integral membrane proteins, such as emerin whose importance will be highlighted in this study, and a perinuclear space (PNS) continuous with the ER lumen separating both membranes (figure 1). Nuclear pore complexes (NPCs) are extremely selective bidirectional transporters that join the INM and the ONM. They hinder the passage of nonspecific macromolecules while allowing the free diffusion of water, sugars, and ions. Moreover, they provide an anchor for many nuclear processes, such as: gene activation and cell cycle regulation (Wente & Rout, 2010). Moreover, underlying the INM is a meshwork of fibrous proteinaceous type V intermediate filaments, called the nuclear lamina (Fawcett, 1966; Yosef Gruenbaum & Foisner, 2015; Pappas, 1956) that associate with NPCs (Aaronson & Blobel, 1975). They were first discovered in the 1950s by transmission electron microscopy in invertebrates (Gerace, Blum, & Blobel, 1978). Then in the 1970s, they were isolated from mammalian nuclei and their major polypeptides were identified (Aaronson & Blobel, 1975; Ciska & Moreno Díaz de la Espina, 2013). Subsequent studies correlated them with different roles, namely: regulating the nuclear structure, granting mechanical support for the nucleus and its membrane, organizing chromatin, distributing NPCs,

associating between the nucleoskeleton and cytoskeleton, and regulating signaling pathways (T Dechat, Adam, Taimen, Shimi, & Goldman; Dittmer & Misteli, 2011; DuBois et al., 2012; Ho & Lammerding, 2012). The nuclear envelope (NE) is also traversed by flexible structures, named Linkers of Nucleoskeleton and Cytoskeleton (LINC) complexes that were initially identified in *C. elegans* studies which revealed their indispensable role in nuclear positioning within the cell (Malone, Fixsen, Horvitz, & Han, 1999; Razafsky & Hodzic, 2015; Starr & Han, 2002; Starr et al., 2001). Recent studies have also shown that LINC complexes allow for nucleocytoplasmic coupling contributing to the transmittance of forces from the extracellular matrix (ECM) into the cytoskeleton and further into the nucleus to mediate mechanotransduction cascades (Lombardi et al., 2011).

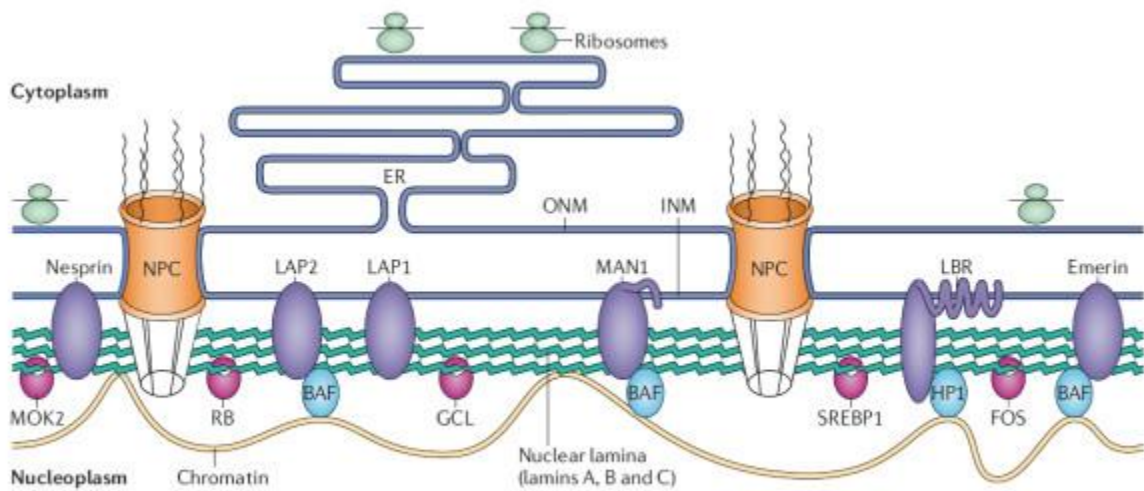


Figure 1: Structure of the nuclear envelope; a modified figure from (Chi, Chen, & Jeang, 2009). The nuclear envelope is composed of the outer nuclear membrane (ONM) is continuous with the ER membrane, the inner nuclear membrane (INM) that harbors many integral membrane proteins, and the perinuclear space that separates them. Undereath the INM, is the nuclear lamina that is composed of A, B, and C-type lamins.

2. Nuclear lamins and nuclear lamina

a. Expression of lamin isoforms

As previously mentioned, underlying the INM is a meshwork of type V intermediate filaments, termed the nuclear lamina. Three lamin genes, *LMNA*, *LMNB1*, and *LMNB2*, are found in mammals encoding four major lamin isoforms and three minor ones. The *LMNA* gene codes for A-type lamins that include the major isoforms A and C and the minor ones A Δ 10 and C2. Whereas, B-type lamins are encoded by two separate genes: *LMNB1* gene coding for the major isoform B1, and *LMNB2* gene coding for the major B2 and the minor B3 isoforms. At least one type of B-lamins is expressed in every mammalian cells, whereas A-type lamins are differentially regulated (Yosef Gruenbaum & Foisner, 2015; Lehner, Stick, Eppenberger, & Nigg, 1987; Rober, Weber, & Osborn, 1989; C. Stewart & Burke, 1987).

Cloning studies showed that lamins are present in all metazoan cells with *LMNB1* gene being the most evolutionarily conserved among the different species (Lyakhovetsky & Gruenbaum, 2014; Zimek & Weber, 2011). Hence, it is postulated that an *LMNB1-like* gene was the antecedent of all lamin and IF proteins now present (A. Peter & Stick, 2012). Moreover, it is suggested that in lower organisms, such as *C. elegans*, the lone B-type lamin satisfies the functions of both types of vertebrate lamins. However, the only invertebrate species that expresses more than one lamin gene are *Ciona intestinalis* that has two *lamin-B* genes, and *Drosophila melanogaster* that has one *lamin-A* gene and one *lamin-B* gene (Yosef Gruenbaum et al., 1988; Dieter Riemer, Wang, Zimek, Swalla, & Weber, 2000; D Riemer & Weber, 1994). On the other hand, unlike mammals, fish, *Xenopus*, reptiles, and birds have three B-type lamin genes, namely: *LB1*, *LB2*, and *LB3/LIII* (Hofemeister, Kuhn, Franke, Weber, & Stick, 2002).

Interestingly, recent studies showed that lamin-like genes are present in some single-cell organisms. For example, the NE protein NE81 in *Dictyostelium discoideum* has a structure that resembles metazoan lamins and is critical for nuclear integrity, mechanical stability, and chromatin organization (Krüger et al., 2012). However, most unicellular organisms, including the extensively studied *Saccharomyces cerevisiae*, do not have lamin genes (Lyakhovetsky & Gruenbaum, 2014). Also, plants lack lamin genes. Nevertheless, their LINC genes can be regarded as functional analogs of animal lamins since they are confined at the nuclear periphery and interact with SUN1/SUN2 that are INM integral membrane proteins mediating nucleocytoplasmic coupling in mammals (Ciska, Masuda, & de la Espina, 2013; Graumann, 2014).

b. Structural organization and assembly of lamins

Based on structural differences between lamins and cytoplasmic IFs, the formers are classified as type V IFs (Steinert & Roop, 1988). Like other IF proteins, lamins possess a tripartite structure made of a highly conserved α -helical coiled-coil rod (head) domain that spans more than half of the lamin molecule. It encompasses four six heptad repeats (1A, 1B, 2A and 2B) that are connected by malleable linker domains (L1, L12 and L2). Yet, lamins have 42 more residues in coil 1B than that of vertebrate cytoplasmic IFs (Herrmann & Aebi, 2004). In addition, like all IFs, lamins possess a globular C-terminal (tail) domain that harbors lamin-specific motifs, namely a nuclear localization signal (NLS), an immunoglobulin (Ig) fold difference motif, and a C-terminal CaaX (C: cysteine, a: aliphatic amino acid, X: any amino acid) motif that undergoes successive post-translational modifications (figure 2). First, the addition of a farnesyl group to the cysteine residue of the CAAX box is mediated by farnesyl

transferase. Next, the last three amino acids undergo proteolytic cleavage by the action of the metallopeptidases ZMPSTE24 or FACE1. Lastly, a methyl group is added to the C-terminal cysteine by isoprenylcysteine carboxyl methyltransferase (Rusiñol & Sinensky, 2006). A-type lamins then undergo an additional post-translational cleavage step mediated by ZMPSTE24 that cleaves 15 amino acids found upstream of the farnesylated cysteine leaving a tyrosine residue at the carboxyl end (figure 3). Additionally, A-type lamins differ from B-type lamins by having a neutral isoelectric point pK while the latter have an acidic one (Gerace et al., 1978).

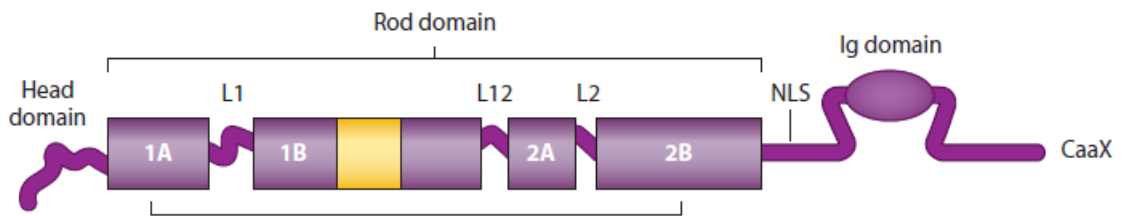


Figure 2: Structural organization of lamins; figure modified from (Yosef Gruenbaum & Foisner, 2015). Lamins are composed of a long rod domain that is flanked by an amino terminal head and a carboxy terminal tail that harbors a NLS, immunoglobulin domain, and a CaaX box.

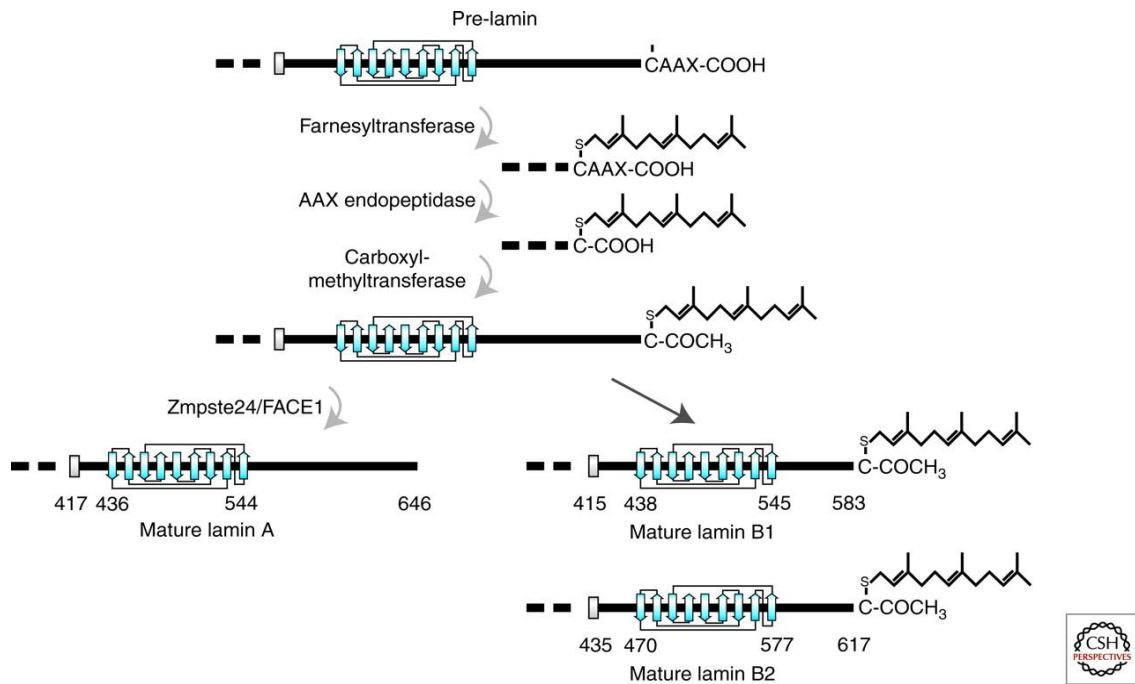


Figure 3: Post-translational modifications of lamins; figure modified from (Thomas Dechat, Adam, Taimen, Shimi, & Goldman, 2010). The pre-lamin protein filament gets farnesylated at its CaaX box. Then the aaX motif gets cleaved by an endopeptidase and a methyl group is added to the cysteine residue. A-type lamins then undergo further processing whereby the last 15 amino acids upstream of the farnesylated cysteine get cleaved.

In the 1990s, *in vitro* studies revealed that lamins form dimers by parallel coiled-coil interactions of their rod domain, which then form polar head-to-tail polymers that associate laterally to produce a paracrystalline array of proteins (Heitlinger et al., 1991). However, these arrays are most probably not applicable to lamin organization *in vivo* since they are only observed after great overexpression of lamins (Klapper et al., 1997). In *C. elegans*, cryoelectron tomography analyses revealed that the basic assembly unit in lamins is a 5-6nm wide protofilament that contains two antiparallel head-to-tail polymers of lamin dimers. Subsequently, the association of 3-4 protofilaments forms the 10nm wide lamin protein filament (Ben-Harush et al., 2009). These results suggest that *ex vivo*, the lamin protofilaments form further complex structures than *in vitro* (Grossman et al., 2012). It is still not known why lamins

assemble differently *in vitro* in comparison with *in vivo*. Yet, possible justifications highlight the complex associations of lamins with their partner proteins and/or chromatin *in vivo* (Yosef Gruenbaum & Foisner, 2015).

c. Important functions of lamins

i. Maintenance of nuclear architecture and cellular integrity

Cytoplasmic and nuclear IF networks have an essential role in maintaining the integrity of cells and tissues. Similarly, the status of lamin polymerization is correlated with maintaining structural and mechanical nuclear stability during interphase. In agreement, *Xenopus* eggs depleted from lamins exhibited small and fragile nuclei (Moir et al., 2000; Newport, Wilson, & Dunphy, 1990). Moreover, when nuclei from the same organism expressed a dominant negative lamin mutant that disrupts lamin polymerization, irregularly shaped nuclei were formed (Spann, Moir, Goldman, Stick, & Goldman, 1997). The same pattern was observed when this mutant protein was expressed in mammalian cells whereby despite the normal formation of the NE and NPCs, the former became more prone to rupture upon centrifugation and similar kinds of mechanical stress. Moreover, point mutations in *LMNA* gene result in Emery-Dreifuss muscular dystrophy (EDMD) in humans (Gisèle Bonne et al., 1999) that is accompanied with gross structural changes in the NE along with mislocalization of emerin (Funakoshi, Tsuchiya, & Arahata, 1999). Therefore, the interaction of emerin and lamins stabilizes the NE. An interesting real-time PCR analysis – conducted in different cell types expressing varying lamin A/C levels – studied the different cellular nuclear responses to stress. It established that low levels of lamin A/C disturbed chromatin packing and was inadequate to protect against stress. While when its

expression was 30 times higher – in heart and skeletal muscles – rapid nuclear distension was hindered (Carmosino et al., 2014; Swift et al., 2013). Importantly, an increase in the expression of lamin A/C in mechanically-stressed tissues activates the serum response factor (SRF) signaling pathway that controls actin dynamics and the expression of certain sarcomeric proteins (Balza & Misra, 2006; Vartiainen, Guettler, Larijani, & Treisman, 2007).

ii. Regulation of nuclear import/export

Several studies have suggested that lamins directly anchor and position NPCs. Plus, in mammalian cells, the distribution of the latter along the NE is highly associated with the distribution of both types of lamins whereby they are enriched in lamin B-associated areas. However, lamin A/C associates with the NE at NPC-free stretches (Fiserova & Goldberg, 2010; Maeshima et al., 2006). Remarkably, highly mobile clusters of NPCs were identified in yeast cells lacking the lamina structure (Belgareh & Doye, 1997; Bucci & Wente, 1997). In *Xenopus*, high-resolution scanning electron microscopy showed a direct attachment of lamins to the center of NPCs (Goldberg & Allen, 1996). This suggests that lamins not only influence NPCs' positioning, but also their conformation and nuclear trafficking (Fiserova & Goldberg, 2010). So far, Nup153 is the nucleoporin shown to mediate lamin–NPC interactions (Smythe, Jenkins, & Hutchison, 2000; Walther et al., 2001). The N-terminal part of Nup153 allows for its structural maintenance (Walther et al., 2001), whereas its C-terminal FG-domain located at its nucleoplasmic and cytoplasmic sides (Fahrenkrog et al., 2002) provides the binding site for lamins (Smythe et al., 2000). On the other hand, in mammalian cells, Sun1 that provides linkage between actin, lamins, and nuclear components was

also shown to be a strong determinant of NPC distribution (Crisp et al., 2006; Q. Liu et al., 2007).

iii. Chromatin remodeling and organization

In the 1990s, electron microscopy studies on *Drosophila* proposed that chromatin is in direct contact with lamins (Belmont, Zhai, & Thilenius, 1993; Yosef Gruenbaum & Foisner, 2015). Moreover, fluorescence in situ hybridization (FISH) studies unveiled that the localization of chromosomes is not random (Cremer & Cremer, 2010; Y Gruenbaum et al., 1984) whereby the gene-poor ones are more apt to localize in close proximity to the nuclear periphery unlike the gene-rich ones that are most likely localized in the center of the nucleus (Croft et al., 1999). Yet, chromosome localization is not always interrelated with gene density and varies significantly between cell types (Zuleger, Robson, & Schirmer, 2011).

In an interesting study, *Drosophila* ectopically expressing B-type lamin (Dm0) were fused to bacterial DNA arginine methyl transferase (DamID). Then, the methyl groups added by the lamin fusion protein were analyzed (Pickersgill et al., 2006). It was found that lamina-associated domains (LADs) are more present in transcriptionally inactive or gene-poor regions and undergo late replication. This spatial organization is conserved in all mammalian cells (Guelen et al., 2008; Peric-Hupkes et al., 2010). The human genome holds more than 1,300 LADs (10kb-10Mb) that make up around 40% of it. Similar LADs were recognized in other mammalian cells by DamID fusions with lamins B1 and A, emerin, and barrier to autointegration factor (BAF) (Guelen et al., 2008; Kind & van Steensel, 2014; Meuleman et al., 2013) and by immunoprecipitation studies of lamin B1 and lamin A with chromatin (Lund et al., 2013; Sadaie et al., 2013;

Shah et al., 2013). Direct/indirect binding of lamins to gene promoters at the LAD domains may influence gene silencing (D. C. Lee, Welton, Smith, & Kennedy, 2009). Moreover, lamin-binding proteins in the INM are proposed to link heterochromatin to the lamina mediating gene silencing. For example, emerin interacts with histone deacetylase 3 (HDAC3) and inactivates its catalytic activity (Demmerle, Koch, & Holaska, 2012). Recently, it was shown that both LBR and LEM (lamina associated polypeptide-2: LAP2, Emerin and MAN1) protein complexes tether heterochromatin to the nuclear periphery in the same manner (Solovei et al., 2013). In most mammalian cells, LBR is mainly expressed early in the development whereas lamin A is expressed later (Yosef Gruenbaum & Foisner, 2015). Therefore, either one of them is able, at a given time, to control signaling by forming repressive heterochromatin sinks. On the other hand, this association of LADs with the nuclear lamina may hinder the interactions of promoters within LADs with their enhancers, hence blocking their signal cascade mechanism (Amendola & van Steensel, 2014).

There are at least two possible mechanisms that explain why lamins associate with specific regions of heterochromatin and not others. The first possible explanation proposes that specific DNA sequences in LADs aid in lamina targeting. In agreement with this proposition, it was found that repetitive GAGA sequences are enriched in lamina-associated sequences in mouse *IgH* and *Cyp3a* loci (Zullo et al., 2012). However, similar LADs in mammals were found to be A/T rich (Meuleman et al., 2013). The second explanation proposes that particular epigenetic marks may help in the tethering of the heterochromatin to the lamina. In support with this, in *C. elegans*, a chronological mechanism exists whereby H3K9me2 formation is mediated by MET-2 that in turn mediates the peripheral localization of chromatin. This founds a repressive

heterochromatin environment that is rich in H3K9me3 (Yosef Gruenbaum & Foisner, 2015).

iv. DNA replication, repair, and transcription

Several studies have linked lamins with DNA replication. In cultured mouse 3T3 cells, lamin B1 was found to co-localize with replication foci in late S phase (Thomas Dechat et al., 2010; Moir, Montag-Lowy, & Goldman, 1994). While, in human fibroblasts, lamins A/C were detected at sites of early replication (Kennedy, Barbie, Classon, Dyson, & Harlow, 2000). Additionally, in *Xenopus* nuclei, DNA replication was inhibited upon the depletion of lamin B3 (Shumaker et al., 2005; Shumaker et al., 2008). Importantly, evidence revealed that A and B type lamins harbor PCNA (proliferating cell nuclear antigen) binding site at their Ig-fold difference and thus play a direct role in DNA replication (Shumaker et al., 2008). Recently, it was also suggested that the lamins impose an indirect effect on replication whereby their assembly ensures a functional NE that conserves the contents of the nucleoplasm, including important replication factors, such as DNA polymerases and PCNA (Walter, Sun, & Newport, 1998).

The mechanisms implicated in lamins' involvement in DNA repair are still unclear. So far, it was found that the expression of mutant lamin isoforms hinders the formation of DNA repair foci (B. Liu et al., 2005; Manju, Muralikrishna, & Parnaik, 2006). Likewise, progeria phenotype – caused by a mutated truncated pre-lamin A protein – was accompanied by genetic instability, telomere dysfunction, and improper DNA repair mechanisms (Gonzalez-Suarez, Redwood, & Gonzalo, 2009; Gonzalez - Suarez et al., 2009).

Several studies have linked lamins with regulation of transcription. In hamster and *Xenopus* cells, it was shown that the expression of dominant negative lamin A precisely inhibited RNA polymerase II activity (Spann, Goldman, Wang, Huang, & Goldman, 2002). Moreover, in HeLa cells, the same pattern of polymerase II inhibition was observed upon the over-expression of lamin A/C or quietening of lamin B1 (Kumaran & Spector, 2008; Shimi et al., 2008). Also, the association of lamins with several transcription factors suggests that they could be involved in the latter's regulatory pathways (Andrés & González, 2009; Heessen & Fornerod, 2007). For example, lamin A/C interacts with the transcription factors: sterol response element binding protein 1 (SREBP1), c-Fos, and MOK2 (Dreuillet, Harper, Tillit, Kress, & Ernoult - Lange, 2008; Dreuillet, Tillit, Kress, & Ernoult - Lange, 2002; Harper, Tillit, Kress, & Ernoult - Lange, 2009). c-Fos interaction with lamin A/C at the NE suppresses the binding of activating protein 1 (AP-1) which hinders the activity of extracellular signal-regulated kinase (ERK) 1/2 (González, Navarro-Puche, Casar, Crespo, & Andrés, 2008; Ivorra et al., 2006).

v. Cell proliferation and differentiation

As previously mentioned, B-type lamins are ubiquitously expressed throughout development (Carmosino et al., 2014; Harborth, Elbashir, Bechert, Tuschl, & Weber, 2001). On the other hand, expression of lamin A/C is limited to differentiated cells and is first identified on days 9 and 12 in extraembryonic mice tissues and the embryo, respectively (Rober et al., 1989). Interestingly, embryonic carcinoma cells and adult cells that do not undergo full differentiation, express little or no Lamin A/C (Rober et al., 1989; C. Stewart & Burke, 1987). It was also observed that lamin B knockout mice

die at birth due to neuronal apoptosis (Coffinier et al., 2010), while those with lamin A/C knockout mice die weeks after birth, despite the development of all their tissues, mainly due to severe muscular dystrophy (Jahn et al., 2012; Kubben et al., 2011). These findings are in agreement with the recently highlighted role of lamin A/C in the differentiation and maturation of myocytes. In addition, the differentiation of stem cells into fat cells was shown to be enhanced by sustaining low levels of lamin A/C, while their differentiation into bone cells was improved by high levels of it (Swift et al., 2013). Also, lamin A/C expression was found to trigger the accumulation of the mechanosensitive transcriptional regulator Yes-associated protein (YAP1) that activates genes responsible for cellular proliferation and represses those responsible for the induction of apoptosis (Zhao, Li, Lei, & Guan, 2010).

Numerous changes in nuclear organization are paralleled by changes in lamin organization with evidence correlating them with diverse lamin functions during cell cycle. In agreement, distribution of nuclear lamins was shown to vary through the cell cycle (Gerace & Blobel, 1980). The most intense modifications in lamin organization occur during its disassembly that occurs along with NE disassembly during late prophase. This is triggered by the phosphorylation of lamins by p34cdc2 kinase at their rod domain, leading to their depolymerization into monomers, dimers, and tetramers (Dessev, Iovcheva-Dessev, Bischoff, Beach, & Goldman, 1991; M. Peter, Nakagawa, Doree, Labbe, & Nigg, 1990). Consequently, the reassembly following mitosis is mediated by lamin dephosphorylation at the same residues (M. Peter et al., 1990). The role of the lamins following mitosis remains controversial. Two proposed models have been stated regarding this. The first one suggests that lamin interactions with the NE components occur early in the reassembly process and are essential for proper nuclear

structure and integrity. While the second model suggests that after the nuclear membrane vesicles fuse around lamins, and after they are incorporated with NPCs, lamins are imported into the nucleus. Much evidence for both models has emerged in *in vitro* nuclear assembly studies (Moir et al., 2000).

vi. Cardiac development and MKL1 signaling

In *lmna*^{-/-} mice and *lmna*^{N195K/N195K} cells, impaired downstream signaling of the mechanosensitive transcription factor megakaryoblastic leukaemia 1 (MKL1) is detected (Ho, Jaalouk, Vartiainen, & Lammerding, 2013). MKL1 is indispensable for cardiac development and function (Olson & Nordheim, 2010). It is normally found in the cytoplasm bound to cytoplasmic G-actin. Then, upon mitogenic or mechanical triggers, G-actin undergoes polymerization in response to the activated RhoA, and MKL1 is consequently liberated from it exposing its NLS sequence found in its actin-binding domain. This allows for the accumulation of MKL1 in the nucleus permitting its co-activation of serum response factor (SRF). The latter then activates genes responsible for cellular motility and contractility, such as actin, vinculin, and SRF (Vartiainen et al., 2007). SRF also activates structural sarcomeric proteins (Balza & Misra, 2006). Notably, in *lmna*^{-/-} and *lmna*^{N195K/N195K} mice, their cardiac tissues had lower transcript levels of SRF and actin than their wildtype littermates (Ho et al., 2013).

B. Interactions of lamins with integral proteins of the inner nuclear membrane

I. Overview

The INM harbors hundreds to conceivably thousands of proteins (Schirmer & Gerace, 2005). Emerging studies on these proteins have revealed their vital roles in

maintaining nuclear structure and positioning (Meister & Taddei, 2013; Mekhail & Moazed, 2010; Rothballer & Kutay, 2013). For example, SUN proteins play crucial roles in nucleocytoplasmic coupling through their interaction with specific ONM proteins that bind to actin, microtubule-organizing centers (MTOCs), IFs, and dynein. Numerous proteins of the SUN and LEM domain-containing families assist in transcriptional regulation, DNA repair, and meiotic recombination by acting as scaffold differences for nuclear factors. Consequently, a myriad of human diseases are related to mutations in the genes encoding them. In metazoan cells, the function of these proteins is partly dependent on their interactions with lamins and LAPs; (Schreiber & Kennedy, 2013; Simon & Wilson, 2011, 2013; C. L. Stewart, Roux, & Burke, 2007). Hence, understanding the targeting, distribution, and regulation of the different INM proteins in different cell types under normal and stress conditions is essential to interpret the mechanisms of manifestation of these disorders (Katta, Smoyer, & Jaspersen, 2014).

2. Inner nuclear membrane protein emerin

a. Overview

Emerin is expressed in all the cells (Koch & Holaska, 2014; Manilal, thi Man, Sewry, & Morris, 1996; Nagano et al., 1996). Along with Lap2 β and MAN1, it is a member of the LEM-domain proteins that bind to BAF (Margalit, Brachner, Gotzmann, Foisner, & Gruenbaum, 2007; Segura-Totten & Wilson, 2004). The emerin gene (*EMD*) is made up of 6 exons and 5 introns. It is situated on the X-chromosome and codes for the emerin protein (29kD) that has 254 amino acids. This protein has an N-terminal nucleoplasmic domain, a C-terminal transmembrane domain, and a luminal domain. The LEM-domain is found on the N-terminus and has a conserved helix-loop-helix fold

difference with a sole function of binding to BAF (a second DNA-binding LEM-like domain is an exception Lap2 proteins) (Cai et al., 2001). Emerin and the other LEM-domain proteins are involved in securing chromatin to the NE. After its synthesis, emerin is inserted into the ER and then into the NE. Because of its small size, emerin can diffuse through NPCs while it is still anchored to the membrane (Ellis, Craxton, Yates, & Kendrick-Jones, 1998; Ostlund, Ellenberg, Hallberg, Lippincott-Schwartz, & Worman, 1999; Östlund, Sullivan, Stewart, & Worman, 2006). It also binds A-type lamins inside the nucleus which is required for its correct localization to the NE (Holaska, Wilson, & Mansharamani, 2002).

b. Functions of emerin

i. Regulation of transcription factors

Emerin interacts with numerous transcription factors, such as germ cell-less (GCL) (Holaska, Lee, Kowalski, & Wilson, 2003), Bcl-2-associated transcription factor 1 (Bclaf1) (Haraguchi et al., 2004), Lim-domain-only 8 (Lmo7) (Holaska, Rais-Bahrami, & Wilson, 2006), β -catenin (Markiewicz et al., 2006), and BAF (K. K. Lee et al., 2001).

GCL is identified as a transcription repressor since it binds the E2F-DP3 heterodimer through the DP3 subunit inactivating its transcriptional activity (de la Luna, Allen, Mason, & La Thangue, 1999). Moreover, GCL directly binds the regulatory binding domains RBD-1 and RBD-2 of emerin (Holaska et al., 2003) leading to the repression of E2F-DP3-dependent gene transcription that is implicated in S-phase entry and cell proliferation control (Holaska & Wilson, 2006). Accordingly, emerin-null cells exhibit higher proliferation rates than their WT controls (Markiewicz et al., 2006).

On the other hand, Bcalf1 is critical in development; whereby Bcalf1-null mice experience immunological complications and premature death (McPherson et al., 2009). It also serves as an mRNA splicing factor and regulates transcription accordingly (Haraguchi et al., 2004; Merz, Urlaub, Will, & Lührmann, 2007; Saitoh et al., 2004). Given that Bcalf1 directly binds to emerin's RBD-1 and RBD-2 and its roles in splicing and development, it is proposed that emerin is also implicated in its regulation of mRNA splicing site choice (Koch & Holaska, 2014).

Lmo7 binds to emerin to be able to shuttle between the cell exterior and the nucleus; the deregulation of the latter inhibits the nuclear localization of the former (Ooshio et al., 2004). This binding represses the ability of Lmo7 to activate its target genes, including emerin, thus serving as a negative feedback loop to control the expression of emerin (Holaska et al., 2006). Interestingly, Lmo7 is expressed in high levels in the heart and skeletal muscles, which implies that its communication with emerin could be related to the EDMD disease mechanism (Putilina et al., 1998; Semenova, Wang, Jablonski, Levorse, & Tilghman, 2003). In alignment with this, Lmo7 activates promoters of crucial myogenic differentiation genes that are downregulated after myotube formation, such as MyoD, Myf5, and Pax3; this overlaps with an increase in emerin expression (Dedeic, Cetera, Cohen, & Holaska, 2011). Moreover, Lmo7 is anticipated to play significant roles in mature muscle and tendons in the adaptation to mechanical stress (Koch & Holaska, 2014).

Beta-catenin is a Wnt signaling transcription factor that directly binds to emerin via its APC-like domain (Markiewicz et al., 2006). Subsequently, emerin prevents the activity of β -catenin by inhibiting its accumulation in the nucleus. Remarkably, knockdown of β -catenin also led to a decrease in the expression levels of

emerin mRNA and its nuclear accumulation. This suggests that both emerin and β -catenin regulate each other's expression levels, localization, and activity (Tilgner, Wojciechowicz, Jahoda, Hutchison, & Markiewicz, 2009). In addition, Wnt signaling is vital for the maintenance and differentiation of myogenic progenitor cells (Brack, Conboy, Conboy, Shen, & Rando, 2008; Otto et al., 2008); this proposes that emerin binding to β -catenin is imperative for myogenic differentiation (Koch & Holaska, 2014).

BAF is key component of the nuclear lamina since it binds all LEM-domain proteins (de Oca, Shoemaker, Gucek, Cole, & Wilson, 2009). It is a member of two emerin-containing complexes; one of them is a regulatory complex harboring HDAC1 and HDAC3 (Holaska & Wilson, 2007), signifying that this complex suppresses chromatin at the NE. Moreover, decreased BAF expression and the subsequent improper localization of emerin to the cytoplasm leads to Nestor-Guillermo progeria syndrome (NGPS) (Cabanillas et al., 2011; Puente et al., 2011).

ii. Maintaining nuclear structure

Emerin is highly implicated in maintaining nuclear architecture. It was shown that emerin-null cells exhibit decreased elasticity and a more supple nuclear membrane (Lammerding et al., 2005). These structural defects may be responsible for the increased fragility observed in EDMD patient cells (A. Rowat, Lammerding, & Ipsen, 2006). Importantly, MKL1, as previously mentioned, accumulates in the nucleus upon mechanical stimulation to increase actin polymerization. This structural response is mediated by its interaction with emerin. Hence, if this interaction is lost, actin dynamics

and cellular integrity are jeopardized (Ho et al., 2013; Miralles, Posern, Zaromytidou, & Treisman, 2003; Mouilleron, Guettler, Langer, Treisman, & McDonald, 2008).

C. Lamins and oxidative stress

Several studies have shown that the stability and expression of lamins are changed in response to oxidative stress. Additionally, lamin expression is highly regulated by p53, pRb, and telomere functions that are chief regulators of cell cycle progression, apoptosis, and senescence (Rahman-Roblick et al., 2007; Shimi & Goldman, 2014). Progerin, a truncated form of lamin A, is also expressed during normal aging by telomere dysfunctions (Cao et al., 2011; Scaffidi & Misteli, 2006). In opposition, lamin B1 expression is significantly reduced during oncogenic stress, senescence, and DNA damage (Dreesen et al., 2013; Freund, Laberge, Demaria, & Campisi, 2012; Shimi et al., 2011). This downregulation during senescence is induced by the pRb–E2F pathway since *LMNB1* is downstream of it (Hallstrom, Mori, & Nevins, 2008). Importantly, lamins harbor amino acid residues that can be oxidized. Accordingly, elevated ROS levels during senescence were shown to lead to the oxidation of cysteine residues present on the lamin A tail domain inhibiting inter- and intramolecular disulfide bond formation (Pekovic et al., 2011). In agreement with this observation, A-type lamins are one of the most heavily phosphorylated proteins upon ERK1/2 activation (Finkel & Holbrook, 2000; Kosako et al., 2009; Lewis et al., 2000). Moreover, posttranslational farnesylation of lamin A is affected by oxidative stress; whereby prelamin A was shown to accumulate in old vascular smooth muscle cells (VSMCs) that feature less Zmpste24/FACE-1 levels in response to oxidative stress (Ragnauth et al., 2010). As for lamin B levels, cancer cells featured lamin B1

degradation upon their oxidization by ROS species (Chiarini, Whitfield, Pacchiana, Armato, & Dal Pra, 2008).

D. Laminopathies

1. Overview

To date, more than 450 mutations have been mapped only to *LMNA* and are linked to 14 laminopathic diseases (figure 4). Startlingly, only a few diseases have been associated with mutations in *LMNB1* and *LMNB2* which further proves the embryonic lethality of B-type mutations (Dutta, Bhattacharyya, & Sengupta, 2016; Schreiber & Kennedy, 2013). Some laminopathies result in deformed nuclei that lack integrity (Folker, Östlund, Luxton, Worman, & Gundersen, 2011; Worman, Ostlund, & Wang), while others result in stiffened ones (Dahl et al., 2006; Verstraeten, Ji, Cummings, Lee, & Lammerding, 2008). Both changes lead to poor responses to mechanical stress in load bearing tissues, mainly muscles (Dutta et al., 2016). Similarly, silencing components of the LINC complex also leads to nuclear deformities and altered responses to mechanical stress. This supports the faulty nucleocytoskeletal coupling and mechanotransduction cascades detected in cells with *LMNA* mutations (Zwerger et al., 2013).

Lamin A

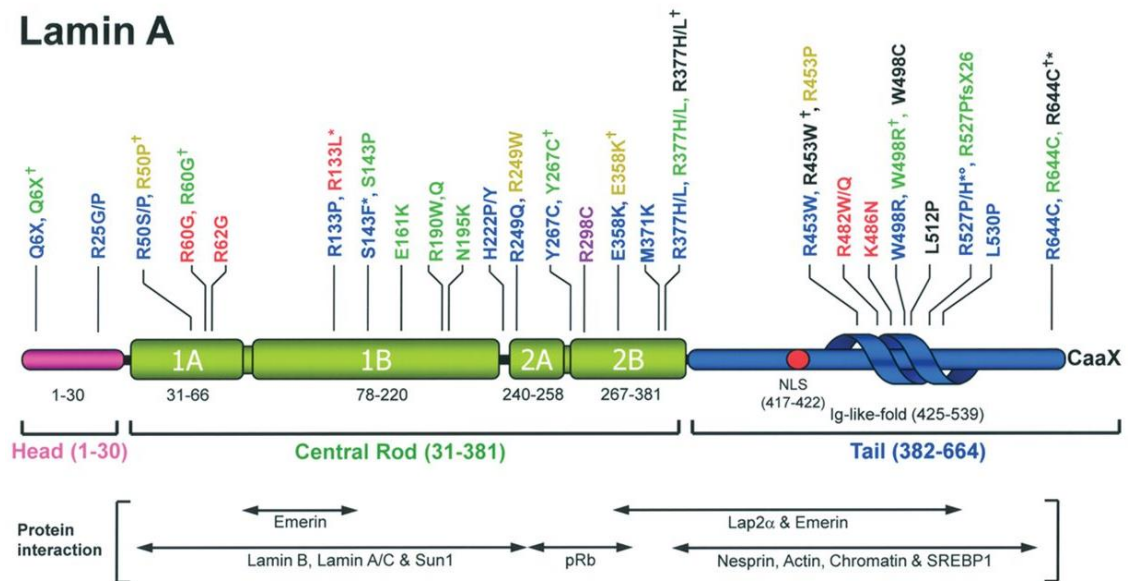


Figure 4: Distribution of mutations and laminopathies along Lamin A (Scharner, Gnocchi, Ellis, & Zammit, 2010). More than 500 mutations spread along the length of the *LMNA* gene with no correlation between the area mutated and the resulting disease phenotype.

2. Laminopathies affecting the muscular tissues

Emery-Dreifuss muscular dystrophy, dilated cardiomyopathy, limb girdle muscular dystrophy, and heart-hand syndrome are the phenotypic laminopathic manifestations in muscular tissues. However, only the first two diseases are of interest to this study.

a. Emery-Dreifuss muscular dystrophy 2

Autosomal dominant Emery-Dreifuss muscular dystrophy (EDMD2) was the first characterized myopathic phenotype (Gisèle Bonne et al., 1999; Maggi, Carboni, & Bernasconi, 2016). It is recognized by early ankle and spine contractures, muscle degeneration, scapulo-humero-peroneal weakness, conduction defects, and an increased risk of sudden cardiac attacks (Emery, 2000; Meune et al., 2006). Unlike EDMD2, X-linked EDMD (EDMD1) is caused by mutations in the *EMD* gene; its patients have a

lower risk of tachyarrhythmia and DCM (BÉCANE et al., 2000; Boriani et al., 2003; Pasotti et al., 2008). Mutations in *LMNA* gene are responsible for around 45% of the EDMD2 cases (Pagon et al., 2013; Pillers & Von Bergen, 2016) with an autosomal dominant inheritance pattern; though autosomal recessive inheritance has likewise been defined (G Bonne et al., 2000). Although patients with the X-linked or autosomal dominant forms of this disease are clinically similar; the latter individuals are more prone to lose the ability to walk by foot (Gorelick, Testai, Hankey, & Wardlaw, 2014).

b. Dilated cardiomyopathy

Dilated cardiomyopathy (DCM) is a heart muscle disease distinguished by a reduced systolic function accompanied by the dilation of the left or both ventricles. Yet, these abnormalities are manifested in the absence of abnormal loading conditions or coronary artery disease (CAD) (Dubowitz, 1977; Tesson et al., 2014). After hypertension and CAD, DCM is the 3rd leading cause of heart failure (HF) in the United States with remarkable morbidity and mortality rates (Maron et al., 2006). To date, more than 60 genes – mostly with an autosomal dominant inheritance pattern – have been linked with DCM (Taylor, Carniel, & Mestroni, 2006). Moreover, incomplete age-related penetrance is detected in the majority of DCM cases. Interestingly, it was testified that in under 20 years of age, 7% of *LMNA* mutation carriers show cardiac-defect phenotypes. This increases to 66% for ages between 20 and 39 years, 86% for ages between 40 and 59 years, and 100% for ages over 60 years (Pasotti et al., 2008). This disease, like other *LMNA*-related diseases, exhibits much variability, especially in the time of onset, rate of progression, and range of phenotypes (Tesson et al., 2014). In agreement with this, a single family displayed 3 different DCM phenotypes: pure DCM,

DCM with EDMD-like symptoms, and DCM with LGMD-like symptoms (Brodsky et al., 2000).

E. Hydrogen peroxide inducible clone-5

1. Overview

Hic-5 is a member of the paxillin protein family that acts as nuclear receptor coactivators lacking the methyltransferase activity (M. D. Heitzer & D. B. DeFranco, 2006; Kasai et al., 2003). Hic-5 also belongs to group III family of proteins that contain the LIM domain and are distinguished by their localization to both, FAs and the nucleus (Dawid, Breen, & Toyama, 1998). Within FA complexes, Hic-5 links several intracellular signaling molecules to membrane receptors, such as vinculin and FAK (Thomas, Hagel, & Turner, 1999). Recently, Hic-5 was associated with peroxisome proliferator-activated receptor gamma (PPAR γ), androgen receptor (AR), and glucocorticoid receptor (GR) (Yang, Guerrero, Hong, DeFranco, & Stallcup, 2000). Indeed, the alternative names of Hic-5, ARA55 (androgen receptor activator) and TGF β 1I1 (transforming growth factor β induced transcript 1) are due to its function as an AR coactivator and to being induced by TGF β , respectively. Furthermore, Hic-5 also interacts with and regulates other transcription factors, such as its upregulation of the activity of SP-1 and its inhibition of the transcriptional activity of Smad3 (Shibanuma, Kim - Kaneyama, Sato, & Nose, 2004; Wang, Song, Sponseller, & Danielpour, 2005).

2. *Hic-5* structure, isoforms, and tissue distribution

Hic-5 harbors a long intron between its N- and C- terminal domains suggesting that it has evolved from the merging of two dissimilar genes (Mashimo, Shibamura, Satoh, Chida, & Nose, 2000; Shibamura, Mori, & Nose, 2011). Its N-terminus harbors four highly conserved LD motifs (paxillin has five) that are rich in leucine and asparagine residues mediating *Hic-5*'s interactions with structural and regulatory proteins. These proteins in turn coordinate changes in the dynamics of actin, cytoskeleton, and gene expression (Shibamura et al., 2004). Whereas, the C-terminus of *Hic-5* has four LIM domains – each harboring two zinc fingers (just like paxillin) – that mediate protein-protein interactions involved in organ development, cytoskeleton organization, and cell lineage specification (Fujimoto et al., 1999) (figure 5).

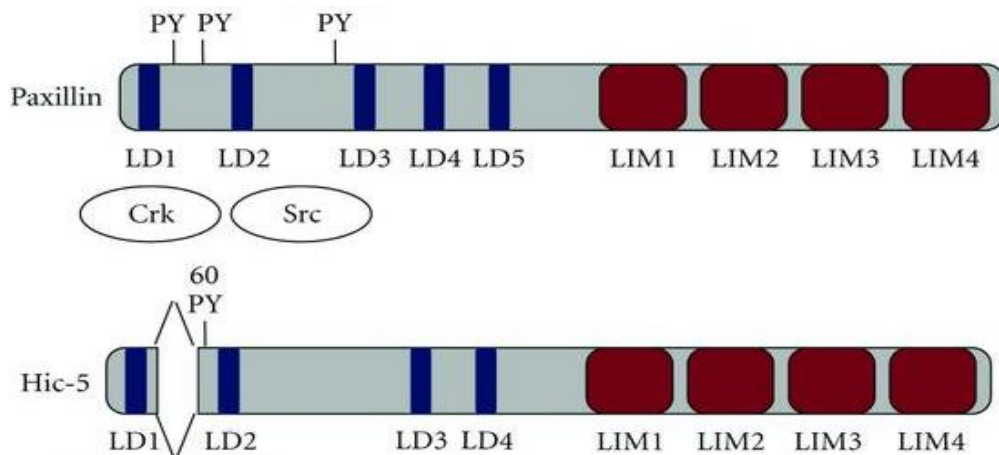


Figure 5: Comparison between the structures of paxillin and *Hic-5* (Schaller, 2001). Paxillin and *Hic-5* share extensive structure homology whereby they both have 4 LIM domains, yet *Hic-5* has 4 LD motifs while the former has 5.

The table below (table 1) summarizes the 10 major isoforms of *Hic-5* that result from alternative splicing. These isoforms are conserved among many species and are classified into either alpha or beta subfamilies according to differences in their LD

motifs. However, they retain identical LIM domains. In addition, the alpha isoform is more abundantly expressed and its 1st isoform has been chosen to be the 'canonical' sequence of this protein. Hence, all positional information in the table below are in comparison with it.

Isoform	Name	Length	Mass (Da)	Amino Acids Special Features
1	Alpha	461	50,101	Canonical sequence
2	Beta	444	48,228	1-17 missing
3	Alpha-B	483	51,988	1-43 different
4	Alpha-E	415	45,266	62-107 missing
5	Beta-G	402	44,059	1-59 missing, 60-82 different
6	Alpha-C	61	6,605	61 different, 62-461 missing
7	Beta-B/D	350	38,289	1-111 missing
8	Beta-C	44	4,732	1-17 & 62-461 missing, 61 different
9	Beta-E/F	399	43,798	1-62 missing, 63-138 different
10	Alpha-D	351	38,669	1-110 missing, 111-148 different

Information in this table are derived from: <http://www.uniprot.org/uniprot/O43294>

The restricted tissue distribution of Hic-5 and paxillin demonstrates a unique feature of these nuclear receptor coactivators. Immunohistochemistry (IHC) studies have revealed a selective expression of Hic-5 in smooth muscles and myoepithelial cells. Yet, unlike paxillin, it was not identified in epithelial cells, including the colon, stomach, skin, liver and mammary glands (Yuminamochi et al., 2003). Furthermore, Hic-5 and paxillin are expressed differentially within the same organ. For instance, in the prostate, Hic-5 is found in the stromal compartment while paxillin is in the epithelial

one (Li et al., 2000). This suggests that they act as cell type specific scaffold differences at discrete cellular compartments regulating diverse signaling pathways at sites proximal and distal to the starting signal (M. D. Heitzer & D. B. DeFranco, 2006).

3. *Hic-5* functions

a. Adaptor-like nuclear receptor co-activator

Hic-5 shuttles between FAs and the nucleus. In agreement, many studies have demonstrated its ability in regulating the expression of the *c-fos* and *p21^{CIP1}* genes (Kim-Kaneyama, Shibamura, & Nose, 2002; Shibamura et al., 2004). Yet, this regulation was not detected with paxillin. In the nucleus, hic-5 also serves as a scaffold difference for the formation of the transcriptional complex similar to that of integrin signaling at FAs (Shibamura et al., 2011). For example, in T47D breast cancer cells harboring an incorporated mouse mammary tumor virus (MMTV) promoter, hic-5 was shown to associate with *GR*, *p21*, and *c-fos* promoters. Yet, since hic-5 does not have HAT or methyltransferase activities, its effect on histones is most likely indirect through the recruitment of different chromatin modifying coactivators. In fact, hic-5 was shown to interact at glucocorticoid responsive promoters with translation initiation factor 2 (TIF-2), Ras-related C3 botulinum toxin substrate 3 (RAC3), CREB-binding protein (CBP), and p300 coactivators (M. Heitzer & D. DeFranco, 2006). In the same study, partial hic-5 ablation resulted in a decrease in GR transactivation and recruitment suggesting an important role of hic-5 in maintaining the assembly of coactivator complexes that are essential for an effective glucocorticoid-induced transcription (M. D. Heitzer & D. B. DeFranco, 2006).

Moreover, hic-5 and paxillin serve as adaptor molecules in the integrin complex and contribute to the regulation of integrin signaling. Accordingly, it was shown that hic-5 competes with paxillin and negatively regulates FAK (Nishiya, Tachibana, Shibamura, Mashimo, & Nose, 2001). Nevertheless, in most cases under normal conditions, cell growth and motility are barely affected by hic-5 expression. Hence, as long as a normal adhesion status is sustained, hic-5 seems to not be mandatory for a proper focal adhesions' status (Shibamura et al., 2011).

In addition, at nuclear receptor-responsive promoters, hic-5 associates with nuclear receptor co-repressor 1 (NCoR) complexes in the absence of glucocorticoids highlighting its ability to directly interact with transcription co-regulators, and not essentially through nuclear receptors. Given that, and the presence of Hic-5 on GR-responsive promoters, it is postulated that hic-5 may coordinate the release of corepressors and the recruitment of coactivators upon stimulation by glucocorticoids (M. Heitzer & D. DeFranco, 2006).

b. Response to oxidative stress signals

A recent study revealed that upon oxidative stimulants like H₂O₂, hic-5 localizes and accumulates in the nucleus; whereas other FA proteins and even paxillin stay in the cytoplasm. More precisely, Hic-5's C-terminus positively contributes to its nuclear localization, unlike its N-terminus that negatively contributes to this process by harboring an oxidative-sensitive nuclear export sequence (NES). Leptomycin B (LMB), an inhibitor of NES, causes the retaining of hic-5 in the nucleus. It was also demonstrated that the NES harbored by hic-5 comprises of a leucine-rich section and two cysteines residues. Dominant negative mutants also showed that hic-5 is involved in

expression of *c-fos* (downstream effector of the TF Jun family; normally expressed upon oxidative stress) after H₂O₂ treatment. Therefore, hic-5 has a novel feature of shuttling between FAs and the nucleus through an oxidant-sensitive NES, reconciling redox signaling to the nucleus (Pignatelli, Tumbarello, Schmidt, & Turner, 2012).

c. Response to TGF- β

Hic-5 was first characterized by its induction by both, H₂O₂ and TGF β (Fernandez et al., 2015; Shibamura, Mashimo, Kuroki, & Nose, 1994). NADPH oxidase (Nox4), an essential component of FAs, significantly reduces their number if depleted (Hilenski, Clempus, Quinn, Lambeth, & Griendling, 2004; Lyle et al., 2009). A recent study identified two of its downstream effectors, namely: *Hic-5* and *Hsp27*. Upon TGF β stimulation, PI3K and Smad3 expression increase, which allows for an increase in Nox4 expression through separate signaling pathways (Michaeloudes, Sukkar, Khorasani, Bhavsar, & Chung, 2011). This in turn stimulates an increase in the expression of both proteins – *Hic5* and *Hsp27* – and allows for their physical interaction that is crucial for the accurate localization of *Hic-5* to FAs. This step is functionally extremely relevant since it facilitates the increase in the TGF β -induced cell adhesion, strength, and migration (Fernandez et al., 2015).

On the other hand, epithelial-mesenchymal transition (EMT) is stimulated by TGF- β that up regulates expression levels of *Hic-5* promoting the induction of an invasive phenotype. *Hic-5* in turn stimulates the phosphorylation of Src which also phosphorylates *Hic-5*, creating a positive feedback loop. *Hic-5* also stimulates the induction of ROCK and p38 MAPK by RhoC and Rac1, respectively. These 2 pathways

are implemented in mediating matrix degradation and hence increased invasion (Pignatelli et al., 2012).

d. Myogenesis and muscle differentiation

A thorough analysis of the function and expression of Hic-5 in C₂C₁₂ myoblasts established that myoblasts express no less than 6 different Hic-5 isoforms, with Hic-5 α and Hic-5 β being the most dominant ones and distinctively expressed during myogenesis. Moreover, during differentiation, any induced changes (up- or down-regulation) in Hic-5 expression cause a significant increase in apoptosis. On the other hand, Death Associated LIM-Only Protein (DALP) is radically induced at the end of metamorphosis when intersegmental muscles are dedicated to die. Notably, DALP and Hic-5 share extensive similarity in structure and sequence and are both able to block differentiation and enhance cell death after the transfer of C₂C₁₂ into a differentiation medium (Z.-L. Gao, Deblis, Glenn, & Schwartz, 2007; Hu et al., 1999). In addition, ectopic expression of Hic-5 α allows for differentiation to occur; but this is not the case for either Hic-5 β or antisense Hic-5 that hinder myoblast fusion. Also, variations in Hic-5 expression restrict normal laminin dynamics and expression; while ectopic laminin can liberate the obstruction of myoblast differentiation and survival induced by Hic-5. All these Hic-5 effects were shown to be mediated via integrin signaling pathways (Z.-L. Gao et al., 2007).

e. Downstream effector of MKL1/SRF pathway

As previously mentioned, myocardin-related transcription factor A (MRTF-A; also known as MKL1) is a transcriptional cofactor that regulates the activity of SRF,

and hence regulating the expression of many contractile genes that are crucial for myofibroblast differentiation (Crider, Risinger, Haaksma, Howard, & Tomasek, 2011; Varney et al., 2016). TGF- β promotes Rho-A- and ROCK- dependent assembly of stress fibers leading to the nuclear import of MRTF-A. Subsequently, focal adhesion and contractile genes are induced (Small et al., 2010; Trembley, Velasquez, de Mesy Bentley, & Small, 2015). Hic-5 also docks at FAs and interacts with their proteins, such as focal adhesion kinase (FAK) and vinculin through its LIM domains (Nishiya, Shirai, Suzuki, & Nose, 2002). In addition, in cells that undergo cyclic stretching, Hic-5 translocates from its FA sites to stress fibers (Kim-Kaneyama et al., 2005; Yund, Hill, & Keller, 2009). Notably, when myofibroblasts with hypertrophic scars (HTS) were treated with Hic-5 siRNA, cell cycle progression was induced, and the production of TGF- β and type I collagen, and the expression of α -SMA were decreased suggesting a fundamental role for Hic-5 in myofibroblasts. Interestingly, *in vitro* normal human dermal fibroblasts (NHDFs), expression of TGF- β upon the induction of Hic-5 was found to occur prior to the induction of α -SMA (Dabiri, Tumbarello, Turner, & Van De Water, 2008a, 2008b; Mori et al., 2012) (figure 6). This expression is mechanosensitive and essential for the canonical and non-canonical pathways, namely SMAD3 and SRF-MRTF-A, respectively. Essentially, expression of Hic-5 was necessary for TGF- β to promote growth of stress fibers and the differentiation of myofibroblasts due to extracellular stiffness. This was also accompanied by the nuclear translocation of MRTF-A in a TGF- β dependent manner and the induction of α -SMA. These findings suggest that there exists a novel mutual regulation of the localization of MRTF-A by Hic-5; the latter's expression being regulated by the former defines a novel positive feed forward loop inducing the myofibroblast phenotype (Varney et al., 2016).

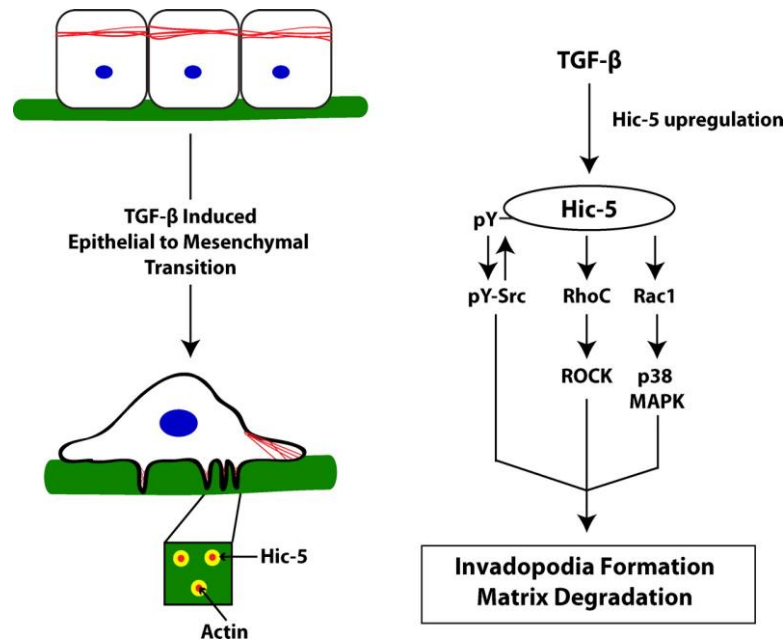


Figure 6: Pathways downstream of Hic-5 activation during EMT (Pignatelli et al., 2012). TGF- β acts upstream of Hic-5 that in turn activates several pathways that lead to the alteration of smooth muscle actin dynamics allowing for EMT to occur.

G. Gap in knowledge, study rationale, and hypothesis

Despite the arising interest in the laminopathic field, an important question still remains unanswered: How can mutations in the ubiquitously expressed *LMNA* gene cause a diverse array of tissue specific phenotypes? Many hypotheses have been proposed to explicate the tissue specific aspects of laminopathies, the two most important ones are the structural hypothesis and the gene regulation hypothesis. The structural hypothesis proposes that mutations in the *LMNA* gene weaken the lamina structure increasing nuclear fragility which ultimately leads – specifically in mechanically stressed tissues – to augmented cell death and disease progression (Broers, Hutchison, & Ramaekers, 2004; Burke & Stewart, 2002; Hutchison & Worman, 2004). However, in spite of the fact that *LMNA* mutations disrupt nuclear stability, a direct connection between the nuclear structural defects and the diverse dreadful muscular phenotypes witnessed in laminopathies has not been recognized.

Hereafter, our study is interested in the gene regulation theory that proposes that since lamins are implicated in the regulation of multiple signaling pathways, then the weakened lamina structure observed in laminopathies would lead to altered gene regulation and faulty interactions with tissue specific TFs underlying the variant disease phenotypes (Ho & Lammerding, 2012). We therefore rationalize that there exists a deregulation in Hic-5 expression and function in lamin A/C and emerin – associated myopathies.

H. Objective of the study and specific aims

Our long-term objective is to test whether the expression level of Hic-5 is deregulated in myopathic laminopathies and whether it is implicated in their pathogenesis. Hereafter, our specific aims are:

Specific Aim 1: To validate whether *hic-5* is differentially expressed at the transcriptional level in mouse embryo fibroblasts MEFs derived from mouse models of myopathic laminopathies in comparison to wild-type controls cultured *in vitro* under baseline and oxidative stress conditions.

Specific Aim 2: To assess whether *hic-5* is differentially expressed at the protein level in MEFs derived from mouse models of myopathic laminopathies in comparison to wild-type controls cultured *in vitro* under baseline and oxidative stress conditions.

Specific Aim 3: To investigate putative modulations in *hic-5* expression and distribution in MEFs derived from mouse models of myopathic laminopathies in comparison to their heterozygote littermates and wild-type controls cultured *in vitro* under baseline and oxidative stress conditions.

I. Significance of the study

Investigating the effects of oxidative stress in specific lamin A/C mutations on the expression and distribution patterns of the mechanosensitive focal adhesion adaptor protein Hic-5 will provide new perceptions into the molecular mechanisms underlying the tissue-specific phenotypes detected in muscular laminopathies. Finding that Hic-5 is differentially implicated in these diseases opens the window for further investigations of its down- and upstream effector proteins so that further conformational *in vitro* and *in vivo* studies provide insights into possible therapeutic targets that could alleviate or demolish the harsh pathogenic phenotypes of muscular laminopathies.

CHAPTER II

MATERIALS AND METHODS

A. Cell Lines

Since the heart is composed of around 60% fibroblasts and 40% muscle cells necessitating the existence of crosstalk between the two cell types, and the fact that in the laminopathies field, fibroblasts are frequently used as surrogate models for proof of principle to determine the physiological doses of any treatment before moving to C₂C₁₂ muscle cells that are associated with technical hurdles and high costs, all experiments in this study were performed using immortalized mouse embryo fibroblast (MEF) lines for preliminary testing of our hypotheses. Three mutant models (to be discussed below) versus their wild-type *Lmna*^{+/+} MEF controls were kindly provided to our lab by Dr. Jan Lammerding (Cornell, NY) to be used in this study.

Lmna^{-/-} mouse models were generated by removing exons 8 to part of exon 11 of the *Lmna* gene. Loss of full length transcripts and lamin A/C proteins was then confirmed by Northern Blot and Western Blot analysis, respectively (Sullivan et al., 1999). Hence, these MEFs represent a surrogate model of the autosomal dominant type of EDMD2. At birth, these mice resemble their wild-type littermates but their postnatal growth is underdeveloped and characterized by the onset of muscular dystrophy. Notably, loss of lamin A/C proteins did not affect the distribution of lamins B1 and B2. However, the integrity of the NE was compromised and complemented by mislocalization of emerin from it. Moreover, these cells had an improper nuclear morphology that was often highly elongated in comparison to the roughly ovoid nuclei

of their WT controls (Lammerding et al., 2004; Lombardi & Lammerding, 2011; Sullivan et al., 1999).

Lmna^{N195K/N195K} MEFs represent a knock out/knock in mouse model with a missense mutation in the *Lmna* gene causing a substitution of asparagine by lysine at amino acid 195 (Mounkes, Kozlov, Rottman, & Stewart, 2005). They represent a surrogate model of the DCM phenotype. Anomalies in the NE of MEFs obtained from these mice were observed accompanied by nuclear herniations which are a result of both, the clustering of nuclear pore complexes and the loss of heterochromatin from the nuclear periphery. Moreover, their nuclei were elongated as opposed to their wild-type controls (Lammerding et al., 2004; Lombardi & Lammerding, 2011; A. C. Rowat et al., 2013).

Emd^{-Y} mouse model was produced by the directed deletion of exons 2-6 in the X-linked *Emd* gene. Whole loss of the *Emd* transcript and emerin protein was verified by Northern Blot, Western Blot, and immunofluorescence staining. Hence, they represent a surrogate model of the X-linked recessive EDMD phenotype. The nuclei of MEFs obtained from this model were visibly normal without any morphological modifications or changes in the distribution of other NE proteins (Melcon et al., 2006).

1. Cell Culture

Adherent MEF cells were propagated in tissue culture using Dulbecco's Modified Eagle's Medium DMEM-AQ media (Cat.# D0819, Sigma-Aldrich), complemented with 1% penicillin-streptomycin (Cat.# DE17-602E, Lonza), 10% Fetal bovine serum (Cat.# F9665, Sigma-Aldrich), and 1% sodium pyruvate (Cat.# S8636, Sigma-Aldrich). When the cells reached 80-100% confluence, they were washed once

with 5ml of 1X Phosphate Buffered Saline without Ca and Mg (PBS) (Cat.# 17-517Q, Lonza). Then, 1.5ml of 1X Trypsin (Cat.# , Lonza) were added to detach the cells from the plate after an incubation at 37°C and 5% CO₂ for 5-7min. Afterwards, cells were re-suspended in 6.5ml of the DMEM-AQ complete media and centrifuged at 600xg at 4°C for 5min. The cell pellet was then re-suspended in 1ml of the complete media. Consequently, the desired volume of cells – according to split ratio – was pipetted into a new 10cm plate pre-filled with 10ml of the complete growth medium.

2. Cell Count

Trypan blue vital exclusion stain was employed to precisely determine the number of living cells in a 10cm plate. The counting was done post the resuspension of the cell pellet in 1ml of the complete DMEM AQ medium, whereby a sample of the cells was taken and diluted by 1:10 for counting using a hemocytometer. Then, a suitable volume of the cells (depending on seeding density) was taken and mixed with its complementary volume of complete media.

B. RNA Extraction

RNA samples were taken from *Lmna*^{+/+}, *Lmna*^{-/-}, *Lmna*^{N195K/N195K}, *Emd*^{t/Y} MEFs under the following conditions:

1. Baseline Conditions

All four types of MEFs were seeded in 6cm plates at 13x10⁴ cells/ml in the complete DMEM AQ media until they reached 100% confluence. Then, they were washed once with PBS(1X), and RNA was extracted using the TRI Reagent (TRIzol,

Cat.# T9424, Sigma-Aldrich) according to the protocol of the manufacturer.

Subsequently, the extracted RNA samples were stored at -70°C to be later quantified and assessed for purity using the Nanodrop Spectrophotometer (Thermonanodrop 2000C, Central Research Science Lab (CRSL) facility, AUB).

2. H_2O_2 -Induced Oxidative Stress Conditions

$Lmna^{+/+}$, Emd^{-Y} , and $Lmna^{N195K/N195K}$ MEFs were seeded in 12 well plates at 6.5×10^4 cells/ml while $Lmna^{-/-}$ MEFs were seeded also in 12 well plates but at 8×10^4 cells/ml in the complete media till they reach 100% confluence. Then, they were treated with either 0.1 or 0.5 μM of H_2O_2 (Hydrogen Peroxide Solution-34.5-36.5%, Cat.# 18304-L, Sigma-Aldrich) for 5, 15, 30 and 60min. The latter was prepared fresh every time by serial dilutions of a sample of the stock (15.14mol/L) into 1mol/L, 0.1mol/L, 1mmol/L, and into 50 $\mu\text{mol/L}$. From the final dilution, 4 μL and 20 μL were added for the 0.1 μM and 0.5 μM treatments, respectively. These concentrations were formerly optimized by Ms. Lara Kamand to be able stress the MEF cells without triggering apoptosis (Kamand, 2012). After these treatments, the cells were washed once with PBS (1X) and RNA extraction from $Lmna^{+/+}$ MEFs was done using the RNeasy Kit (QUAIGEN) and that of $Lmna^{N195K/N195K}$, Emd^{-Y} , and $Lmna^{-/-}$ MEFs using TRI Reagent (TRIzol, Cat.# T9424, Sigma-Aldrich) according to the protocol of the manufacturer. As controls, untreated cells equivalent to each time point were used.

C. Reverse Transcription

Half a μg or 1 μg of every RNA sample was reverse transcribed into cDNA using the iScript cDNA Synthesis Kit (Cat.# 170-8891, Bio-Rad). In short, each sample

was mixed with 4µl of the 5X iScript Reaction Mix, 1µl of the iScript reverse transcriptase enzyme, and a specific volume of nuclease free sterile water (Amresco) to reach total volume of 20µl in a pre-cooled RNase free PCR tube using barrier tips. Then, reverse transcription was completed in the DNA engine machine (Peltier thermal cyclers, Bio-Rad) whereby annealing was done for 5min at 25°C, extension for 30min at 42°C, and finally inactivation of the iScript reverse transcriptase for 5min at 85°C. All cDNA samples were stored at -20°C.

D. Quantitative Real-Time PCR

Real-Time PCR quantification was performed using the iQ SYBR Green Supermix (Cat.# S4438, Sigma-Aldrich) with specific primer pairs for each gene (table 2) that were formerly certified and computationally derived from the MGH/Harvard Medical School Primer Bank Database (www.pga.mgh.harvard.edu/primerbank).

Table 2: A list showing the sequences of the forward and the reverse primers that were used to quantify the transcriptional expression of <i>Hic-5</i> and the <i>18S</i> reference genes by Real-Time PCR.	
Gene (species)	Primer Sequences
<i>Hic-5</i> (mouse)	Forward Primer: 5'-TACAGCACGGTATGCAAGCC-3' Reverse Primer: 5'-GCAACCGATCTAGCTCACAGAG-3'
<i>18S</i> (mouse)	Forward Primer: 5'-TCAAGAACGAAAGTCGGAGG-3' Reverse Primer: 5'-GGACATCTAAGG GCATCACA-3'

Every cDNA sample was diluted by 1:20 by adding 5µl of cDNA and 95µl of nuclease free sterile water into a pre-cooled sterile 1.5mL microfuge tube using barrier tips. Then, 4µl of the diluted cDNA was added to 6.5µL of the nuclease free sterile water, 1µL of the 1:10 diluted forward primer, 1µL of the 1:10 diluted reverse primer, and 12.5µL of the Supermix to reach a final volume of 25µL. Each sample was prepared

in duplicates on ice and its quantification was performed using the Real-Time PCR machine (c-1000 Touch thermal cycler, Bio-Rad, CRSL facility, AUB). The protocol was made of the following steps: 50°C for 2min for initial heating, 95°C for 10min to open the double-stranded DNA helix, 60°C for 1min to ensure proper annealing, and finally 72°C for 30sec for extension. This process was repeated for 40 cycles with a final extension step for 10min at 72°C. Experimental results were analyzed using the Bio-Rad CFX Manager Software.

E. Protein extraction, SDS-PAGE & western blot analysis

1. Protein extraction

Protein isolates were extracted from *Lmna*^{+/+}, *Lmna*^{-/-}, *Lmna*^{N195K/N195K}, *Emd*^{-Y} MEFs under the following conditions:

a. Baseline conditions:

Lmna^{+/+}, *Lmna*^{-/-}, *Lmna*^{N195K/N195K}, *Emd*^{-Y} MEFs were seeded in 6cc plates at 13x10⁴ cells/ml in DMEM AQ complete media to reach 100% confluence. Then, they were washed twice with 1.5mL pre-cooled PBS (1X), lysed using 150µL RIPA lysis buffer (Cat.# R-0278, Sigma-Aldrich) freshly complemented with 1:1000 Protease Inhibitor Cocktail (Cat.# P-8340, Sigma-Aldrich), and incubated for 20min in the cold room ProBlot™ Rocker. Subsequently, lysates were lodged off the plates using micropipette tips and transferred into pre-cooled sterile microfuge tubes to be centrifuged at 12000xg, 4°C for 10min. After that, supernatants holding the protein extracts were transferred to other sterile precooled microfuge tubes and stored at -20°C.

b. H₂O₂-induced oxidative stress conditions

All MEFs were seeded in 12 well plates at 6.5×10^4 cells/mL in the complete media till they reach 100% confluence. Then they were treated with 0.1 or 0.5 μ M H₂O₂ for 5, 15, 30 and 60min. Next, they were washed twice with 1mL pre-cooled PBS (1X), lysed using 80 μ L RIPA lysis buffer freshly supplemented with 1:1000 Protease Inhibitor Cocktail, and processed as mentioned above.

2. *Sample protein quantification*

Protein quantification was done in 96 well plates. The first two lanes were used for standardization using specific dilutions of 1mg/ml of BSA (Bovine Serum Albumin, Cat.# 0332, Amresco) in deionized distilled water (ddH₂O). The standards were prepared in duplicates with the following BSA content: 0.0, 2.0, 4.0, 6.0, 8.0, and 10.0 μ g. Then, 5 μ l of each sample was placed in duplicates in the subsequent lanes. Afterwards, 200 μ l of the Optiblot Bradford Reagent (Cat.# ab119216, Abcam) was added to each well and measurement of protein contents was performed using the SpectraMax ascent software (Multiskan EX, Thermo lab Systems).

3. *SDS-PAGE: Sodium dodecyl sulfate-polyacrylamide gel electrophoresis*

a. Casting and running the gel

Protein isolates were resolved by a 4% Tris-HCl. Resolving and stacking gels were casted using short plates and 1.5mm integrated spacers. To prepare a 1.5mm thick lower gel, 3.2ml of 30% Acrylamide (Cat.# 161-0158, Bio-Rad) were mixed with 2ml of 1.5M Tris-HCl pH 8.8 (Cat.# 161-0798, Bio-Rad) and 2.8ml of deionized distilled water. Then 140 μ l of APS (Ammonium Persulfate, Cat.# 161-0700, Bio-Rad) and 20 μ l

of TEMED (Tetramethylethylenediamine, Cat.# 0761, Ultra-pure grade, Amresco) were added to the mixture, simultaneously. Then, the latter was poured till the lower green mark of the casting frame, directly covered with a top layer of isobutanol, and left for 30min to polymerize. Likewise, a 1.5mm thick upper gel was prepared by adding 750 μ l of 30% Acrylamide/Bis to 1250 μ l of 0.5M Tris-HCl pH 6.8 (Cat.# 161-0799, Bio-Rad) and 3ml of deionized distilled water. Afterwards, 140 μ l of APS and 20 μ l of TEMED were added simultaneously to the previous mixture, and the stacking gel solution was emptied between the glass plates after decanting the formerly added isobutanol. The comb was then seated between the glass plates, and the upper gel was left to polymerize for 10min. On the other hand, 1X running buffer was prepared by dissolving 14.4g of glycine (Cat.# 161-0724, Bio-Rad), 2.5g of Tris-base (Cat.# 161-0719, Bio-Rad), and 1g of SDS (Sodium Dodecyl Sulfate, Cat.# 161-0302, Bio-Rad) in 1L of deionized distilled. When solidified, the casted gels were positioned in the clamping frame of the running chamber with the short plate facing interiorly, and the chamber was filled with 1X running buffer. The combs were then removed slowly.

b. Preparing and loading the samples

Samples of 40 μ g of protein were prepared by adding an appropriate volume of the protein isolates, deionized distilled water, and 5X loading buffer (glycerol, SDS, 0.5M Tris-HCl pH 6.8, and dashes of bromophenol blue) freshly supplemented with 10% β -mercaptoethanol. Then, they were denatured at 95°C for 5min in a thermobloc machine and immediately placed on ice to be loaded afterwards to the bottom of the wells. 10 μ l of Precision Plus Protein standard (Cat.# 161-0373, Bio-Rad) was used as a molecular weight marker. The electrophoretic cell was then enclosed with its lid; and

the SDS-PAGE was run at 200V for 45min with ice-buckets surrounding the running chamber.

c. Protein transfer from gel to blot

Post gel-migration, the proteins were transferred from the gel onto a polyvinylidene fluoride (PVDF) transfer membrane (Immuno-Blot™ PVDF Membrane, Cat.# 162-0177, Bio-Rad) that was freshly activated by 100% methanol (Sigma-Aldrich) for 1min and then incubated in cold transfer buffer (1X). The latter was prepared the same as the running buffer; however, instead of the addition of SDS, 200mL of methanol were added to reach a concentration of 20%. Two sponges, two blotting papers, and the gel which was released from its frame were also soaked in the transfer buffer; the rest was poured into the running chamber. The gel-membrane sandwich was then assembled in this order: white cassette, sponge, blotting paper, PVDF membrane, gel, blotting paper, sponge, black cassette. Next, the sandwich was positioned in the transfer unit that was covered in ice. The transfer was then set at 100V for 1.25hrs.

d. Membrane blocking, washing & antibody incubations

Each membrane was incubated at room temperature on a ProBlot™ Rockerat 60rpm for 1hr in 25ml of 5% non-fat dry milk (Regilait) in washing buffer (0.1% PBS-T) to block any non-specific binding sites. The washing buffer was prepared by mixing 100mL of 10X non-sterile PBS without Ca and Mg, 1mL of Tween20 (Polyoxyethylene sorbitol ester, Cat.# P1379, Sigma-Aldrich), and 900mL of deionized distilled water. Afterwards, each membrane was incubated with the Hic-5 primary antibody (H-75, sc-

28748, Santa Cruz) diluted at 1:200 in 5ml of 5% non-fat dry milk in washing buffer at 4°C on a ProBlot™ Rocker 25 at 60rpm overnight. The next day, the membranes were washed for 10min three times in 20ml of the washing buffer at room temperature on a ProBlot™ Rocker 25 at 90 rpm. They were then incubated with a Horseradish peroxidase (HRP)-conjugated secondary antibody, namely goat anti rabbit IgG, 0.8µg/µl, used at 1:2500 (attained from Jackson Immunoresearch and Goat Anti-mouse IgG H&L) provided at 1mg/ml (ab97023, Abcam). This incubation was done in 5ml of 5% non-fat dry milk in washing buffer for 1hr at room temperature on a ProBlot™ Rocker 25 at 60 rpm. Afterwards, the membranes were washed for 5min three times in 20ml washing buffer.

e. X-ray film imaging of western blots

One ml of each of the Reagents A (ab65628) and B (ab65629) that belong to the Western Lightening Chemiluminescence Reagent (ECL Western Blotting Substrate Kit, Abcam) were added to the membrane for 1min. The latter was then transferred to a cassette (Spectroline Monotec Cassette, Spectronics Corp.) and covered with a plastic pouch. The signal was detected by exposing the membranes to X-ray films (AGFA) which were then processed in the XOMAT X-ray film processor (Optimax) in a dark room. Exposure times were primary antibody- and experiment-dependent.

f. Membrane stripping & re-probing with a different primary antibody

Membranes were stripped at room temperature for 45min using 15mL of 0.1M sodium hydroxide (NaOH) made by diluting 1M NaOH in deionized distilled water. Then they were washed for a few minutes with 10mL of the washing buffer and blocked

in 20mL of 5% non-fat dry milk prepared in 0.1% PBS-T at room temperature on a ProBlot™ Rocker 25 at 60rpm for 1hr. Afterwards, they were incubated with 3mL of rabbit polyclonal IgG provided at 200µg/mL of GAPDH primary antibody (FL-335- sc-25778, Santa Cruz Inc.) for normalization at a dilution of 1:200 in 5% non-fat dry milk in washing buffer on a ProBlot™ Rocker 25 at 60 rpm for 1hr. The steps that followed were exactly like the ones mentioned previously.

g. Western blots densitometry analysis

Protein expression levels were computed by densitometry analysis standardized to GAPDH using Image J 1.49 free Java image processing software (downloaded from: <http://imagej.nih.gov/ij/download.html>). The developed X-ray films were scanned on a flatbed scanner and saved in the .tif format at 1200 dpi. Then using Image J software, the scanned films were converted to an 8-bit type gray-scale image. Densitometry was then performed according to the protocol of the software resulting in peak measurements (corresponding to each protein band for a single isoform or the total protein pool) as a percent of the total size of the all the measured peaks. Afterwards, results were pasted into an Excel spreadsheet and the relative density of the peaks was computed in comparison to a standard (WT MEFs for baseline conditions and untreated MEFs for oxidative stress conditions) by dividing the percent value of every lane by that of the standard one. These quotients were then adjusted to the relative density of GAPDH by dividing each value of the former to the corresponding value of the latter.

F. Immunofluorescence staining

MEF cells were seeded in 6 well plates at 13×10^4 cells/mL using 2mL of the complete DMEM AQ media per well on square cover glass slips (Corning) that are 22 x 22 mm wide and 0.17-0.25mm thick to reach 100% confluence. Afterwards for baseline conditions, the cells were washed twice for 5min in 2mL of 1X PBS. However for oxidative stress conditions, prior to the washes, cells were treated just like mentioned previously (two 6-well plates were needed for each repeat). Then, the cells were fixed at room temperature for 20min in 2mL 4% PFA that was freshly prepared by diluting a 16% PFA solution (Paraformaldehyde, Cat.# 15710, Electron Microscopy Sciences) in 1X PBS. Next, cells were rinsed for 5min 2 times in 2mL of 1X PBS and permeabilized at room temperature for 10min with 1.5mL of 0.2% Triton X-100 that was prepared by diluting 10% Triton-X in 1X PBS. The latter was prepared by diluting Triton® X-100 (t-Octylphenoxy polyethoxyethanol, Cat.# T8787, Sigma-Aldrich) in 1X PBS. Subsequently, cells were washed 2 times in 2mL of 1X PBS as stated previously and blocked for 2hrs at room temperature in 2ml of 2% BSA that was prepared by diluting a stock of 10% BSA in 1X PBS stored at -20°C . After that, the blocking media was removed from the wells and they were washed once for 5min in 2mL of 1X PBS. The coverslips were next flipped on a dampened tray covered by a piece of parafilm onto 200 μL of the Hic-5 primary antibody diluted at 1:500 in 1X PBS at 4°C overnight. Following that, coverslips were returned to the plates and washed for 5min 2 times in 2mL of 1X PBS. Then, cells were incubated at room temperature for 1hr in 200 μL prepared at 1:200 in 1X PBS of the Donkey Anti Rabbit Alexa Fluor® 488 (Jackson ImmunoResearch) provided at 1.5 $\mu\text{g}/\mu\text{L}$. Cells were next washed 2 times like before. Secondary only incubated cells were used as negative controls. Lastly, the coverslips

were mounted using 1 drop of the UltraCruz™ Hard-set Mounting Medium given as a 10mL solution containing 1.5µg/ml of 4',6-diamidino-2-phenylindole (DAPI) on clean glass slides. The edges of the coverslips were sealed with 2 coats of transparent nail polish. Finally, the slides were stored in a box at 4⁰C and were imaged 2-3 days afterwards.

G. Microscopic imaging

Image attainment was done using the Upright Fluorescence Microscope (Leica Suite X, CRSL facility) at 20X objective magnification with 3-5 frames per slide. Cells stained for Alexa 488 fluorophore were examined using the 580nm fluorescence filter and that of DAPI were examined with the 440 nm fluorescence filter using one exposure time point for each slide.

H. Statistical analysis

In all the experiments, data were expressed as mean \pm standard error of the mean (SEM) derived from 3-4 independent experiments per group (and for Real-Time PCR in duplicates as well). Statistical analysis was then done using Microsoft Excel Program and IBM SPSS Statistics 20 using two-tailed student t-test for comparing between two groups, or one-way ANOVA and the 2-sided Dunnett or Tukey tests for comparing several groups. Results were considered significantly different at values of $P \leq 0.05$, with the symbols □*' for $P \leq 0.05$, □**' for $P \leq 0.01$ and □***' for $P \leq 0.001$.

CHAPTER III

RESULTS

A. Specific Aim 1: To validate whether *hic-5* is differentially expressed at the transcriptional level in mouse embryo fibroblasts (MEFs) derived from mouse models of myopathic laminopathies in comparison to wild-type controls cultured *in vitro* under baseline and oxidative stress conditions.

1. Under baseline conditions, *hic-5* normalized to *18S* increases in transcript levels in the *Lmna*^{-/-} MEFs and *Emd*^{-Y} MEFs with respect to their wild type controls and to *Lmna*^{N195K/N195K} MEFs. This increase is statistically significant in the former and insignificant in the latter.

To determine the transcriptional expression levels of *hic-5* in the four MEF panels (*Lmna*^{+/+}, *Lmna*^{-/-}, *Lmna*^{N195K/N195K}, and *Emd*^{-Y}) under baseline conditions, their cells were seeded to ensure 100% confluence. Then, quantitative Real-Time PCR (qRT-PCR) experiments were done following RNA extraction and reverse transcription. Under baseline conditions, Real-Time PCR quantification data show that *hic-5* normalized to the transcriptional levels of *18S* reference gene in *Lmna*^{-/-} MEFs significantly increase by 1.3-fold difference (± 0.1) and 1.7-fold difference (± 0.1) with respect to the control *Lmna*^{+/+} MEFs (P -value <0.05) and *Lmna*^{N195K/N195K} MEFs (P -value <0.01), respectively. *Emd*^{-Y} MEFs show a similar – yet statistically insignificant – increasing pattern of *hic-5* normalized *18S* of 1.0-fold difference (± 0.1) and 1.3-fold difference (± 0.1) with respect to *Lmna*^{+/+} and *Lmna*^{N195K/N195K} MEFs (P -value >0.05 for both), respectively. On the other hand, *hic-5* normalized *18S* transcript levels are

insignificantly less in $Lmna^{N195K/N195K}$ MEFs by 0.4-fold difference (± 0.1) with respect to the control $Lmna^{+/+}$ MEFs ($P\text{-value} > 0.05$). Data signify mean fold difference \pm SEM of three independent repeats, each performed in duplicates (figure 7).

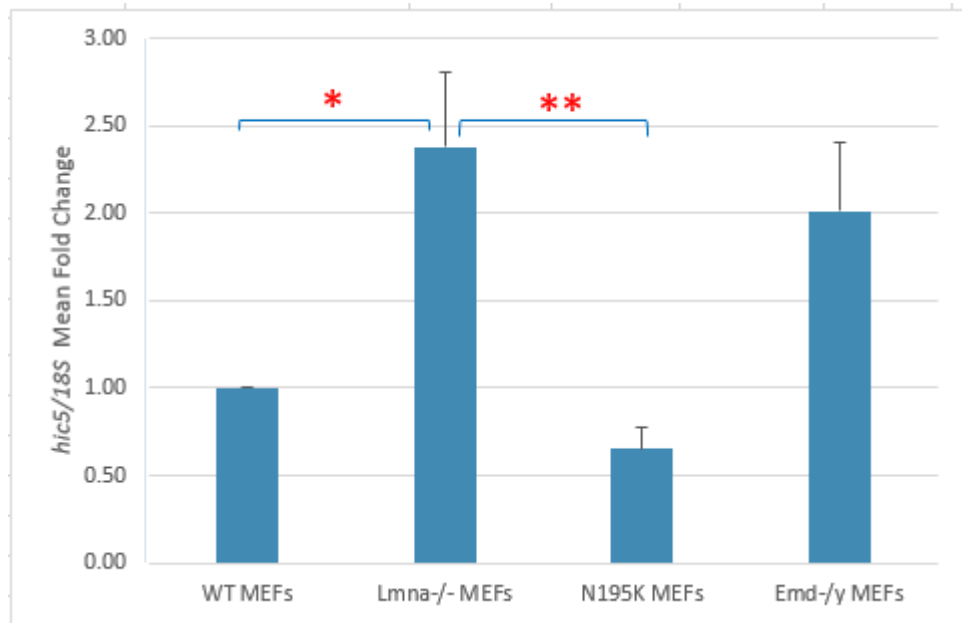


Figure 7: Mean fold difference change in *hic-5* transcript expression in the four MEF cell lines ($Lmna^{+/+}$, $Lmna^{-/-}$, $Lmna^{N195K/N195K}$, and $Emd^{-/Y}$) at baseline conditions. Real-Time PCR quantification data suggest that the *hic-5* transcript expression normalized to that of the *18S* reference gene is down-regulated in $Lmna^{N195K/N195K}$ MEFs but upregulated in $Lmna^{-/-}$ and $Emd^{-/Y}$ MEFs with respect to WT MEFs. Data represent mean fold difference \pm SEM in comparison to WT controls derived from 3 independent experiments; each performed in duplicates. Results were checked for statistical significance by one-way ANOVA and t-test. One asterisk represents a statistical significance ($P < 0.05$). Two asterisks represent a statistical significance ($P < 0.01$).

2. In WT ($Lmna^{+/+}$) MEFs, *hic-5* normalized to 18S significantly decreases in transcript levels 15min post 0.1 μ M and 0.5 μ M treatments with H_2O_2 with respect to their untreated controls.

To quantify the response of *hic-5* to H_2O_2 -induced oxidative stress in the four MEF panels, $Lmna^{+/+}$, $Lmna^{-/-}$, $Lmna^{N195K/N195K}$, and $Emd^{-/Y}$ MEFs were seeded to reach full confluence and then exposed to 0.1 μ M and 0.5 μ M of H_2O_2 for 5, 15, 30 and 60min.

RNA extraction, cDNA synthesis, and qPCR assessment were then performed on each cell line. Real-Time PCR quantification data suggest that *hic-5* normalized to the transcriptional levels of *18S* in *Lmna*^{+/+} MEFs significantly decrease by 0.2-fold difference (± 0.1) and 0.25-fold difference (± 0.1) with respect to their untreated controls (P -value < 0.05 for both) 15min post treatment with 0.1 μ M and 0.5 μ M of H₂O₂, respectively. A similar – yet statistically insignificant decrease – was observed 60min post both treatments by 0.4-fold difference (± 0.1) and 0.25-fold difference (± 0.1) with respect to their untreated controls, respectively (P -value > 0.05 for both). On the other hand, *hic-5* normalized to *18S* levels remain almost unchanged directly and 30min post both treatments. Data signify mean fold difference \pm SEM of three independent repeats, each performed in duplicates (figure 8).

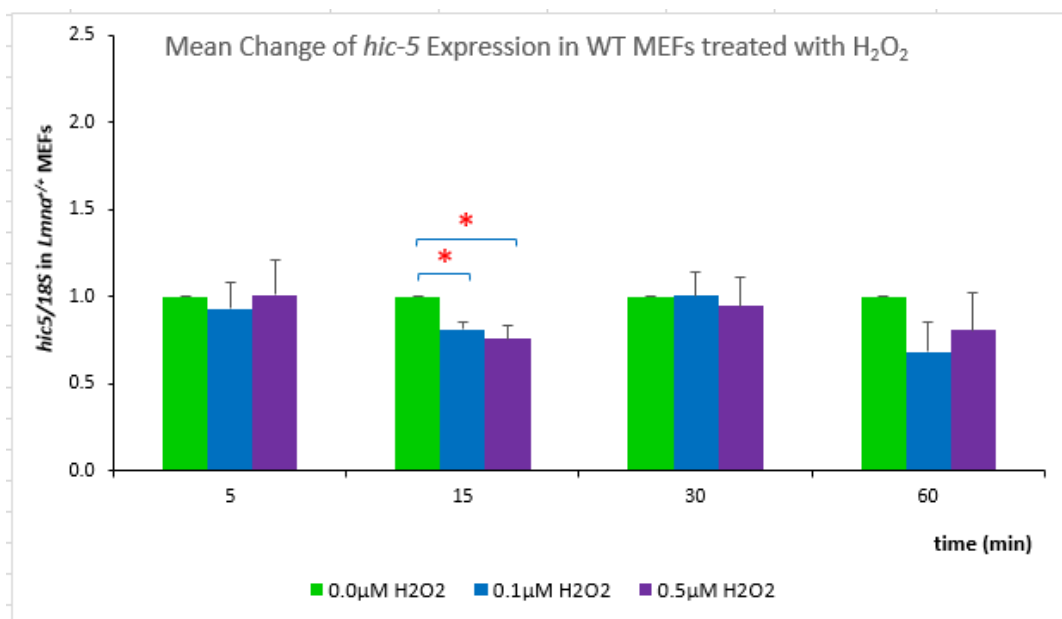


Figure 8: Mean fold difference change in *hic-5* transcript expression in *Lmna*^{+/+} MEF cells cultured at 100% confluence under 0.1 μ M or 0.5 μ M of H₂O₂–induced oxidative stress conditions for 5, 15, 30, and 60min. Data from Real-Time PCR quantification designate early and late reductions in transcript expression of *hic-5* normalized to that of *18S* reference gene in comparison to their untreated controls (0.0 μ M H₂O₂). Data represent mean fold difference change \pm SEM derived from 3 independent experiments; each performed in duplicates. Results were checked for statistical significance by one-way ANOVA. One asterisk represents a statistical significance ($P < 0.05$).

3. In *Lmna*^{-/-} MEFs, *hic-5* normalized to *18S* increases directly (statistically significant) and *1hr* (statistically insignificant) after 0.5 μ M treatment with H_2O_2 with respect to their untreated controls. Whereas, 30min post treatment with 0.1 μ M H_2O_2 , these lamin knockout MEFs demonstrate an early-late increase in *hic-5* normalized to *18S* with respect to their untreated controls.

Real-Time PCR quantification data upon treatment with 0.5 μ M of H_2O_2 show that levels of *hic-5* normalized to *18S* increase significantly and immediately in *Lmna*^{-/-} MEFs by 0.9-fold difference (± 0.2) with respect to their untreated controls (P -value < 0.05). Similar increases of 0.2-fold difference (± 0.1) and 1.2-fold difference (± 0.1) are observed 15min and 60min after this treatment with respect to their untreated controls. Yet, they are statistically insignificant with a P -value > 0.05 for both. On the other hand, upon treating these MEFs with 0.1 μ M of H_2O_2 , no alterations in *hic-5* normalized to *18S* transcriptional levels are observed except after 30min whereby it significantly increases by 0.4-fold difference (± 0.1) with respect to the untreated controls (P -value < 0.05). Data signify mean fold difference \pm SEM of three independent repeats, each performed in duplicates (figure 9).

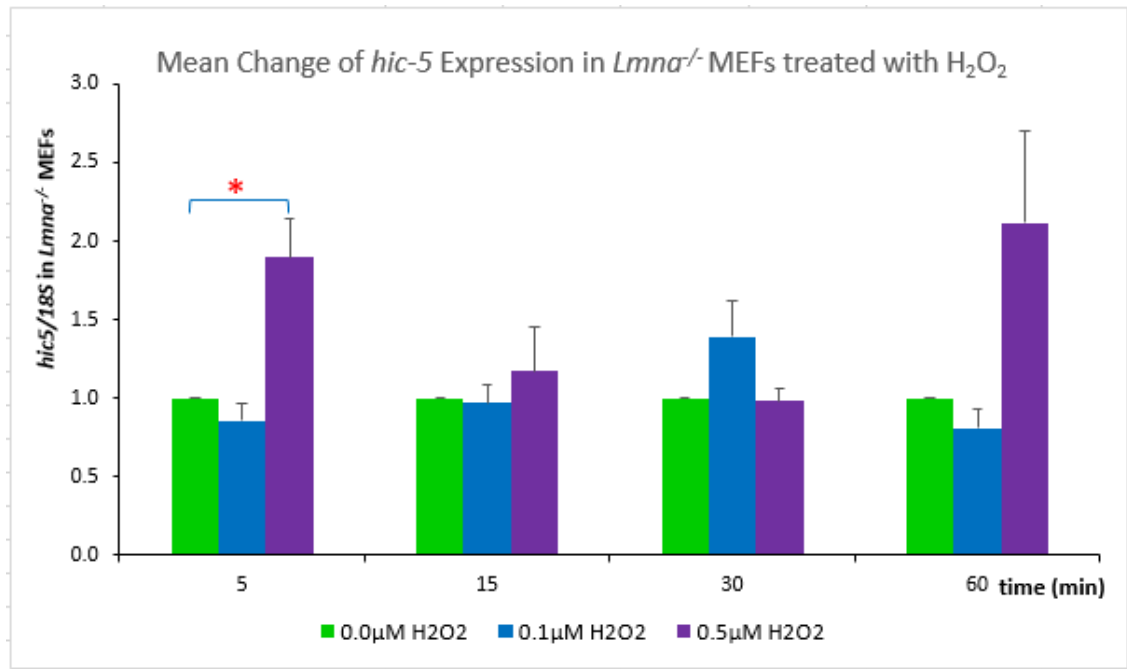


Figure 9: Mean fold difference change in *hic-5* transcript expression in *Lmna*^{-/-} MEF cells cultured at 100% confluence under 0.1 μM or 0.5 μM of H₂O₂-induced oxidative stress conditions for 5, 15, 30, and 60 min. Data from Real-Time PCR quantification designate immediate, early, and late reductions in transcript expression of *hic-5* normalized to that of *18S* reference gene in these knockout MEFs upon 0.5 μM H₂O₂ treatment in comparison to their untreated controls (0.0 μM H₂O₂). While upon 0.1 μM H₂O₂ treatment, no significant alterations are observed. Data represent mean fold difference change ± SEM derived from 4 independent experiments; each performed in duplicates. Results were checked for statistical significance by one-way ANOVA. One asterisk represents a statistical significance ($P < 0.05$).

4. In *Lmna*^{N195K/N195K} MEFs, directly and early after 0.1 μM and 0.5 μM treatments with H₂O₂, *hic-5* normalized to *18S* significantly increases in transcript levels with respect to the untreated controls.

Real-Time PCR quantification data suggest that *hic-5* normalized to the transcriptional levels of *18S* reference gene in *Lmna*^{N195K/N195K} MEFs increases upon both treatments (0.1 μM and 0.5 μM of H₂O₂) at all time points (5 min, 15 min, 30 min, and 60 min); whereby a statistically significant increase by 1.0-fold difference (±0.1) and 0.4-fold difference (±0.1) with respect to the untreated controls (P -value < 0.05 for both) is observed after 5 min of 0.5 μM treatment and 15 min of both treatments,

respectively. Whereas, these increases are statistically insignificant 30min post both treatments and are changed by 0.3-fold difference (± 0.1) and 0.45-fold difference (± 0.1) with respect to the untreated controls (P -value >0.05 for both). *Hic-5* levels also increase 60min post these treatments by 0.1-fold difference (± 0.1) and 0.4-fold difference (± 0.1) with respect to the untreated controls, respectively (P -value >0.05 for both). Data signify mean fold difference \pm SEM of three independent repeats, each performed in duplicates (figure 10).

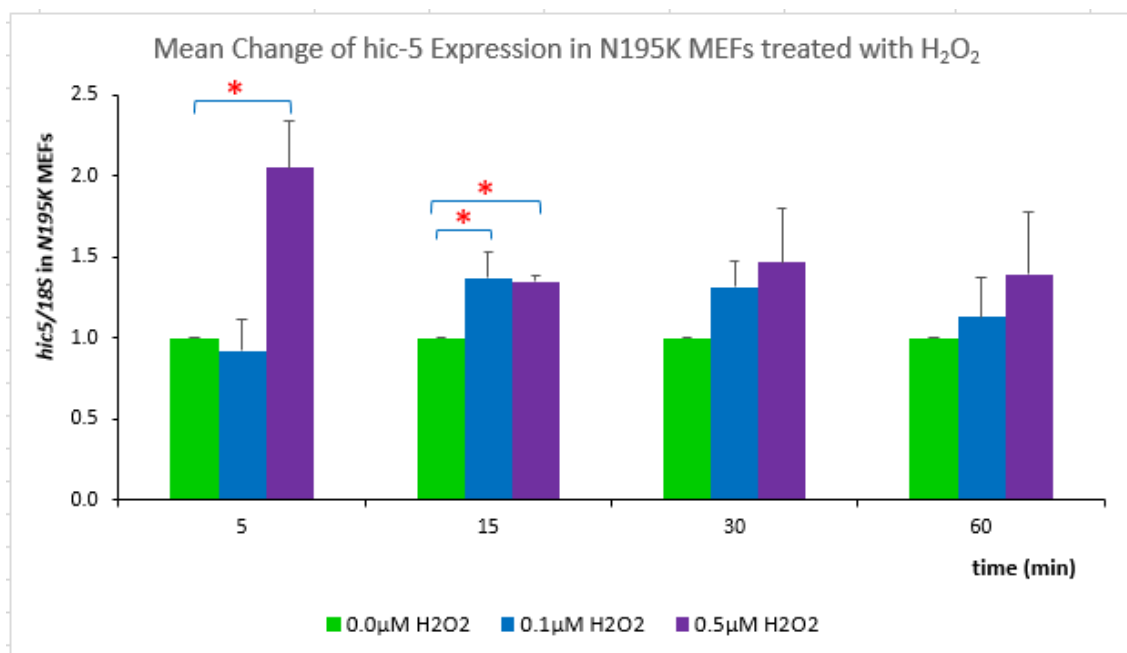


Figure 10: Mean fold difference change in *hic-5* transcript expression in *Lmna*^{N195K/N195K} MEF cells cultured at 100% confluence under 0.1 μM or 0.5 μM of H₂O₂-induced oxidative stress conditions for 5, 15, 30, and 60min. Data from Real-Time PCR quantification designate an immediate increase in transcript expression of *hic-5* normalized to that of *18S* reference gene in these MEFs upon 0.5 μM H₂O₂ treatment in comparison to the untreated controls (0.0 μM H₂O₂). While upon 0.1 μM H₂O₂ treatment, insignificant immediate reduction followed by a sustained upregulation are detected in *hic-5* transcript levels. Data represent mean fold difference change \pm SEM derived from 4 independent experiments; each performed in duplicates. Results were checked for statistical significance by one-way ANOVA. One asterisk represents a statistical significance ($P < 0.05$).

5. In *Emd*^{-Y} MEFs, upon treatments with 0.1 μ M and 0.5 μ M of H₂O₂ for different time points (5min, 15min, 30min, and 60min), *hic-5* normalized to *18S* demonstrates slight fluctuations in transcript levels that are statistically insignificant with respect to their untreated controls.

Real-Time PCR quantification data in *Emd*^{-Y} MEFs suggest that *hic-5* normalized to *18S* decreases in a statistically insignificant manner by 0.15-fold difference (± 0.1), 0.2-fold difference (± 0.1), and 0.3-fold difference (± 0.1) 5min, 15min, and 60min post the 0.1 μ M treatment with respect to the untreated controls (*P*-value > 0.05 for all). On the other hand, upon 0.5 μ M H₂O₂ treatment of these MEFs, an insignificant immediate decrease in *hic-5* normalized to *18S* transcript levels followed by an insignificant increase as more time elapses are observed. Accordingly, it decreases by 0.1-fold difference (± 0.1) and 0.15-fold difference (± 0.1) after 5min and 15min and then increases by 0.1-fold difference (± 0.1) and 0.15-fold difference (± 0.1) after 30min and 60min with respect to their untreated controls (*P*-value > 0.05 for all). Data signify mean fold difference \pm SEM of three independent repeats, each performed in duplicates (figure 11).

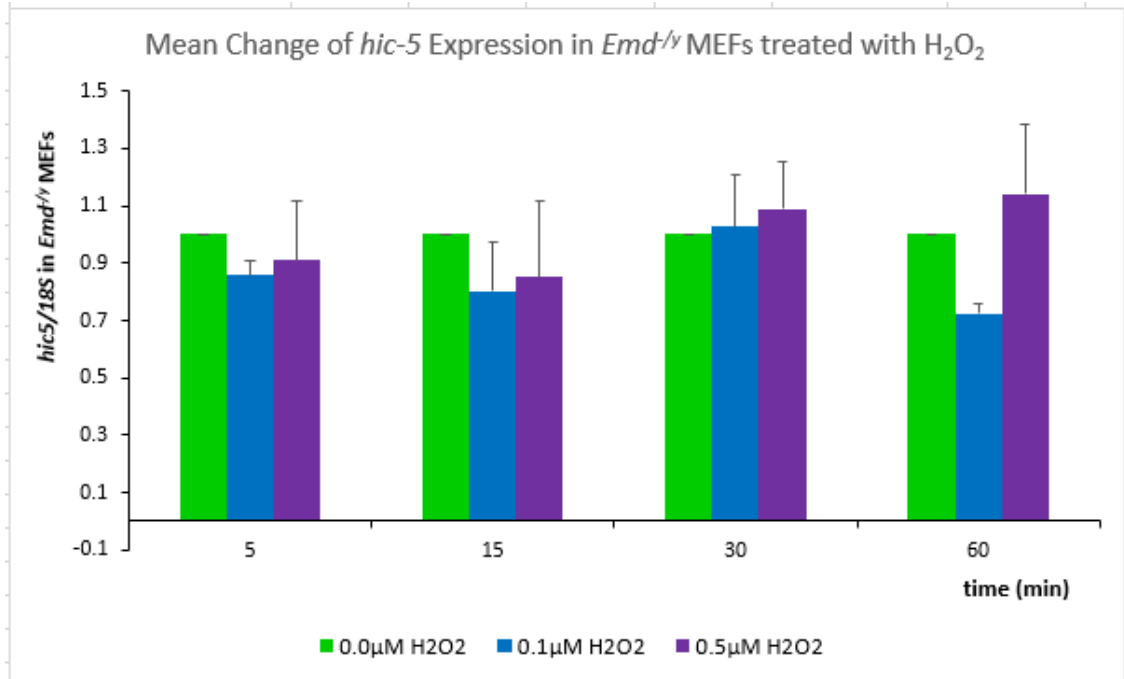


Figure 11: Mean fold difference change in *hic-5* transcript expression in *Emd*^{+/y} MEF cells cultured at 100% confluence under 0.1 μM or 0.5 μM of H₂O₂-induced oxidative stress conditions for 5, 15, 30, and 60 min. Data from Real-Time PCR quantification designate an immediate-early reduction in transcript expression of *hic-5* normalized to that of *18S* reference gene in these MEFs upon both treatments in comparison to their untreated controls (0.0 μM H₂O₂). Transcript expression of *hic-5* then slightly increases 30 min post both treatments and further increases after 60 min upon the 0.5 μM H₂O₂ treatment but decreases upon the 0.1 μM H₂O₂ treatment. Data represent mean fold difference change ± SEM derived from 4 independent experiments; each performed in duplicates. Results were checked for statistical significance by one-way ANOVA.

B. Specific Aim 2: To assess whether hic-5 is differentially expressed at the protein level in mouse embryo fibroblasts (MEFs) derived from mouse models of myopathic laminopathies in comparison to wild-type controls cultured *in vitro* under baseline and oxidative stress conditions.

1. Under baseline conditions, hic-5 α is upregulated in the three laminopathic cell lines (Emd^{Y} MEFs, $Lmna^{N195K/N195K}$ MEFs, and $Lmna^{-/-}$ MEFs) with respect to the WT ($Lmna^{+/+}$ MEFs) controls. This upregulation is highly significant in the complete lamin knockout panel ($Lmna^{-/-}$ MEFs).

To determine any modulation at the protein level in hic-5 expression under baseline conditions, cells of the four MEF panels ($Lmna^{+/+}$, $Lmna^{-/-}$, $Lmna^{N195K/N195K}$, and Emd^{Y}) were seeded to reach 100% confluence. Then, protein extraction from total cell lysates, SDS-PAGE, and Western Blot analysis were performed using an antibody that specifically detects three (hic-5 α , hic-5 α B, and hic-5 β) of the isoforms of hic-5. Qualitative analysis was performed by the visual detection and comparison of densitometry signals developed on autoradiography films. Finally, semi-quantitative densitometry analyses using Image J software were performed. Since protein levels of hic-5 α B and hic-5 β demonstrate much variability between the different cell lines and within each line; and since they aren't always detected between the numerous independent repeats performed on each cell line (up to N=9) despite using fresh protein lysates and high amounts of loaded protein (40 μ g), the results shown and analyzed are only performed on the canonical hic-5 α isoform.

Under baseline conditions, image J analysis of densitometry signals of hic-5 α normalized to the loading control GAPDH show an increase in the protein levels between $Lmna^{-/-}$, $Lmna^{N195K/N195K}$ and Emd^{Y} mutant MEFs in comparison to their WT

(*Lmna*^{+/+}) MEFs control. A statistically insignificant 1.0-fold difference (± 0.1) increase in hic-5 α protein expression is detected in both the *Lmna*^{N195K/N195K} MEFs and *Emd*^Y MEFs in comparison to the WT controls (P -value >0.05). However, the 3.0-fold difference increase (± 0.1) in hic-5 α protein expression in the *Lmna*^{-/-} MEFs is highly statistically significant with respect to the WT controls (P -value <0.001). Data signify mean fold difference \pm SEM of three independent repeats (figure 12).

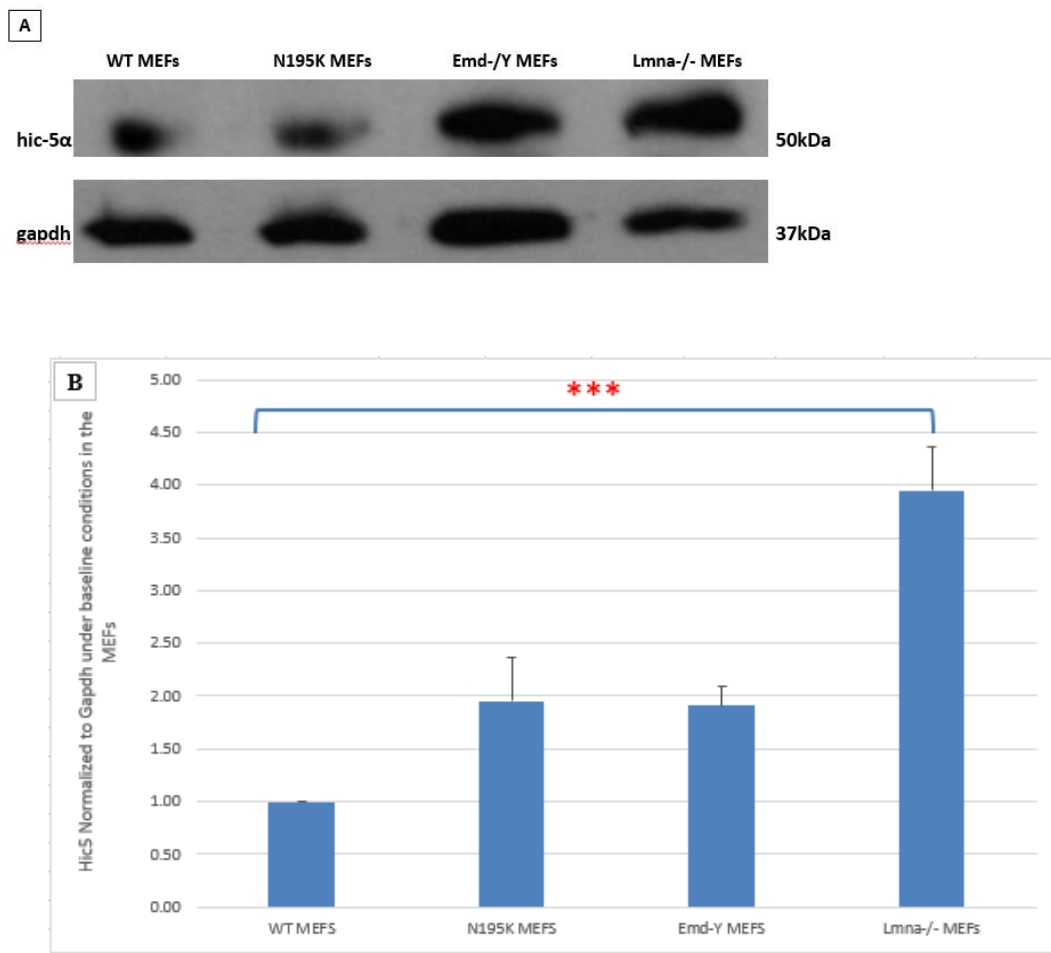


Figure 12: Western Blot analysis of hic-5 α protein expression in *Lmna*^{-/-}, *Lmna*^{N195K/N195K}, and *Emd*^Y mutant MEFs cell lines in comparison to the control WT cells cultured at 100% confluence under baseline conditions. Panel A; representative blot. Panel B; image J quantification and analyses show an increase in hic-5 α densitometry signal normalized to that of the GAPDH loading control in the mutant MEFs in comparison to the control WT cells. Data represent mean fold difference change \pm SEM derived from 3 independent experiments. Results were checked for statistical significance by one-way ANOVA. Three asterisks represent a statistical significance ($P<0.001$).

2. Upon treatment with 0.1 μ M and 0.5 μ M of H₂O₂, the protein levels of hic-5 α are slightly altered in the WT (*Lmna*^{+/+} MEFs) at the different time points (5, 15, 30, and 60min) demonstrating a significant decrease upon 30min of their exposure to 0.5 μ M of H₂O₂ with respect to the untreated controls.

To evaluate the response of hic-5 to H₂O₂-induced oxidative stress, *Lmna*^{+/+}, *Lmna*^{-/-}, *Lmna*^{N195K/N195K}, and *Emd*^{-Y} MEFs were seeded to reach 100% confluence while guaranteeing uniformity in cell-cell contact profiles in each tested sample and between independent repeats. Then, cells were exposed to 0.1 μ M and 0.5 μ M of H₂O₂ for 5, 15, 30 and 60min. Afterwards, total protein extraction, SDS-PAGE, Western Blot densitometry, and image J analysis were performed.

Upon treating the *Lmna*^{+/+} MEFs with both 0.1 μ M and 0.5 μ M of H₂O₂, image J analysis of densitometry signals suggest an immediate 0.35-fold difference (± 0.1) increase and 0.7-fold difference (± 0.1) increase in hic-5 α protein levels normalized to GAPDH with respect to the untreated controls, respectively. Yet, these increases are not statistically significant (*P-value* > 0.05). Protein levels of hic-5 α then decrease with respect to their initial increase as time elapses to 30min and then normalize again 60min post the 0.5 μ M treatment. Accordingly, hic-5 α protein levels demonstrate a 0.2-fold difference (± 0.1) increase, 0.7-fold difference (± 0.1) decrease, and 0.1-fold difference (± 0.1) decrease 15, 30, and 60min post 0.5 μ M treatment of H₂O₂ with respect to their untreated controls, respectively. These changes are statistically insignificant for the 15min and 60min time points with a *P-value* > 0.05 but significant post 30min of this treatment with a *P-value* < 0.05. However, upon 0.1 μ M treatment of H₂O₂, hic-5 α protein levels demonstrate statistically insignificant alterations of 0.4-fold difference decrease (± 0.1), 0.5-fold difference decrease (± 0.1), and 0.4-fold difference increase (± 0.1) after

15, 30, and 60min with respect to their untreated controls, respectively (P -value >0.05 for all). Data signify mean fold difference \pm SEM of three independent repeats (figure 13).

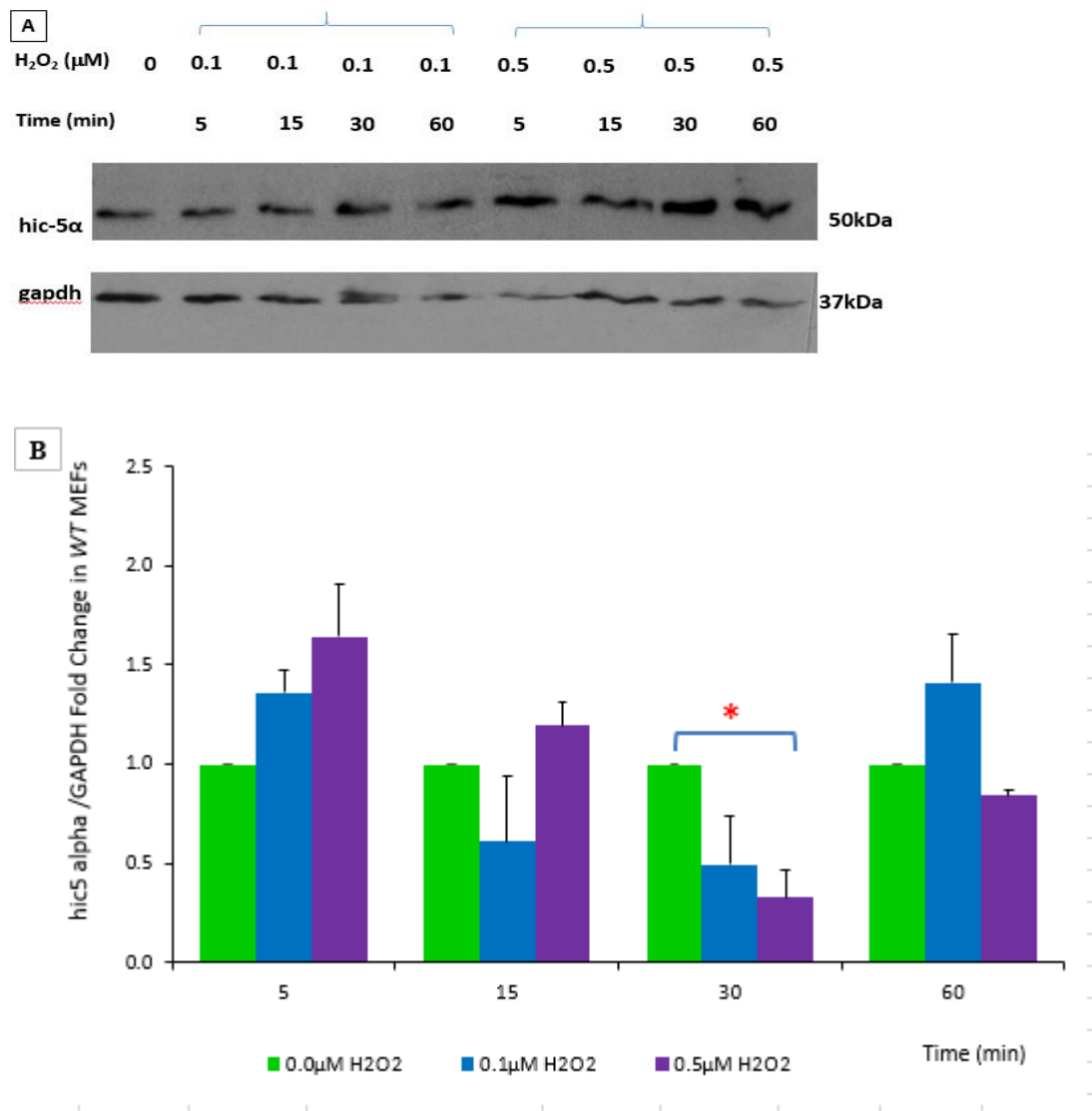


Figure 13: hic-5 α protein expression in *Lmna*^{+/+} MEF cells cultured at 100% confluence under 0.1 μ M or 0.5 μ M H₂O₂-induced oxidative stress conditions for 5, 15, 30 and 60min. Panel A; representative blot. Panel B; image J quantification and analysis of the hic-5 α densitometry signal normalized to that of the GAPDH loading control data show an immediate-early increase in hic-5 α protein expression followed by a late decrease in the 0.5 μ M H₂O₂ treated WT MEFs in comparison to their untreated controls. Whereas, upon 0.1 μ M H₂O₂ treatment, these MEFs demonstrate immediate and late increases interspersed by decrease in hic-5 α protein. Data represent mean fold difference change \pm SEM derived from 3 independent experiments. Results were checked for statistical significance by one-way ANOVA. One asterisk represents a statistical significance ($P < 0.05$).

3. Upon treatment with 0.1 μ M of H₂O₂, the protein levels of hic-5 α in *Lmna*^{-/-} MEFs decrease insignificantly with respect to their untreated controls throughout the different time points. However, when these knockout MEFs were treated with 0.5 μ M of H₂O₂, hic-5 α demonstrates an increase in protein expression which is significant only after 1 hour of treatment.

Upon treatment of *Lmna*^{-/-} MEFs with H₂O₂, image J analysis of densitometry signals suggest a decrease in hic-5 α protein levels normalized to GAPDH upon the 0.1 μ M treatment and an increase in their levels upon the 0.5 μ M treatment with respect to their untreated controls at the different time points. Accordingly, upon the latter treatment, hic-5 α protein levels normalized to GAPDH increase by 0.25-fold difference (± 0.1), 0.3-fold difference (± 0.1), and 0.5-fold difference (± 0.1) after 5, 15, and 30min of treatment with respect to their untreated controls, respectively. Yet, these changes are not statistically significant (*P-value* > 0.05 for all). Protein expression of hic-5 also increases – yet significantly – by 0.75-fold difference (± 0.1) after 60min of this treatment with respect to the untreated controls (*P-value* < 0.05). On the other hand, all decreases observed upon the 0.1 μ M treatment are statistically insignificant (*P-value* > 0.05 for all) and are as follows: 0.2, 0.4, 0.1, and 0.05 (± 0.1) fold difference-change after 5, 15, 30, and 60min, respectively. Data signify mean fold difference \pm SEM of three independent repeats (figure 14).

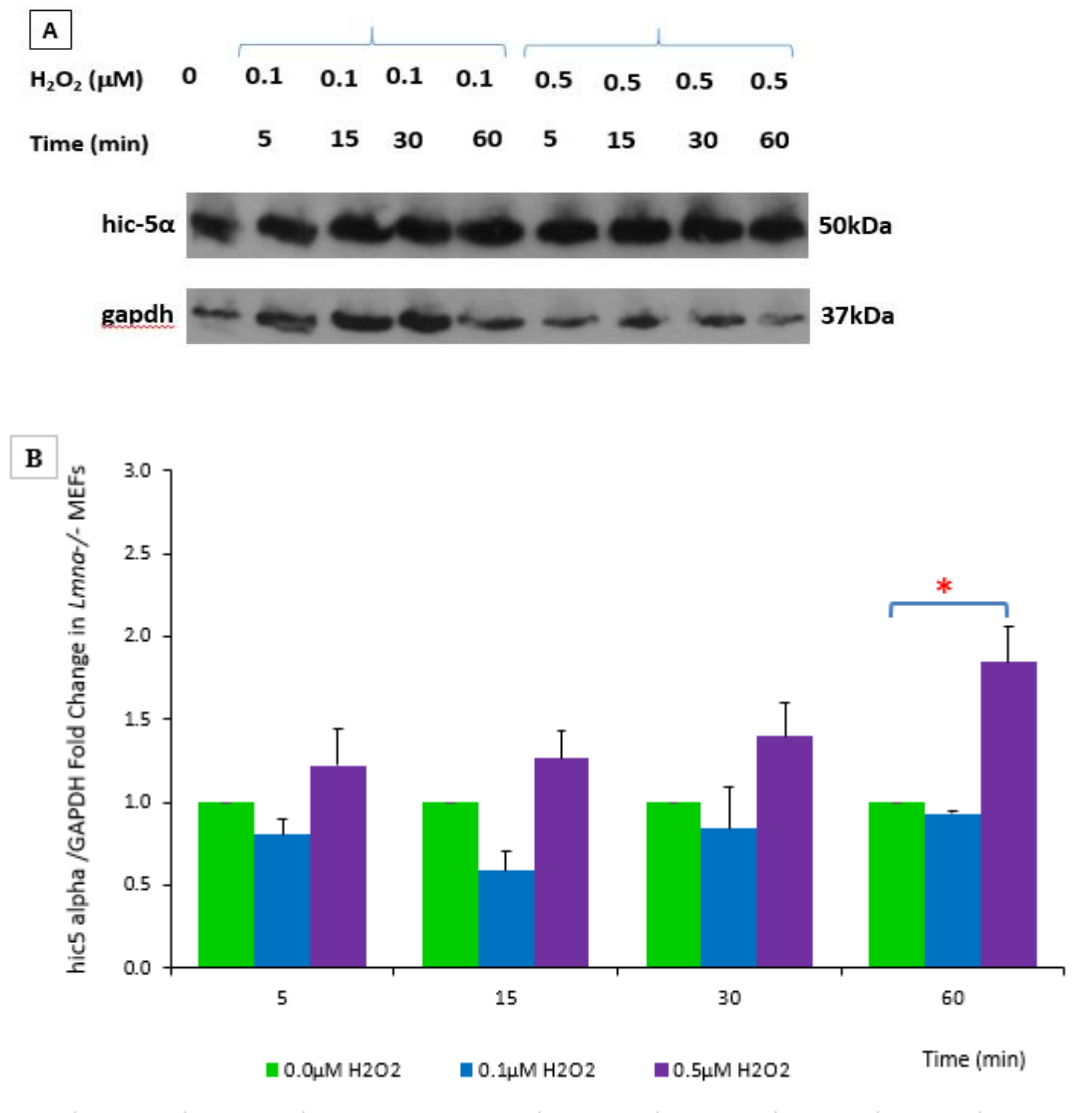


Figure 14: hic-5 α protein expression in *Lmna*^{-/-} MEF cells cultured at 100% confluence under 0.1 μ M or 0.5 μ M H₂O₂-induced oxidative stress conditions for 5, 15, 30 and 60min. Panel A; representative blot. Panel B; image J quantification and analysis of the hic-5 α densitometry signal normalized to that of the GAPDH loading control data show an increase in hic-5 α protein expression at all time points in the 0.5 μ M H₂O₂ treated lamin knock out MEFs in comparison to their untreated controls. In opposition with that, upon 0.1 μ M H₂O₂ treatment, hic-5 α protein expression shows an insignificant decrease at all time points. Data represent mean fold difference change \pm SEM derived from 3 independent experiments. Results were checked for statistical significance by one-way ANOVA. One asterisk represents a statistical significance ($P < 0.05$).

4. Upon treatment with 0.1 μ M and 0.5 μ M of H₂O₂, the protein levels of hic-5 α in *Lmna*^{N195K/N195K} MEFs show a significant increase with respect to their untreated controls directly after the treatment (5min and 15min, respectively) which then significantly decrease as more time elapses.

Upon treatment of *Lmna*^{N195K/N195K} MEFs with 0.1 μ M of H₂O₂, image J analysis of densitometry signals demonstrate an immediate increase in hic-5 α protein levels normalized to GAPDH with respect to their untreated controls. They then decrease afterwards as more time elapses. Accordingly, hic-5 α levels in these MEFs significantly increase with a 1.5-fold difference change (± 0.1) 5min after this treatment with respect to their untreated controls (*P*-value < 0.05). However, 15min and 30min post the 0.1 μ M treatment, hic-5 α protein levels also increase – statistically insignificant though (*P*-value > 0.05) – by 0.6 and 0.25-fold difference (± 0.1) change, respectively. Then an hour post this treatment, hic-5 α levels significantly decrease by a 0.5-fold difference change (± 0.1) with respect to the untreated controls (*P*-value < 0.05). On the other hand, upon treating *Lmna*^{N195K/N195K} MEFs with 0.5 μ M of H₂O₂, an immediate increase in hic-5 α protein levels that peaks 15min post treatment is observed. These levels of increase then decrease with time. Accordingly, a statistically insignificant 0.5-fold difference (± 0.1) increase is observed in these MEFs 5min post the treatment with respect to their untreated controls (*P*-value > 0.05). Then, it significantly increases by 3-fold difference (± 0.1) with respect to the untreated controls (*P*-value < 0.01). Afterwards, the *Lmna*^{N195K/N195K} MEFs treated with 0.5 μ M of H₂O₂ demonstrate an insignificant (*P*-value > 0.05) 0.25 and a significant (*P*-value < 0.05) 0.45 (± 0.1) fold difference increases in hic-5 α protein levels 30min and 60min post treatment with respect to their untreated

controls. Data signify mean fold difference \pm SEM of three independent repeats (figure 15).

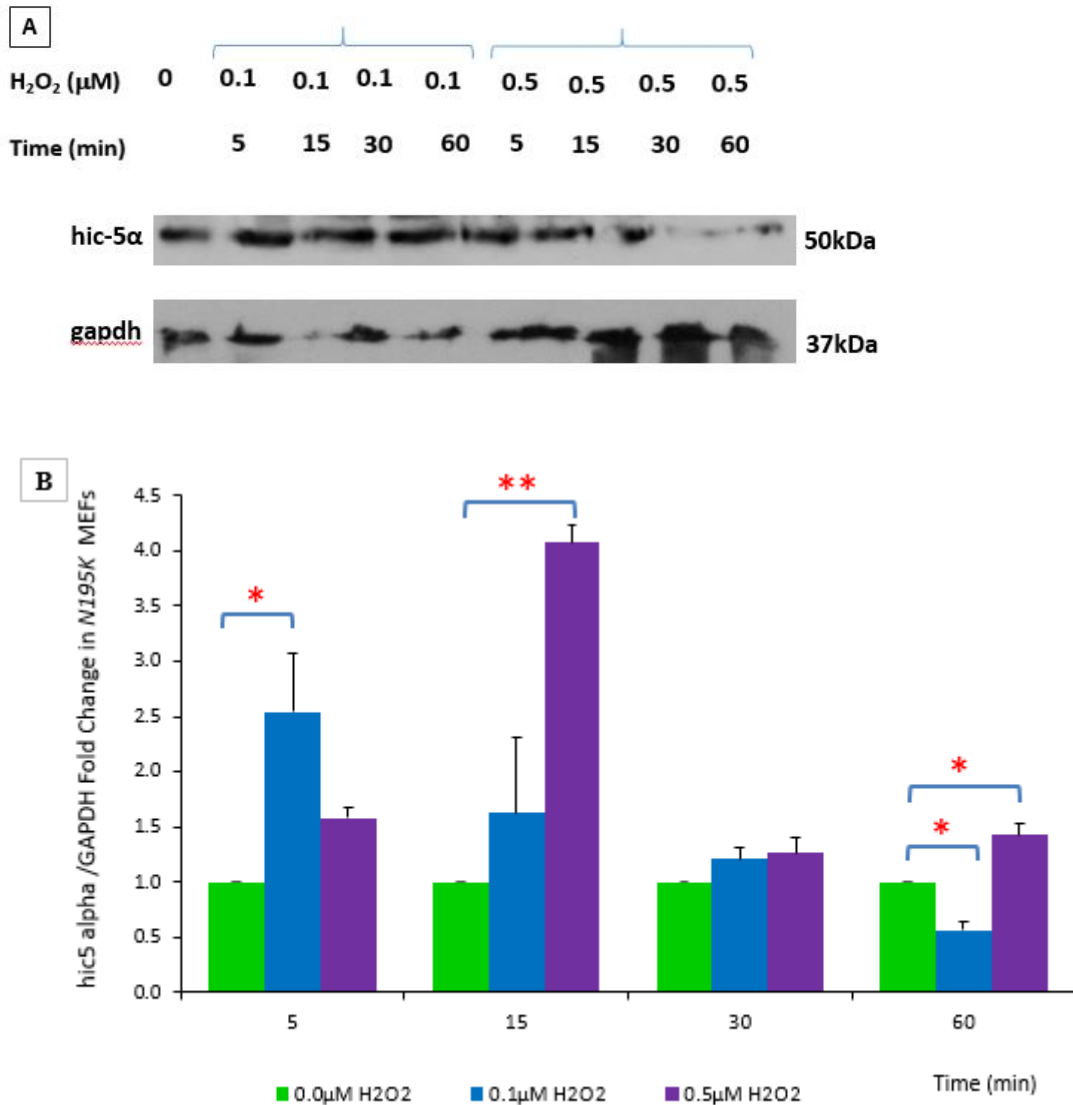


Figure 15: hic-5 α protein expression in *Lmna*^{N195K/N195K} MEF cells cultured at 100% confluence under 0.1 μ M or 0.5 μ M H₂O₂-induced oxidative stress conditions for 5, 15, 30 and 60min. Panel A; representative blot. Panel B; image J quantification and analysis of the hic-5 α densitometry signal normalized to that of the GAPDH loading control data show an increase in hic-5 α protein expression at all time points that peaks the most 15min post the 0.5 μ M H₂O₂ treatment in comparison to their untreated controls. Whereas upon 0.1 μ M H₂O₂ treatment, hic-5 α protein expression shows an immediate increase that decreases as time elapses until it becomes less than its expression in the untreated controls. Data represent mean fold difference change \pm SEM derived from 3 independent experiments. Results were checked for statistical significance by one-way ANOVA. One asterisk represents a statistical significance ($P < 0.05$). Two asterisks represent a statistical significance ($P < 0.01$).

5. Upon treatment with 0.1 μM of H_2O_2 , the protein levels of hic-5 α in $\text{Emd}^{\text{f/y}}$ MEFs show direct-early significant increases with respect to their untreated controls that then decrease with time. Whereas, when they are treated with 0.5 μM of H_2O_2 , hic-5 α demonstrates highly significant increases in protein levels that fluctuate as time elapses with respect to their untreated controls.

Upon treatment of $\text{Emd}^{\text{f/y}}$ MEFs with 0.5 μM of H_2O_2 , image J analysis of densitometry signals demonstrate an increase at all time points in hic-5 α protein levels normalized to GAPDH with respect to their untreated controls. Whereas, this pattern of expression is similar when these MEFs are treated with 0.1 μM of H_2O_2 , except that it decreases at the final time point with respect to the untreated controls. Hence, in accordance with the previously stated patterns, hic-5 α protein levels normalized to GAPDH significantly increase by 3.4-fold difference (± 0.1) ($P\text{-value} < 0.001$), 0.4-fold difference (± 0.1) ($P\text{-value} < 0.01$), 4.2-fold difference (± 0.1) ($P\text{-value} < 0.001$), and 1.2-fold difference (± 0.1) ($P\text{-value} < 0.05$) with respect to the untreated controls 5, 15, 30, and 60min post 0.5 μM H_2O_2 treatment, respectively. So, the highest peaks of increase in hic-5 α protein levels seem to take place 5 and 30min after this treatment. On the other hand, post 0.1 μM H_2O_2 treatment, hic-5 α protein levels significantly increase the most after 15min by 3.5-fold difference (± 0.1) with respect to the untreated controls ($P\text{-value} < 0.001$). They also shows increases after 5min and 30min of this treatment by statistically significant 0.65-fold difference (± 0.1) ($P\text{-value} < 0.01$) and statistically insignificant 0.45-fold difference (± 0.1) ($P\text{-value} > 0.05$) with respect to the untreated controls, respectively. The protein levels of hic-5 α then decrease 60min after this treatment in a statistically insignificant manner by 0.2-fold difference (± 0.1) with

respect to the untreated controls (P -value >0.05). Data signify mean fold difference \pm SEM of three independent repeats, each performed in duplicates (figure 16).

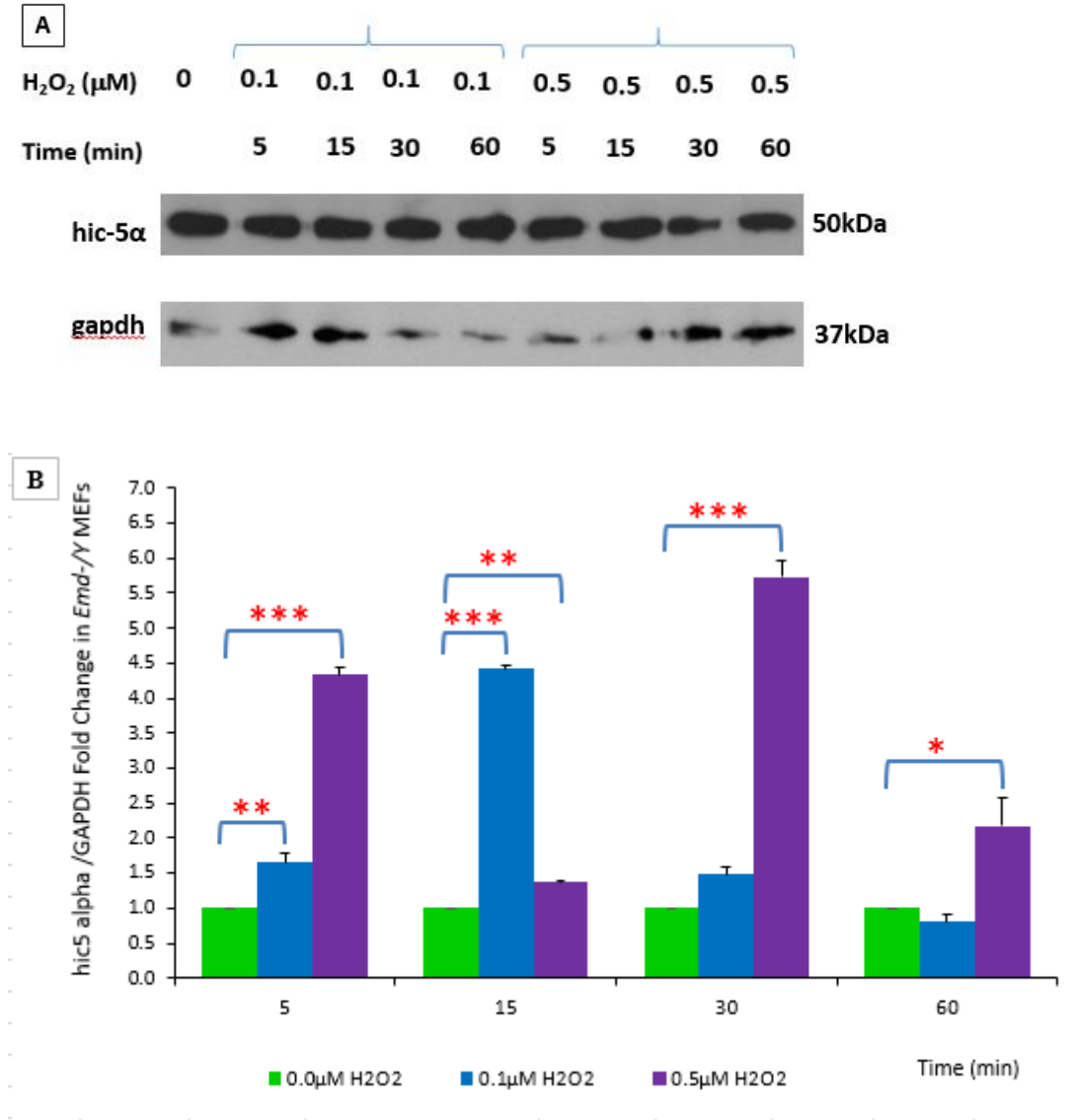


Figure 16: hic-5 α protein expression in *Emd* ^{γ} MEF cells cultured at 100% confluence under 0.1 μ M or 0.5 μ M H₂O₂-induced oxidative stress conditions for 5, 15, 30 and 60min. Panel A; representative blot. Panel B; image J quantification and analysis of the hic-5 α densitometry signal normalized to that of the GAPDH loading control data show an increase in hic-5 α protein expression at the first 3 time points that peaks the most 15min post the 0.1 μ M H₂O₂ treatment in these mutant MEFs in comparison to their untreated controls. Whereas upon 0.5 μ M H₂O₂ treatment, hic-5 α protein expression shows an increase at all time points in comparison with the untreated controls. Data represent mean fold difference change \pm SEM derived from 3 independent experiments. Results were checked for statistical significance by one-way ANOVA. One asterisk represents a statistical significance ($P<0.05$). Two asterisks represent a statistical significance ($P<0.01$). Three asterisks represent a statistical significance ($P<0.001$).

C. Specific Aim 3: To investigate putative modulations in hic-5 expression and distribution in mouse embryo fibroblasts (MEFs) derived from mouse models of myopathic laminopathies in comparison to their heterozygote littermates and wild-type controls cultured *in vitro* under baseline and oxidative stress conditions.

1. Under baseline conditions, hic-5 protein has a similar pattern of expression in $Lmna^{+/+}$, $Lmna^{-/-}$, and $Emd^{-/Y}$ MEF cell lines of significantly high

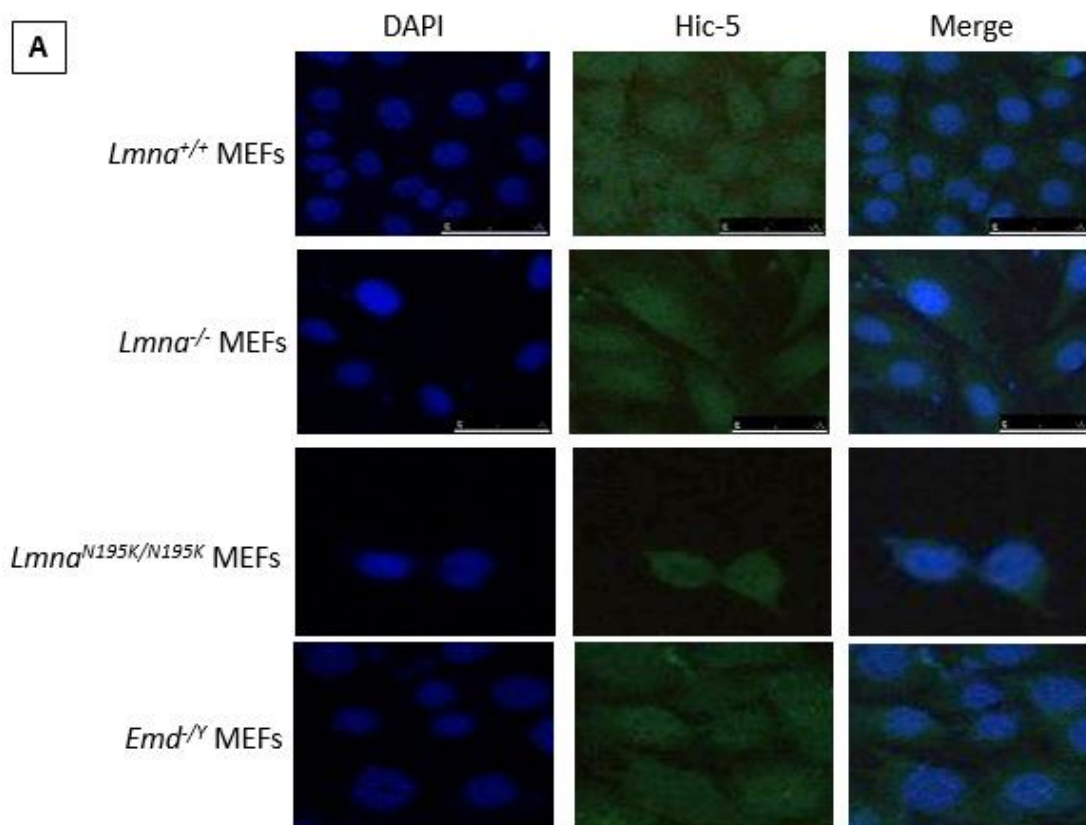
nuclear=cytoplasmic localization in comparison to low nuclear>cytoplasmic.

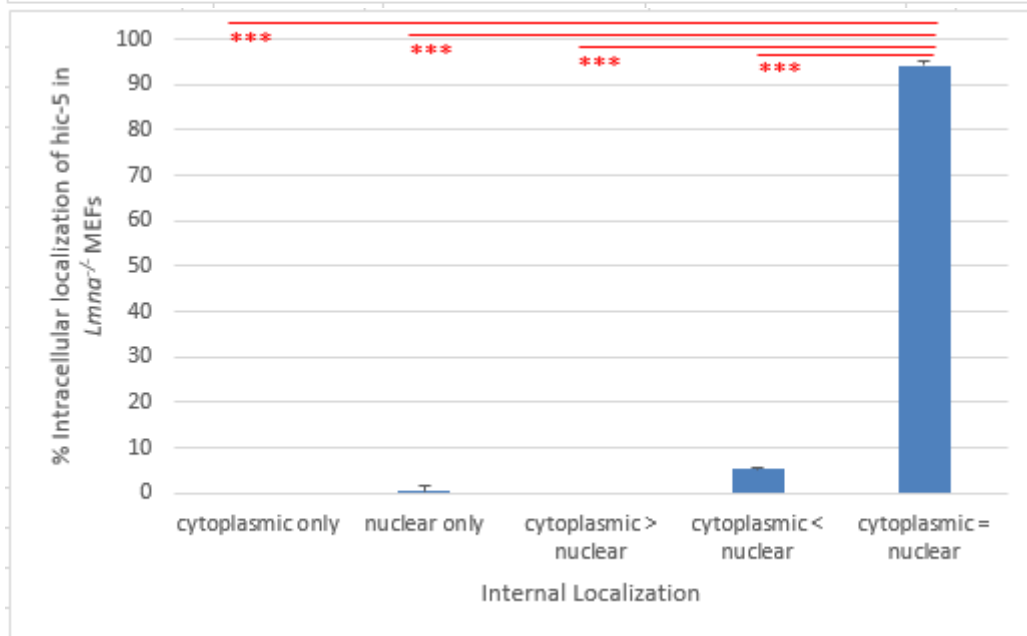
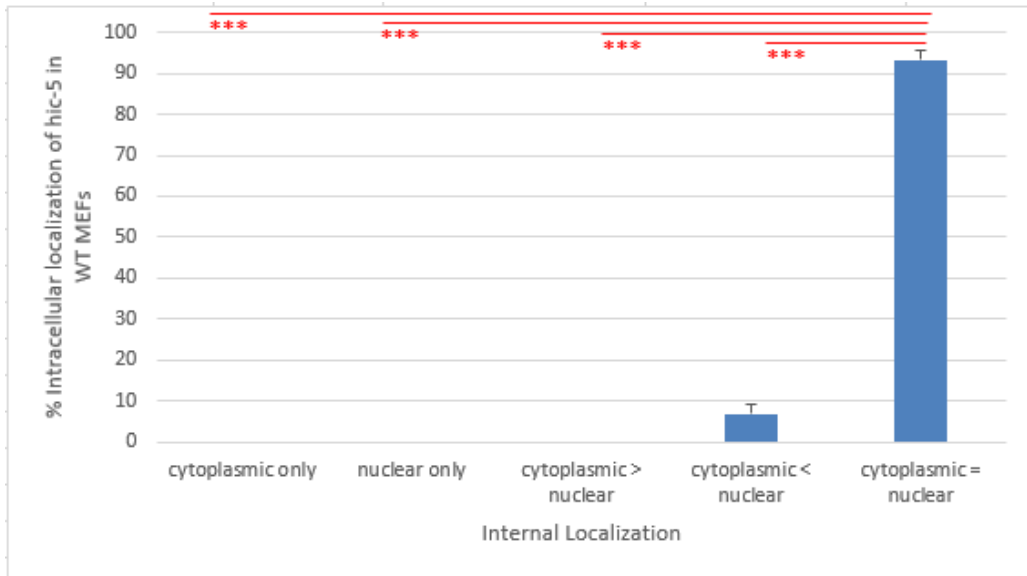
Whereas, $Lmna^{N195K/N195K}$ MEFs show a different pattern of significant high nuclear hic-5 localization in comparison with the nuclear=cytoplasmic ones.

To examine prospective alterations in the intracellular distribution and localization of hic-5 in $Lmna^{+/+}$, $Lmna^{-/-}$, $Lmna^{N195K/N195K}$, and $Emd^{-/Y}$ MEFs under baseline conditions, we performed immunofluorescence staining of PFA fixed cells stained with hic-5 antibody that detects all its isoforms. Using the same exposure time and excitation wave length, we acquired 3-5 image frames per slide for each cell lines. Subsequently, we subcategorized the pattern of hic-5 expression into five categories: nuclear, nuclear > cytoplasmic, nuclear = cytoplasmic, nuclear < cytoplasmic, and cytoplasmic expression. The cells of each frame of each cell line were allocated to one of the five categories, and expressed as a percentage of the total number of cells.

Under baseline conditions, fluorescence images and their semi-quantitative analyses data indicate a significantly high localization of hic-5 in a cytoplasmic = nuclear manner in comparison to cytoplasmic < nuclear distribution in $Lmna^{+/+}$, $Lmna^{-/-}$, and $Emd^{-/Y}$ MEFs. Accordingly, the percentage of cells exhibiting cytoplasmic = nuclear distribution are $86.46\% \pm 0.01$, $88.86\% \pm 0.01$, and $86.04\% \pm 0.01$ significantly more (P -value < 0.001 for all) than cells with cytoplasmic = nuclear distribution in $Lmna^{+/+}$,

Lmna^{-/-}, and *Emd*^{/Y} MEFs, respectively. Whereas, *Lmna*^{N195K/N195K} MEFs have a different internal cellular distribution of hic-5 whereby cells exhibiting only a nuclear localization of this protein are significantly more by 50.93%±0.01 than those exhibiting an equal distribution between the cytoplasm and the nucleus (*P-value*<0.001). Results are represented as mean fold difference in the fluorescence intensity ± SEM of three independent experiments (figure 17).





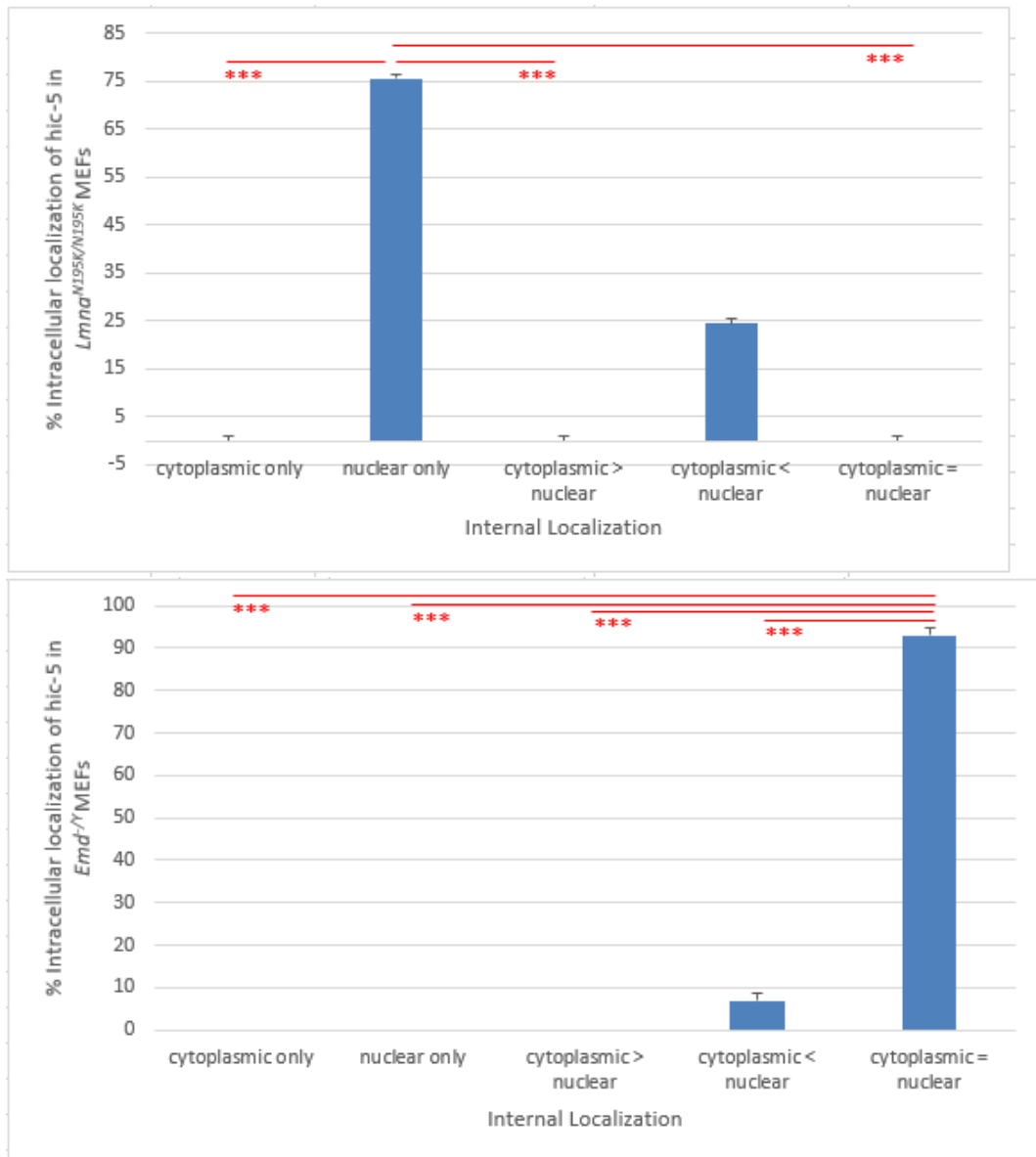


Figure 17: Immunofluorescence staining and semi-quantitative analysis of hic-5 protein cellular internal localization expression in the 4 MEFs panels (*Lmna*^{+/+}, *Lmna*^{-/-}, *Lmna*^{N195K/N195K}, and *Emd*^{-/-}) cultured at 100% confluence under baseline conditions. Panel A; representative upright fluorescence microscope images showing immunofluorescence staining of hic-5 in the 4 MEF cells. DAPI was used to stain the nuclei. Images were acquired at 20X magnification. Panel B: Semi-quantitative assessment of the relative fluorescence intensity of hic-5 reveals that it is highly present in a nuclear = cytoplasmic manner in comparison to nuclear > cytoplasmic in WT, lamin knockout, and emerin knockout MEFs. Whereas, hic-5 is highly expressed in a nuclear manner rather than nuclear = cytoplasmic in *Lmna*^{N195K/N195K} MEFs. Data represent mean \pm SEM derived from 3 independent repeats. Results were checked for statistical significance by one-way ANOVA. Three asterisks represent a statistical significance ($P < 0.001$).

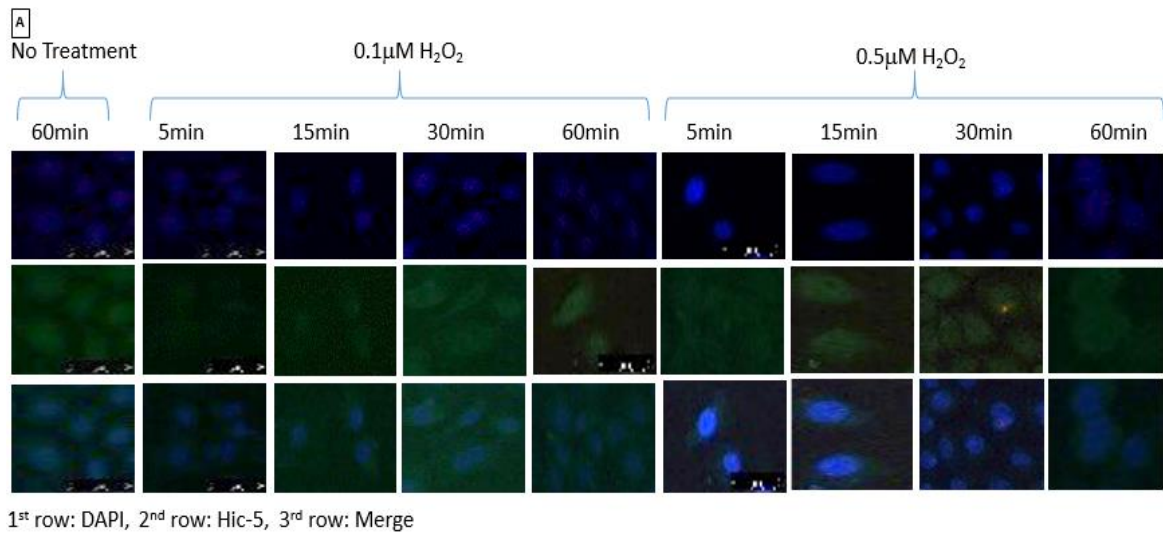
2. Upon treating WT *Lmna*^{+/+} MEFs with 0.1 μ M and 0.5 μ M of H₂O₂ the cellular internal localization of hic-5 shows significantly higher levels of cytoplasmic = nuclear distribution in comparison with its nuclear and nuclear > cytoplasmic distributions across all different time points similar to their untreated controls. Moreover, an immediate decrease in the cytoplasmic = nuclear distribution of hic-5 is observed upon treating the WT MEFs with 0.5 μ M of H₂O₂ in comparison with their untreated controls.

To evaluate the response of hic-5 to H₂O₂-induced oxidative stress, *Lmna*^{+/+}, *Lmna*^{-/-}, *Lmna*^{N195K/N195K}, and *Emd*^{-/Y} MEFs were seeded to reach 100% confluence while ensuring uniformity in spreading and cell-cell contact profiles in each tested sample and independent repeats. Then, they were exposed to 0.1 μ M and 0.5 μ M of H₂O₂ for 5, 15, 30 and 60 minutes. Afterwards, immunofluorescence staining of PFA fixed cells with hic-5 antibody was performed. Using the same exposure time and excitation wave length, we acquired three image frames per slide for each cell lines. Then they were counted and analyzed according to the previously stated criteria to determine the localization within each time point and between different treatments and their time points.

Upon treating the WT MEFs with 0.1 μ M or 0.5 μ M of H₂O₂, fluorescence images and their semi-quantitative analysis data indicate significantly high localization of hic-5 in a cytoplasmic = nuclear manner in comparison to cytoplasmic < nuclear and nuclear distribution between all the time points and the different treatments.

Accordingly, the control untreated MEFs demonstrate significantly 67.84% \pm 4 more cells exhibiting a cytoplasmic = nuclear distribution than the two other mentioned categories (*P*-value<0.001). This difference is reduced significantly by 2.48% \pm 0.01 (*P*-

value < 0.05) and insignificantly by $2.78\% \pm 0.01$ and $6.35\% \pm 0.01$ (P -value > 0.05 for both) in the cells treated for 5min with $0.5\mu\text{M}$ of H_2O_2 , 5min with $0.1\mu\text{M}$ of H_2O_2 , and 15min with $0.5\mu\text{M}$ of H_2O_2 in comparison with that of the untreated controls, respectively. On the other hand, all the other time points of the 2 treatments show statistically insignificant increases by around 2.67% in the nuclear = cytoplasmic distribution of hic-5 in comparison with their untreated controls. Results are represented as mean fold difference in the fluorescence intensity \pm SEM of four independent experiments (figure 18).



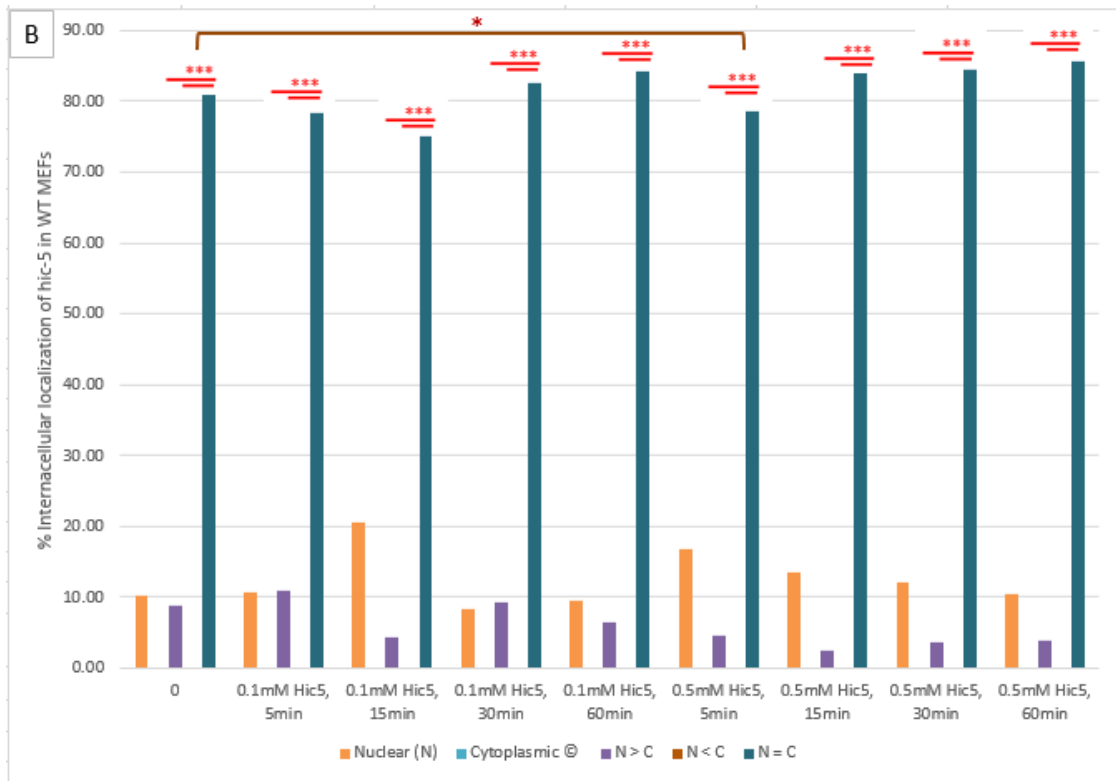


Figure 18: Immunofluorescence staining and semi-quantitative analysis of hic-5 protein cellular internal localization expression in *Lmna*^{+/+} MEFs cultured at 100% confluence under 0.1 μ M or 0.5 μ M H₂O₂-induced oxidative stress conditions for 5, 15, 30 and 60min. Panel A; representative upright fluorescence microscope images showing immunofluorescence staining of hic-5 in the WT MEFs. DAPI was used to stain the nuclei. Images were acquired at 20X magnification. Panel B: Semi-quantitative assessment of the hic-5 protein expression in WT MEFs indicate that it significantly localized more in a nuclear = cytoplasmic manner rather than nuclear and nuclear > cytoplasmic localizations. This pattern is similar among the different time points and different treatments. Results were checked for statistical significance by one-way ANOVA. One asterisk represents a statistical significance ($P < 0.05$). Three asterisks represent a statistical significance ($P < 0.001$).

3. Lamin knockout (*Lmna*^{-/-}) MEFs demonstrate a similar pattern of *hic-5* distribution among the different time points post 0.1 μ M or 0.5 μ M of H₂O₂ treatments with respect to their untreated controls as those of WT MEFs. In addition, *hic-5*'s nuclear > cytoplasmic localization is higher than the nuclear one also upon both treatments and similar to the untreated controls.

Upon treating the lamin knockout (*Lmna*^{-/-}) MEFs with 0.1 μ M or 0.5 μ M of H₂O₂, fluorescence images and their semi-quantitative analysis data show significantly more localization of *hic-5* in a cytoplasmic = nuclear manner by around 60% in comparison to cytoplasmic < nuclear distribution and by around 45% in comparison to the nuclear distribution between all the time points and different treatments (*P*-value < 0.001). Also, cells exhibiting nuclear > cytoplasmic distribution are present approximately 15% more than those with a nuclear distribution only. This increase is found to be statistically significant in all the panels (*P*-value < 0.001), except 5 and 60min post 0.1 μ M H₂O₂ treatment (*P*-value > 0.05). On the other hand, *hic-5* localization in a cytoplasmic = nuclear manner is insignificantly increased by around 3% (*P*-value > 0.05) after the first two time points and the last two points upon treating these MEFs with 0.1 μ M H₂O₂ and 0.5 μ M H₂O₂ in comparison with their untreated controls, respectively. While this localization decreases insignificantly in comparison with the untreated controls by 1.2% \pm 0.01 and 4.78% \pm 0.01 after the 1st and last time point in the 0.1 μ M H₂O₂ treated mutant MEFs (*P*-value > 0.05). Whereas, the nuclear > cytoplasmic localization of *hic-5* decreases insignificantly by around 3% when these MEFs are treated with 0.1 μ M H₂O₂ for 5 and 60min and with 0.5 μ M H₂O₂ for the 1st three time points in comparison with their untreated controls (*P*-value > 0.05). However, its localization there shows increases by around 2.5% in the remaining time points (*P*-

value > 0.05). Results are represented as mean fold difference in the fluorescence intensity \pm SEM of four independent experiments (figure 19).

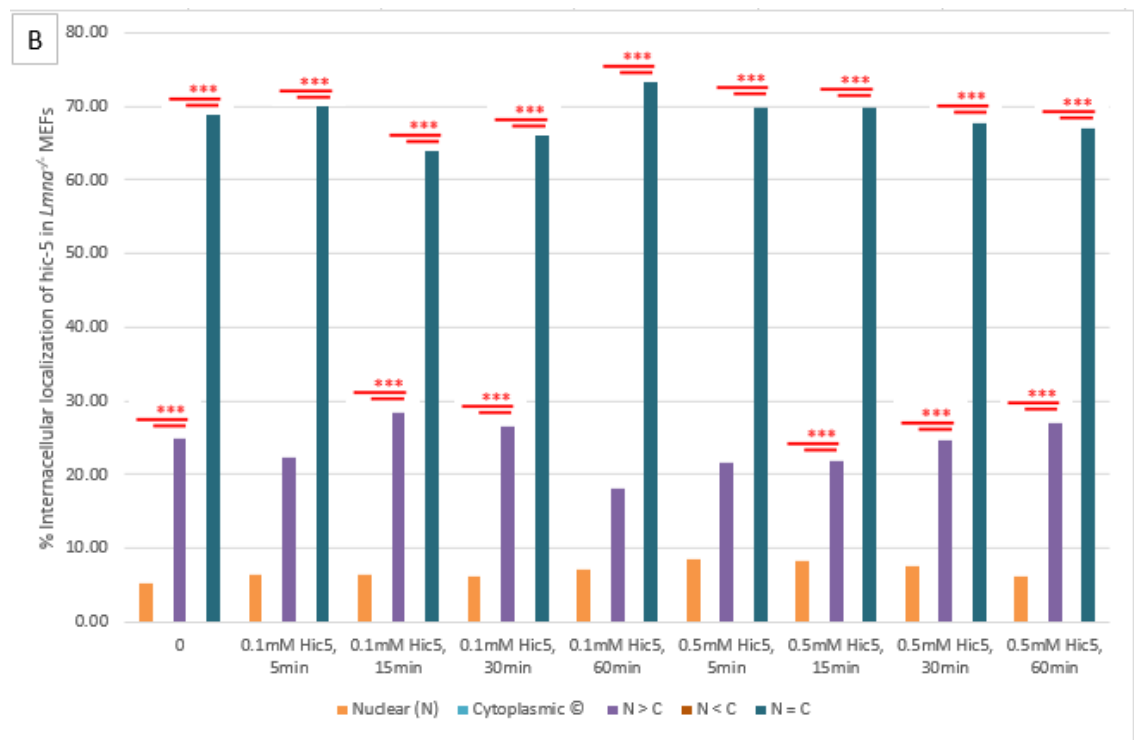
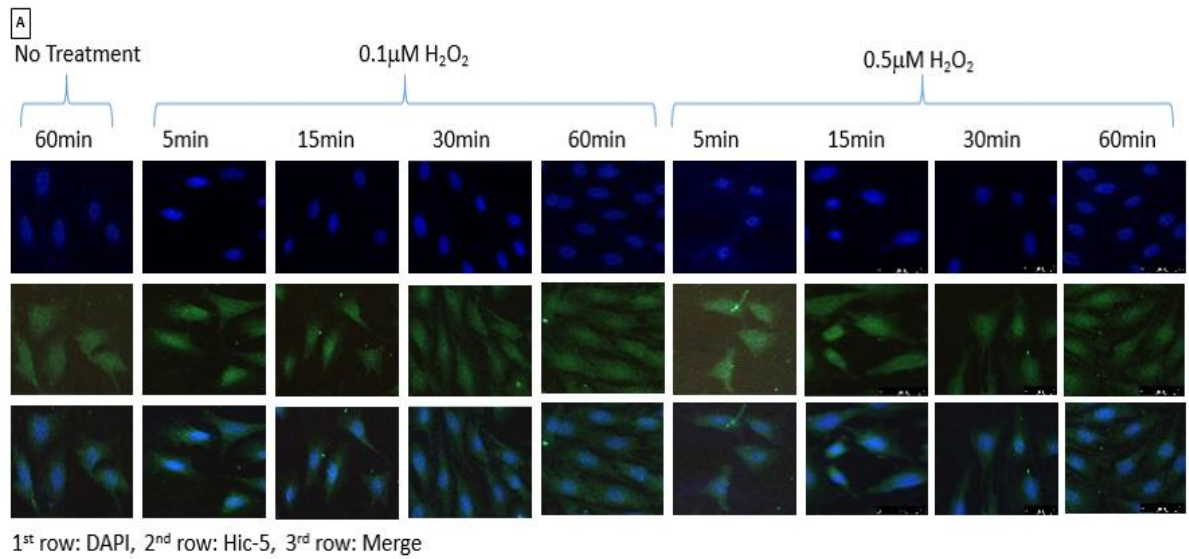


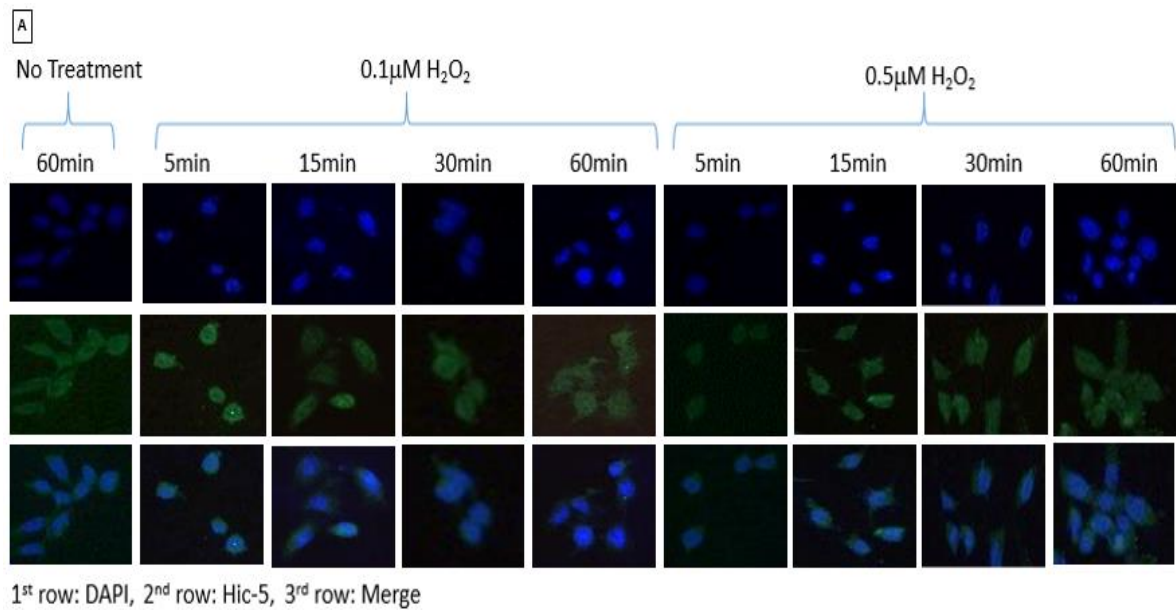
Figure 19: Immunofluorescence staining and semi-quantitative analysis of hic-5 protein cellular internal localization expression in *Lmna*^{-/-} MEFs cultured at 100% confluence under 0.1µM or 0.5µM H₂O₂-induced oxidative stress conditions for 5, 15, 30 and 60min. Panel A; representative upright fluorescence microscope images showing immunofluorescence staining of hic-5 in the lamin knockout MEFs. DAPI was used to stain the nuclei. Images were acquired at 20X magnification. Panel B: Semi-quantitative assessment of the hic-5 protein expression in lamin knockout MEFs signify that it is

significantly present more in a nuclear = cytoplasmic manner rather than nuclear and nuclear > cytoplasmic localizations. Moreover, they show significantly more hic-5 levels in a nuclear > cytoplasmic manner rather than nuclear only. These patterns are similar among the different time points and different treatments. Results were checked for statistical significance by one-way ANOVA. Three asterisks represent a statistical significance ($P < 0.001$).

4. $Lmna^{N195K/N195K}$ MEFs show increasing and decreasing fluctuations in their nuclear hic-5 localization in comparison to the nuclear = cytoplasmic one upon treating them with 0.1 μ M and 0.5 μ M H_2O_2 in comparison with their untreated controls. Yet, the nuclear localization significantly increases while the nuclear = cytoplasmic significantly decreases 15min post 0.1 μ M H_2O_2 treatment in comparison with the untreated controls.

The untreated $Lmna^{N195K/N195K}$ MEFs show insignificantly less nuclear localization of hic-5 by $4.12\% \pm 0.01$ in comparison with its nuclear = cytoplasmic localization ($P\text{-value} > 0.05$). This difference is also seen by $26.98\% \pm 0.01$, $7.87\% \pm 0.01$, and $2.13\% \pm 0.01$ ($P\text{-value} > 0.05$ for all) when these MEFs are treated with 0.1 μ M H_2O_2 for 5min and 0.5 μ M H_2O_2 for 5 and 15min, respectively. However, at the other time points, nuclear localization of hic-5 shows to be on average 20.81% ($P\text{-value} > 0.05$) more than its nuclear = cytoplasmic one. This increase is the most 30min after both treatments. However, the nuclear localization of hic-5 decreases insignificantly by $11.43\% \pm 0.01$ and $1.88\% \pm 0.01$ ($P\text{-value} > 0.05$ for both) 5min after treating the N195K mutant MEFs with 0.1 μ M H_2O_2 and 0.5 μ M H_2O_2 in comparison with their untreated controls, respectively. Then, this localization increases by an average of $10.55\% \pm 0.01$ at all the remaining time points; this increase is the most and highly significant 15min post 0.1 μ M H_2O_2 treatment ($P\text{-value} < 0.01$). On the other hand, the nuclear = cytoplasmic localization of hic-5 insignificantly increases by $11.43\% \pm 0.01$ and $1.88\% \pm 0.01$ ($P\text{-}$

value > 0.05 for both) 5min post 0.1 μ M and 0.5 μ M H₂O₂ treatments with respect to their untreated controls, respectively. However, this localization decreases by an average of 10.55% \pm 0.01 at all the other time points with respect to the untreated ones; this decrease is the most and highly significant 5min post the 0.1 μ M H₂O₂ treatment (*P-value* < 0.01). Results are represented as mean fold difference in the fluorescence intensity \pm SEM of four independent experiments (figure 20).



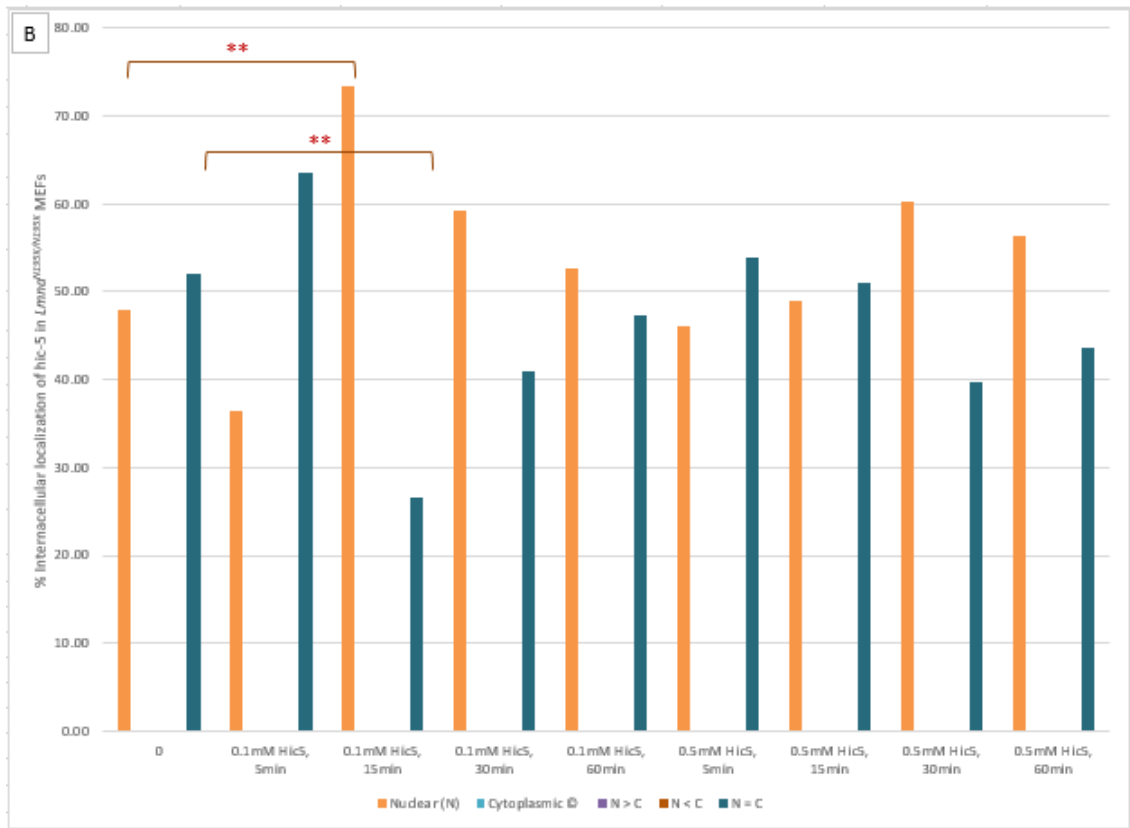
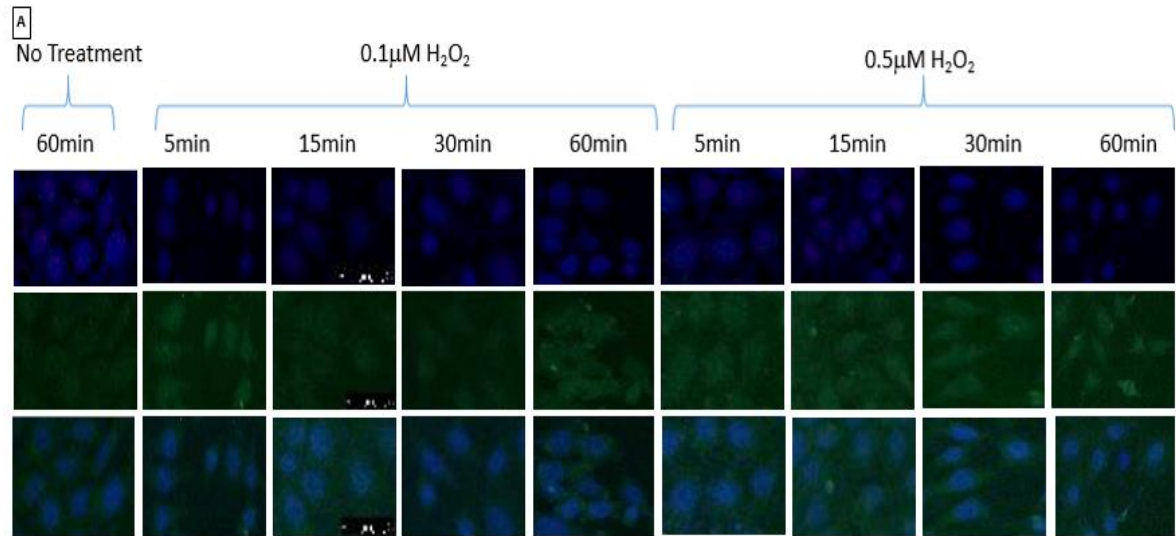


Figure 20: Immunofluorescence staining and semi-quantitative analysis of hic-5 protein cellular internal localization expression in *Lmna*^{N195K/N195K} MEFs cultured at 100% confluence under 0.1 μ M or 0.5 μ M H₂O₂-induced oxidative stress conditions for 5, 15, 30 and 60min. Panel A; representative upright fluorescence microscope images showing immunofluorescence staining of hic-5 in the N195K mutant MEFs. DAPI was used to stain the nuclei. Images were acquired at 20X magnification. Panel B: Semi-quantitative assessment of the hic-5 protein expression in these MEFs show that it is present in either in a nuclear = cytoplasmic manner or nuclear only. hic-5 localization is significantly altered 15min post 0.1 μ M of H₂O₂. Results were checked for statistical significance by one-way ANOVA. Two asterisks represent a statistical significance ($P < 0.01$).

5. Emd^Y MEFs show similar patterns of significantly high nuclear = cytoplasmic distribution of hic-5 within the treated and untreated groups like those of WT and lamin knockout MEFs. Yet, they are the only MEFs among the four tested samples to have a small fraction of their cells harboring hic-5 in a cytoplasmic > nuclear manner.

Fluorescence images and their semi-quantitative analysis data indicate significantly high localization levels of hic-5 in a nuclear = cytoplasmic manner that are approximately 77% more than hic-5's nuclear > cytoplasmic, nuclear < cytoplasmic, and nuclear distributions at all time points and treatment doses ($P\text{-value} < 0.001$). The levels of hic-5 localization in all the aforementioned categories slightly and insignificantly fluctuate by an average of $1.81\% \pm 0.01$ among the different treatments with respect to their untreated controls ($P\text{-value} > 0.05$). Yet, the greatest changes in nuclear > cytoplasmic and nuclear < cytoplasmic hic-5 distribution are observed 15min post the $0.1\mu\text{M}$ H₂O₂ treatment whereby the former category increases by $7.5\% \pm 0.01$ while the latter decreases by $3.82\% \pm 0.01$ with respect to the untreated controls ($P\text{-value} > 0.05$ for both). However, the greatest change in nuclear = cytoplasmic localization of hic-5 is observed 60min post the $0.1\mu\text{M}$ H₂O₂ treatment by which it insignificantly increases by $5.54\% \pm 0.01$ with respect to the untreated controls ($P\text{-value} > 0.05$). Results are represented as mean fold difference in the fluorescence intensity \pm SEM of four independent experiments (figure 21).



1st row: DAPI, 2nd row: Hic-5, 3rd row: Merge

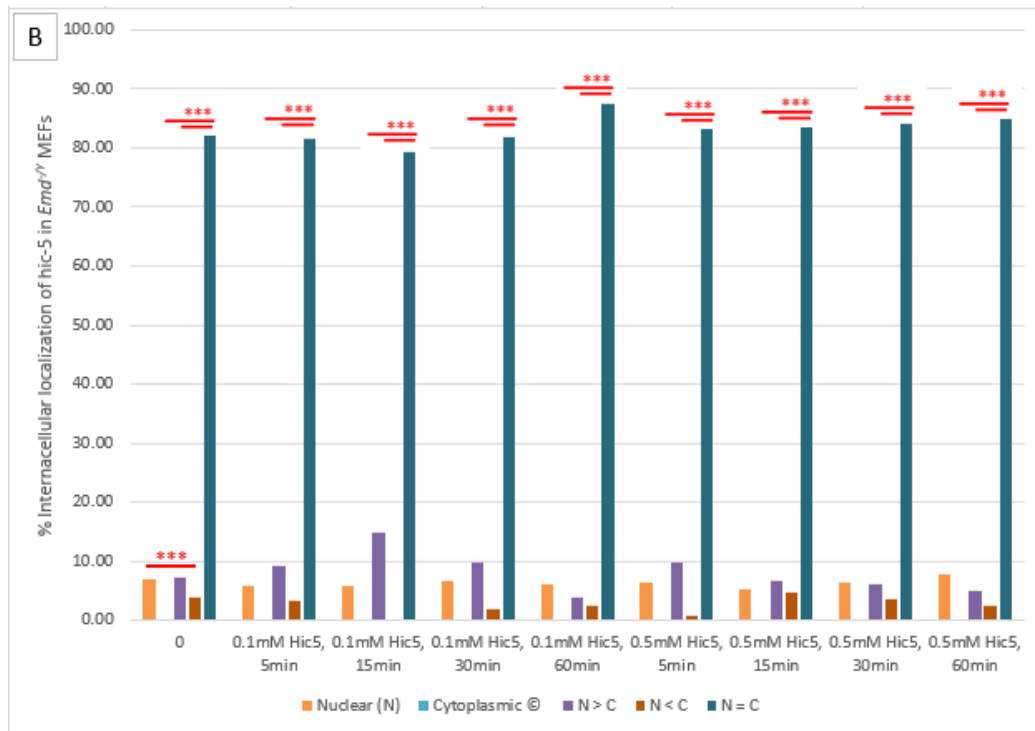


Figure 21: Immunofluorescence staining and semi-quantitative analysis of hic-5 protein cellular internal localization expression in *Emd*^{-/-} MEFs cultured at 100% confluence under 0.1 μ M or 0.5 μ M H₂O₂-induced oxidative stress conditions for 5, 15, 30 and 60min. Panel A; representative upright fluorescence microscope images showing immunofluorescence staining of hic-5 in the emerin null MEFs. DAPI was used to stain the nuclei. Images were acquired at 20X magnification. Panel B: Semi-quantitative assessment of the hic-5 protein expression in these MEFs show that it is significantly present more in a nuclear = cytoplasmic manner rather than nuclear and nuclear > cytoplasmic localizations. Results were checked for statistical significance by one-way ANOVA. Three asterisks represent a statistical significance ($P < 0.001$).

Tables 3 and 4 below give an overview of the previously stated baseline and hydrogen peroxide-induced oxidative stress results.

Table 3: Summary of baseline results			
Cell Type	Real-Time PCR Results (<i>hic-5</i> transcript levels)	Western blot Results (<i>hic-5</i> α protein levels)	Immunofluorescence Results (<i>hic-5</i> subcellular localization)
<i>Lmna</i> ^{+/+} MEFs	control	control	Around 90% equal distribution between nucleus and cytoplasm
<i>Lmna</i> ^{-/-} MEFs	More than WT* and N195K** MEFs	More than WT*** MEFs and the other 2 mutants MEFs	Around 90% equal distribution between nucleus and cytoplasm
<i>Lmna</i> ^{N195K/N195K} MEFs	Less than WT MEFs	More than WT MEFs	Around 75% nuclear localization
<i>Emd</i> ^{-Y} MEFs	More than WT and N195K MEFs	More than WTMEFs	Around 90% equal distribution between nucleus and cytoplasm

One asterisk represents a statistical significance ($P < 0.05$). Two asterisks represent a statistical significance ($P < 0.01$). Three asterisks represent a statistical significance ($P < 0.001$).

Table 4: Summary of H ₂ O ₂ -induced oxidative stress treatments results						
Cell Type	Real-Time PCR Results (<i>hic-5</i> transcript levels with respect to the untreated controls)		Western blot Results (<i>hic-5α</i> protein levels with respect to the untreated controls)		Immunofluorescence Results (<i>hic-5</i> subcellular localization with respect to the untreated controls)	
H ₂ O ₂ concentration (μM)	0.1	0.5	0.1	0.5	0.1	0.5
<i>Lmna</i> ^{+/+} MEFs	Decrease* after 15min	Decrease* after 15min	Decrease* after 30min	Decrease* after 30min	No significant changes	Decrease* in nuclear=cytoplasmic localization after 5min
<i>Lmna</i> ^{-/-} MEFs	No significant changes	Increase* after 5min	No significant changes	Increase* after 60min	No significant changes	No significant changes
<i>Lmna</i> ^{N195K/N195K} MEFs	Increase* after 15min	Increase* after 5 & 15min	Increase* after 5min & decrease* after 60min	Increase after 15** & 60* min	Increase* in nuclear localization after 15min	No significant changes
<i>Emd</i> ^{+/-} MEFs	No significant changes	No significant changes	Increase after 5** & 15*** min	Increase after 5***, 15**, 30***, and 60* min	No significant changes	No significant changes

One asterisk represents a statistical significance ($P < 0.05$). Two asterisks represent a statistical significance ($P < 0.01$). Three asterisks represent a statistical significance ($P < 0.001$).

CHAPTER IV

DISCUSSION

Laminopathies are a family of genetic maladies expressed as diverse pathologies that distress an extensive range of tissues, including skeletal and cardiac muscles. They are manifested due to mutations in the genes coding for lamin proteins and/or NE proteins. *LMNA* gene that codes for lamin A/C is the most mutated gene in the human genome with more than 400 mutations linked to it. Many hypotheses have been proposed to associate the tissue specific phenotypes observed in laminopathies with the ubiquitous expression of the *LMNA* gene. In this study, we focus on the gene regulation hypothesis that postulates that mutations in the *LMNA* gene lead to alterations in the normal gene expression profile either directly through lamin interactions with chromatin, or indirectly by the disruption of protein-protein interactions. In support with this hypothesis, many INM proteins are dependent on lamins A/C for proper localization. Accordingly, diverse proteins may be erroneously placed if their binding sites on lamin A/C are altered by mutations in the latter. This can partly clarify the phenotypic diversity and tissue specific malfunctions observed in laminopathies. In agreement, several studies have validated this correlation in various lamin interacting partners including TFs that work in a tissue specific manner. Our interest in the gene regulation theory along with the numerous findings that support it, aided us in directing our focus to the oxidative stress sensitive gene *hic-5* that has central roles in myogenesis and muscle differentiation. Moreover, muscles are stressed tissues and *hic-5* responds to oxidative stress signals by shuttling between FAs and the nucleus to activating c-fos that has crucial roles in cellular division, differentiation, and

survival. Nonetheless, EDMD and DCM are established in mechanically stressed tissues. As such, we hypothesized that mutations or complete loss of lamins A/C or emerin may affect the transcriptional and translational levels of Hic-5 aiding in disease pathogenesis of DCM and EDMD.

Our results show that under baseline conditions, *hic-5* normalized to *18S* increase significantly by 1.3-fold difference (± 0.1) and 1.7-fold difference (± 0.1) in *Lmna*^{-/-} MEFs and insignificantly by 1.0-fold difference (± 0.1) and 1.3-fold difference (± 0.1) in *Emd*^{-Y} MEFs with respect to their wild type controls and to *Lmna*^{N195K/N195K} MEFs, respectively. In agreement with this finding, under baseline conditions, hic-5 α is upregulated insignificantly in *Emd*^{-Y} MEFs by 1.0-fold difference (± 0.1) and significantly in *Lmna*^{-/-} MEFs by 3.0-fold difference (± 0.1) with respect to the WT controls. The fact that all three mutant MEF panels exhibit increased proliferation rates under baseline conditions may be in support with our findings. Accordingly, when hic-5 translocates into the nucleus, it activates *c-fos* in an Ets, ERE, and Sp1-dependent manner. Yet, hic-5 functions as a nuclear adaptor to these elements and does not directly bind to them. The complex assembly allowed by hic-5 then enables the cooperation of these factors to attain full transcriptional activity (Kim-Kaneyama et al., 2002). Immunofluorescence staining under baseline conditioned also showed that hic-5 protein has a similar pattern of localization in *Lmna*^{+/+}, *Lmna*^{-/-}, and *Emd*^{-Y} MEFs with a significant average of 87.12% (± 0.01) of more nuclear = cytoplasmic localization in comparison to the nuclear > cytoplasmic one, unlike *Lmna*^{N195K/N195K} MEFs which have significantly increased levels of hic-5 localization by 50.93% (± 0.01) in the nucleus rather than the nuclear = cytoplasmic distribution. The fact that N195K mutant MEFs have a more localized nuclear localization would partly explain why hic-5 showed

slight insignificant reductions in transcriptional levels accompanied by slight insignificant increases in its translational levels. It can be postulated that since it is primarily located in the nucleus and not doesn't show extensive nuclear = cytoplasmic localization like the other cell types, then it would harbor slightly lower level of transcripts than the other mutant cell lines. Moreover, the fact that in this DCM model, *hic-5* is almost primarily always located in the nucleus sheds the light on the possibility that is constitutively active in this disease. Yet the increased protein levels might be due to harboring more and different isoforms and to different phosphorylation levels of this protein inside the mutant MEF panels. However, no studies have investigated this relation yet.

In WT (*Lmna*^{+/+}) MEFs, *hic-5* normalized to *18S* significantly decreases in transcript levels by an average of 0.225-fold difference (± 0.1) and in protein levels by an average of 0.625-fold difference (± 0.1) 15 and 30min post 0.1 μ M and 0.5 μ M treatments with H₂O₂ with respect to their untreated controls, respectively. This is preceded by an immediate increase in protein levels by 0.75 fold difference (± 0.1) and a decrease in the cytoplasmic = nuclear distribution of *hic-5* upon the 0.5 μ M H₂O₂ treatment in comparison with the untreated controls. These changes suggest that since these MEFs have less transcript and protein levels of this protein at baseline, immediate translation of the protein is needed after both oxidative stress-inducing treatments. This then causes a decrease in transcript levels that get restored 30min post the treatments allowing for increases in protein level after 60min, accordingly. This restoration is required to withstand the elongated treatments.

In *Lmna*^{-/-} MEFs, *hic-5* normalized to *18S* increases significantly by 0.9-fold difference (± 0.2) directly and insignificantly by 1.2-fold difference (± 0.1) 1hr after

0.5 μ M treatment with H₂O₂ with respect to their untreated controls. Moreover, hic-5 α increases in protein levels with respect to the untreated controls throughout the different time points. This increase is significant by 0.75-fold difference (\pm 0.1) only after 1 hour of treatment. These results suggest that immediate increases in transcript levels allow for immediate increases in the protein levels of hic-5 α post this treatment. Then as transcript levels decrease due to consumption, the protein levels almost remain unchanged with respect to their previous increases possibly due to slow degradation rates. Finally, as this treatment proceeds, lamin knockout MEFs increase their *hic-5* transcript levels in response to it and as a result protein levels increase as well to endure the oxidative-rich micro-environment. On the other hand, 30min post treatment with 0.1 μ M H₂O₂, these lamin knockout MEFs demonstrate a statistically insignificant increase in *hic-5* normalized to *18S* by 0.4-fold difference (\pm 0.1) with respect to the untreated controls. Yet, the protein levels of hic-5 α decrease slightly and consistently by around 0.1-fold difference (\pm 0.05) with respect to their untreated controls at all time points. All these changes – though insignificant – suggest that the decrease in *hic-5* transcript levels observed after the 1st three time points, serves in the building up of protein levels that become significant 30min afterwards. Yet, since the 0.1 μ M treatment of H₂O₂ is generally considered very similar to physiological levels of this molecule, and since lamin knockout MEFs harbor increased pools of *hic-5* in transcript and protein levels in comparison with their WT controls at baseline levels, then it is quite expected not to see much change upon these nearly physiological treatments.

In *Lmna*^{N195K/N195K} MEFs, directly after 0.1 μ M and 0.5 μ M treatments with H₂O₂, *hic-5* normalized to *18S* significantly increases in 1.0-fold difference (\pm 0.1) and 0.4-fold difference (\pm 0.1) with respect to the untreated controls, respectively. Protein

levels also show significant immediate increases with respect to their untreated controls by 0.4 fold difference (± 0.1) and 0.7-fold difference (± 0.1), respectively. Moreover, nuclear localization of hic-5 significantly increases by around 26% while its nuclear = cytoplasmic one significantly decreases by around 15% early post 0.1 μM H_2O_2 treatment in comparison with the untreated controls. However, the increase in transcript levels with respect to controls is somewhat sustained with time unlike the protein levels that decrease with time to insignificantly peak again after 60min of the 0.1 μM treatment. Our results can be explained by that N195K mutant MEFs also have higher protein levels of hic-5 at baseline similar that to that of lamin knockout MEFs in comparison with WT MEFs; yet they are lower. These lower increased levels may partly explain why *Lmna*^{N195K/N195K} MEFs show more response to both treatments than the previously mentioned ones. In addition, the increased nuclear localization observed may serve in the activation of the signaling pathways responsible for combating the increases in ROS levels induced upon the treatment. Hic-5 that has a pI=6.8 (slightly acidic) may also be trapped inside the nucleus since this DCM mutation substitutes the acidic asparagine residue with the basic lysine residue. Hence, this change in charge may be responsible for the almost exclusive nuclear localization of hic-5. Interestingly, the HF1b/Sp4 TF that is expressed in the heart, was recently found to have increased nuclear localization in the N195K DCM model. The fact that this TF factor harbors three zinc fingers in its DNA-binding domains (Mounkes, 2005 #421) and that hic-5 also harbors zinc fingers in its LIM domains, allow us to postulate that a similar pattern of trapping of these TFs inside the nucleus may exist that is mediated by the altered lamina structure. E203G and E203K are two mutations of the rod domain of the *LMNA* gene and are in close proximity to the N195K mutation (Burke, 2002 #426). Therefore,

they may have similar deregulation in *hic-5* expression and distribution to the ones observed in our N195K DCM model.

In *Emd*^{-Y} MEFs, upon treatments with 0.1 μ M and 0.5 μ M of H₂O₂ for different time points, *hic-5* normalized to *18S* demonstrates slight statistically insignificant fluctuations with respect to their untreated controls. However, the protein levels of *hic-5* α show significant increases upon both treatments at the different time points with respect to their untreated controls. The slight insignificant fluctuations observed in transcript levels may also be attributed to the high levels of *hic-5* pool at baseline conditions that are comparable to that of lamin knockouts. Hence, the production of more transcripts would not be needed to respond to such levels of physiologically relevant ROS. Whereas, since *hic-5* α protein levels of the EMD knockout MEFs are similar to those of WT MEFs at baseline, they are then required to increase in response to our used oxidative stress treatments to maintain homeostasis. Yet, this increase despite the almost steady levels of *hic-5* transcripts may be due to quick synthesis of transcript templates keeping them at an almost steady-state accompanied by slower degradation of this protein inside the EMD knockout MEFs. In agreement, muscle-wasting diseases are characterized by increased activation and slower degradation rates of many proteins (Sandri, 2013 #431); hence *hic-5* could be one of them.

In agreement with our oxidative stress induced results, *Hic-5* was previously shown to be associated with increased *c-fos* gene expression in response to 60min exposure to 0.1mM and 0.5mM H₂O₂ treatments in the MC3T3 osteoblast precursor cell lines (Shibanuma et al., 2003). Hence, it is quite interesting that we observed an induction in the transcript and protein levels upon much lower and nearly physiological levels of H₂O₂ in the tested mutant MEF cell lines. Remarkably, it was previously

shown that reorganization of actin stimulates cells to produce ROS including H₂O₂ that serve as mediators linking the change in cellular morphology to nuclear gene expression events (Turner, 2000). These findings go in agreement with our results whereby EDMD and DCM are mainly manifested in mechanically stressed tissues, namely skeletal and cardiac muscles. These tissues respond to mechanical stress cues by cytoplasmic remodeling, mainly in actin dynamics, through mechanotransduction signaling cascades. The recent linkage of actin, MKL-1 and Hic-5 would hence serve an important role in our model. Upon mechanical stimulation and the generation of stress fibers, MKL1 interacts with emerin to accumulate in the nucleus and increase actin polymerization through the activation of the SRF signaling pathway (Ho et al., 2013; Miralles et al., 2003; Mouilleron et al., 2008). As previously stated, Hic-5 acts as a downstream effector of the MKL1/SRF pathway and hence it is induced along with α smooth muscle actin (α -SMA) in response to TGF- β and MKL-1 nuclear localization. Interestingly, a recent study revealed that Hic-5 is essential for the nuclear accumulation of MKL-1, generation of α -SMA, and inducing cellular contractility. This highlights the possibility of a mechanically-dependent positive feedback loop whereby Hic-5 and MKL-1 influence the expression of each other to influence the differentiation status of myofibroblast in response to TGF- β (Varney et al., 2016). This can also be attributed to the generation of ROS species in response to actin dynamics whereby a change in actin polymerization status would allow for increasing levels of ROS that in turn increase levels of Hic-5 hence linking the mechanosensitive pathways with the oxidative ones. Therefore, the delayed increased levels of transcript and protein levels of hic-5 may partly describe the impaired muscle regeneration observed in the studied disease models; whereby since they harbor at baseline increased levels of the Hic-5 protein and

transcripts, their response to oxidative and mechanical stress gets delayed allowing for tension and ROS to build up inside the cells rendering them toxic. Moreover, the pools of Hic-5 that are present at baseline may also be insufficient for responding to stress cues due to altered post-translational modifications, rendering their increased numbers of no apparent benefit to the MEFs. Moreover, the increased levels of hic-5 at baseline in these mutant MEF lines may serve to compensate for the deformed lamina structure that has crucial roles in chromatin packing, protection from stress, and actin dynamics. Hence, they could – more or less – play its role in maintaining regular actin dynamics allowing mechanotransduction signals to propagate despite the mutated link between the cytoplasm and the nucleoplasm. Additionally, since the phosphorylation levels of hic-5 are altered post osmotic stress by CAK β or Fyn (Ishino, Aoto, Sasaski, Suzuki, & Sasaki, 2000), and that A-type lamins are one of the most heavily phosphorylated proteins upon ERK1/2 activation (Finkel & Holbrook, 2000; Kosako et al., 2009; Lewis et al., 2000), it is important to test whether their phosphorylated states are differentially regulated at baseline and upon oxidative stress in the mutant MEF cell lines. Our results also suggest that the expression of hic-5 alfa is spatially and temporally regulated under baseline and oxidative stress conditions in the test laminopathic mutant cell lines. Hence, it would be interesting to test the expression of each of its ten isoforms in response to both treatments and at baseline conditions as well. Yet, the instability and short half-life of this protein make this objective challenging. In agreement with this, several studies have found contradictory results in terms of the differential expression of hic-5 isoforms and their biological functions. For example, some labs have reported that Hic-5 plays an important role in the induction of myogenesis while others reported an inhibitory role in this context (Hu et al., 1999; Shibamura, Iwabuchi, & Nose, 2002).

Adding to the complexity, isoforms of Hic-5 are differentially expressed in tissues (Z. Gao & Schwartz, 2005). We thereby postulate that certain isoforms might be differentially expressed within muscles and among the different cell lines. Interestingly, our western blots have detected – though inconsistently – 7 hic-5 isoforms in the WT MEFs, 2 isoforms in the N195K mutant MEFs and emerin null ones, and only 1 hic-5 isoform in the lamin knockout MEFs. This could partly explain the differences in transcript and protein levels of hic-5 observed at baseline and oxidative stress conditions between the different mutant MEF panels. This also suggests that hic-5 expression is deregulated differently between the different types of muscular laminopathies.

In summary, this study demonstrates a novel finding of hic-5 alteration in transcript and protein levels in muscular laminopathies. Initially, hic-5 abundance was always linked with vascular smooth muscles, we here show that it is highly abundant in fibroblasts linked with skeletal and cardiac muscles and is upregulated in related-laminopathic pathologies. Another key finding is the profuse nuclear localization of hic-5 in the tested DCM model which signifies a high possibility of constitutive action of hic-5 and might be the reason behind its slightly lower transcript levels in this model in comparison to their WT controls.

For future directions, Hic-5 transcript and protein levels under baseline and oxidative stress conditions will be assessed in a more relevant framework such as C₂C₁₂ myoblasts, cardiac myocytes, and cardiac and skeletal muscle tissue sections derived from EDMD and DCM mouse models. We also aim to assess the effects of mechanical stress on Hic-5 transcription, translation, and phosphorylation levels in the aforementioned models. Moreover, we are willing to test whether Hic-5

interacts/associates with lamin A/C protein by performing co-immunoprecipitation assays.

Finally, learning more about the effects of lamin A/C mutations on the differential expression of focal adhesion, oxidative stress-induced, and mechanosensitive genes such as *Hic-5* offers new insights into the cellular and molecular biology of muscular laminopathies through highlighting possible mechanisms accountable for the phenotypic complexity that accompanies them. Such studies provide the building blocks for viable therapies targeting the pathogenic manifestations of lamin A/C mutations in muscular laminopathies.

REFERENCES

- Aaronson, R. P., & Blobel, G. (1975). Isolation of nuclear pore complexes in association with a lamina. *Proceedings of the National Academy of Sciences*, 72(3), 1007-1011.
- Amendola, M., & van Steensel, B. (2014). Mechanisms and dynamics of nuclear lamina–genome interactions. *Current opinion in cell biology*, 28, 61-68.
- Andrés, V., & González, J. M. (2009). Role of A-type lamins in signaling, transcription, and chromatin organization. *The Journal of cell biology*, 187(7), 945-957.
- Balza, R. O., & Misra, R. P. (2006). Role of the serum response factor in regulating contractile apparatus gene expression and sarcomeric integrity in cardiomyocytes. *Journal of Biological Chemistry*, 281(10), 6498-6510.
- BÉCANE, H., Bonne, G., Varnous, S., Muchir, A., Ortega, V., Hammouda, E. H., . . . Eymard, B. (2000). High incidence of sudden death with conduction system and myocardial disease due to lamins A and C gene mutation. *Pacing and Clinical Electrophysiology*, 23(11), 1661-1666.
- Belgareh, N., & Doye, V. (1997). Dynamics of nuclear pore distribution in nucleoporin mutant yeast cells. *The Journal of cell biology*, 136(4), 747-759.
- Belmont, A. S., Zhai, Y., & Thilenius, A. (1993). Lamin B distribution and association with peripheral chromatin revealed by optical sectioning and electron microscopy tomography. *The Journal of cell biology*, 123(6), 1671-1685.
- Ben-Harush, K., Wiesel, N., Frenkiel-Krispin, D., Moeller, D., Soreq, E., Aebi, U., . . . Medalia, O. (2009). The supramolecular organization of the *C. elegans* nuclear lamin filament. *Journal of molecular biology*, 386(5), 1392-1402.
- Bonne, G., Di Barletta, M. R., Varnous, S., Bécane, H.-M., Hammouda, E.-H., Merlini, L., . . . Urtizbera, J.-A. (1999). Mutations in the gene encoding lamin A/C cause autosomal dominant Emery-Dreifuss muscular dystrophy. *Nature genetics*, 21(3), 285-288.
- Bonne, G., Mercuri, E., Muchir, A., Urtizbera, A., Becane, H., Recan, D., . . . Reuner, U. (2000). Clinical and molecular genetic spectrum of autosomal dominant Emery-Dreifuss muscular dystrophy due to mutations of the lamin A/C gene. *Annals of neurology*, 48(2), 170-180.
- Boriani, G., Gallina, M., Merlini, L., Bonne, G., Toniolo, D., Amati, S., . . . Bonvicini, M. (2003). Clinical Relevance of Atrial Fibrillation/Flutter, Stroke, Pacemaker Implant, and Heart Failure in Emery-Dreifuss Muscular Dystrophy A Long-Term Longitudinal Study. *Stroke*, 34(4), 901-908.

- Brack, A. S., Conboy, I. M., Conboy, M. J., Shen, J., & Rando, T. A. (2008). A temporal switch from notch to Wnt signaling in muscle stem cells is necessary for normal adult myogenesis. *Cell stem cell*, 2(1), 50-59.
- Brodsky, G. L., Muntoni, F., Miodini, S., Sinagra, G., Sewry, C., & Mestroni, L. (2000). Lamin A/C gene mutation associated with dilated cardiomyopathy with variable skeletal muscle involvement. *Circulation*, 101(5), 473-476.
- Broers, J. L., Hutchison, C. J., & Ramaekers, F. (2004). Laminopathies. *The Journal of pathology*, 204(4), 478-488.
- Bucci, M., & Wenthe, S. R. (1997). In vivo dynamics of nuclear pore complexes in yeast. *The Journal of cell biology*, 136(6), 1185-1199.
- Burke, B., & Stewart, C. L. (2002). Life at the edge: the nuclear envelope and human disease. *Nature Reviews Molecular Cell Biology*, 3(8), 575-585.
- Cabanillas, R., Cadiñanos, J., Villameytide, J. A., Pérez, M., Longo, J., Richard, J. M., . . . González, D. J. (2011). Néstor–Guillermo progeria syndrome: a novel premature aging condition with early onset and chronic development caused by BANF1 mutations. *American journal of medical genetics Part A*, 155(11), 2617-2625.
- Cai, M., Huang, Y., Ghirlando, R., Wilson, K. L., Craigie, R., & Clore, G. M. (2001). Solution structure of the constant region of nuclear envelope protein LAP2 reveals two LEM - domain structures: one binds BAF and the other binds DNA. *The EMBO Journal*, 20(16), 4399-4407.
- Cao, K., Blair, C. D., Faddah, D. A., Kieckhafer, J. E., Olive, M., Erdos, M. R., . . . Collins, F. S. (2011). Progerin and telomere dysfunction collaborate to trigger cellular senescence in normal human fibroblasts. *The Journal of clinical investigation*, 121(7), 2833-2844.
- Carmosino, M., Torretta, S., Procino, G., Gerbino, A., Forleo, C., Favale, S., & Svelto, M. (2014). Role of nuclear Lamin A/C in cardiomyocyte functions. *Biology of the Cell*, 106(10), 346-358.
- Chi, Y.-H., Chen, Z.-J., & Jeang, K.-T. (2009). The nuclear envelopathies and human diseases. *Journal of biomedical science*, 16(1), 1.
- Chiarini, A., Whitfield, J. F., Pacchiana, R., Armato, U., & Dal Pra, I. (2008). Photoexcited calphostin C selectively destroys nuclear lamin B1 in neoplastic human and rat cells—a novel mechanism of action of a photodynamic tumor therapy agent. *Biochimica et Biophysica Acta (BBA)-Molecular Cell Research*, 1783(9), 1642-1653.

- Ciska, M., Masuda, K., & de la Espina, S. M. D. (2013). Lamin-like analogues in plants: the characterization of NMCP1 in *Allium cepa*. *Journal of experimental botany*, ert020.
- Ciska, M., & Moreno Díaz de la Espina, S. (2013). NMCP/LINC proteins: putative lamin analogs in plants? *Plant signaling & behavior*, 8(12), e26669.
- Coffinier, C., Chang, S. Y., Nobumori, C., Tu, Y., Farber, E. A., Toth, J. I., . . . Young, S. G. (2010). Abnormal development of the cerebral cortex and cerebellum in the setting of lamin B2 deficiency. *Proceedings of the National Academy of Sciences*, 107(11), 5076-5081.
- Cremer, T., & Cremer, M. (2010). Chromosome territories. *Cold Spring Harbor perspectives in biology*, 2(3), a003889.
- Crider, B. J., Risinger, G. M., Haaksma, C. J., Howard, E. W., & Tomasek, J. J. (2011). Myocardin-related transcription factors A and B are key regulators of TGF- β 1-induced fibroblast to myofibroblast differentiation. *Journal of Investigative Dermatology*, 131(12), 2378-2385.
- Crisp, M., Liu, Q., Roux, K., Rattner, J., Shanahan, C., Burke, B., . . . Hodzic, D. (2006). Coupling of the nucleus and cytoplasm role of the LINC complex. *The Journal of cell biology*, 172(1), 41-53.
- Croft, J. A., Bridger, J. M., Boyle, S., Perry, P., Teague, P., & Bickmore, W. A. (1999). Differences in the localization and morphology of chromosomes in the human nucleus. *The Journal of cell biology*, 145(6), 1119-1131.
- Dabiri, G., Tumbarello, D. A., Turner, C. E., & Van De Water, L. (2008a). Hic-5 promotes the hypertrophic scar myofibroblast phenotype by regulating the TGF- β 1 autocrine loop. *Journal of Investigative Dermatology*, 128(10), 2518-2525.
- Dabiri, G., Tumbarello, D. A., Turner, C. E., & Van De Water, L. (2008b). TGF- β 1 slows the growth of pathogenic myofibroblasts through a mechanism requiring the focal adhesion protein, Hic-5. *Journal of Investigative Dermatology*, 128(2), 280-291.
- Dahl, K. N., Scaffidi, P., Islam, M. F., Yodh, A. G., Wilson, K. L., & Misteli, T. (2006). Distinct structural and mechanical properties of the nuclear lamina in Hutchinson–Gilford progeria syndrome. *Proceedings of the National Academy of Sciences*, 103(27), 10271-10276.
- Dawid, I. B., Breen, J. J., & Toyama, R. (1998). LIM domains: multiple roles as adapters and functional modifiers in protein interactions. *Trends in Genetics*, 14(4), 156-162.

- de la Luna, S., Allen, K. E., Mason, S. L., & La Thangue, N. B. (1999). Integration of a growth - suppressing BTB/POZ domain protein with the DP component of the E2F transcription factor. *The EMBO journal*, 18(1), 212-228.
- de Oca, R. M., Shoemaker, C. J., Gucek, M., Cole, R. N., & Wilson, K. L. (2009). Barrier-to-autointegration factor proteome reveals chromatin-regulatory partners. *PloS one*, 4(9), e7050.
- Dechat, T., Adam, S., Taimen, P., Shimi, T., & Goldman, R. Nuclear lamins. *Cold Spring Harb Perspect Biol* 2010; 2: a000547.
- Dechat, T., Adam, S. A., Taimen, P., Shimi, T., & Goldman, R. D. (2010). Nuclear lamins. *Cold Spring Harbor perspectives in biology*, 2(11), a000547.
- Dedeic, Z., Cetera, M., Cohen, T. V., & Holaska, J. M. (2011). Emerin inhibits Lmo7 binding to the Pax3 and MyoD promoters and expression of myoblast proliferation genes. *J Cell Sci*, 124(10), 1691-1702.
- Demmerle, J., Koch, A. J., & Holaska, J. M. (2012). The nuclear envelope protein emerin binds directly to histone deacetylase 3 (HDAC3) and activates HDAC3 activity. *Journal of Biological Chemistry*, 287(26), 22080-22088.
- Dessev, G., Iovcheva-Dessev, C., Bischoff, J. R., Beach, D., & Goldman, R. (1991). A complex containing p34cdc2 and cyclin B phosphorylates the nuclear lamin and disassembles nuclei of clam oocytes in vitro. *The Journal of cell biology*, 112(4), 523-533.
- Dittmer, T. A., & Misteli, T. (2011). The lamin protein family. *Genome biology*, 12(5), 1.
- Dreesen, O., Chojnowski, A., Ong, P. F., Zhao, T. Y., Common, J. E., Lunny, D., . . . Stewart, C. L. (2013). Lamin B1 fluctuations have differential effects on cellular proliferation and senescence. *The Journal of cell biology*, 200(5), 605-617.
- Dreuillet, C., Harper, M., Tillit, J., Kress, M., & Ernoult - Lange, M. (2008). Mislocalization of human transcription factor MOK2 in the presence of pathogenic mutations of lamin A/C. *Biology of the Cell*, 100(1), 51-61.
- Dreuillet, C., Tillit, J., Kress, M., & Ernoult - Lange, M. (2002). In vivo and in vitro interaction between human transcription factor MOK2 and nuclear lamin A/C. *Nucleic acids research*, 30(21), 4634-4642.
- DuBois, K. N., Alsford, S., Holden, J. M., Buisson, J., Swiderski, M., Bart, J.-M., . . . Barry, J. D. (2012). NUP-1 Is a large coiled-coil nucleoskeletal protein in trypanosomes with lamin-like functions. *PLoS Biol*, 10(3), e1001287.
- Dubowitz, V. (1977). *Muscle disorders in childhood*: Karger Publishers.

- Dutta, S., Bhattacharyya, M., & Sengupta, K. (2016). Implications and Assessment of the Elastic Behavior of Lamins in Laminopathies. *Cells*, 5(4), 37.
- Ellis, J. A., Craxton, M., Yates, J., & Kendrick-Jones, J. (1998). Aberrant intracellular targeting and cell cycle-dependent phosphorylation of emerin contribute to the Emery-Dreifuss muscular dystrophy phenotype. *Journal of Cell Science*, 111(6), 781-792.
- Emery, A. E. (2000). Emery–Dreifuss muscular dystrophy—a 40 year retrospective. *Neuromuscular Disorders*, 10(4), 228-232.
- Fahrenkrog, B., Maco, B., Fager, A. M., Köser, J., Sauder, U., Ullman, K. S., & Aepli, U. (2002). Domain-specific antibodies reveal multiple-site topology of Nup153 within the nuclear pore complex. *Journal of structural biology*, 140(1), 254-267.
- Fawcett, D. W. (1966). On the occurrence of a fibrous lamina on the inner aspect of the nuclear envelope in certain cells of vertebrates. *American Journal of Anatomy*, 119(1), 129-145.
- Fernandez, I., Martin-Garrido, A., Zhou, D. W., Clempus, R. E., Seidel-Rogol, B., Valdivia, A., . . . San Martin, A. (2015). Hic-5 Mediates TGFβ–Induced Adhesion in Vascular Smooth Muscle Cells by a Nox4-Dependent Mechanism. *Arteriosclerosis, thrombosis, and vascular biology*, 35(5), 1198-1206.
- Finkel, T., & Holbrook, N. J. (2000). Oxidants, oxidative stress and the biology of ageing. *Nature*, 408(6809), 239-247.
- Fiserova, J., & Goldberg, M. W. (2010). Relationships at the nuclear envelope: lamins and nuclear pore complexes in animals and plants. *Biochemical Society Transactions*, 38(3), 829-831.
- Folker, E. S., Östlund, C., Luxton, G. G., Worman, H. J., & Gundersen, G. G. (2011). Lamin A variants that cause striated muscle disease are defective in anchoring transmembrane actin-associated nuclear lines for nuclear movement. *Proceedings of the National Academy of Sciences*, 108(1), 131-136.
- Freund, A., Laberge, R.-M., Demaria, M., & Campisi, J. (2012). Lamin B1 loss is a senescence-associated biomarker. *Molecular biology of the cell*, 23(11), 2066-2075.
- Fujimoto, N., Yeh, S., Kang, H.-Y., Inui, S., Chang, H.-C., Mizokami, A., & Chang, C. (1999). Cloning and characterization of androgen receptor coactivator, ARA55, in human prostate. *Journal of Biological Chemistry*, 274(12), 8316-8321.
- Funakoshi, M., Tsuchiya, Y., & Arahata, K. (1999). Emerin and cardiomyopathy in Emery–Dreifuss muscular dystrophy. *Neuromuscular Disorders*, 9(2), 108-114.

- Gao, Z.-L., Deblis, R., Glenn, H., & Schwartz, L. M. (2007). Differential roles of HIC-5 isoforms in the regulation of cell death and myotube formation during myogenesis. *Experimental cell research*, 313(19), 4000-4014.
- Gao, Z., & Schwartz, L. M. (2005). Identification and analysis of Hic - 5/ARA55 isoforms: Implications for integrin signaling and steroid hormone action. *FEBS letters*, 579(25), 5651-5657.
- Gerace, L., & Blobel, G. (1980). The nuclear envelope lamina is reversibly depolymerized during mitosis. *Cell*, 19(1), 277-287.
- Gerace, L., Blum, A., & Blobel, G. (1978). Immunocytochemical localization of the major polypeptides of the nuclear pore complex-lamina fraction. Interphase and mitotic distribution. *The Journal of Cell Biology*, 79(2), 546-566.
- Goldberg, M. W., & Allen, T. D. (1996). The nuclear pore complex and lamina: three-dimensional structures and interactions determined by field emission in-lens scanning electron microscopy. *Journal of molecular biology*, 257(4), 848-865.
- Gonzalez-Suarez, I., Redwood, A. B., & Gonzalo, S. (2009). Loss of A-type lamins and genomic instability. *Cell Cycle*, 8(23), 3860-3865.
- Gonzalez - Suarez, I., Redwood, A. B., Perkins, S. M., Vermolen, B., Lichtensztejin, D., Grotzky, D. A., . . . Sullivan, T. (2009). Novel roles for A - type lamins in telomere biology and the DNA damage response pathway. *The EMBO journal*, 28(16), 2414-2427.
- González, J. M., Navarro-Puche, A., Casar, B., Crespo, P., & Andrés, V. (2008). Fast regulation of AP-1 activity through interaction of lamin A/C, ERK1/2, and c-Fos at the nuclear envelope. *The Journal of cell biology*, 183(4), 653-666.
- Gorelick, P. B., Testai, F., Hankey, G., & Wardlaw, J. M. (2014). *Hankey's clinical neurology*: CRC Press.
- Graumann, K. (2014). Evidence for LINC1-SUN associations at the plant nuclear periphery. *PLoS One*, 9(3), e93406.
- Grossman, E., Dahan, I., Stick, R., Goldberg, M. W., Gruenbaum, Y., & Medalia, O. (2012). Filaments assembly of ectopically expressed *Caenorhabditis elegans* lamin within *Xenopus* oocytes. *Journal of structural biology*, 177(1), 113-118.
- Gruenbaum, Y., & Foisner, R. (2015). Lamins: nuclear intermediate filament proteins with fundamental functions in nuclear mechanics and genome regulation. *Annual review of biochemistry*, 84, 131-164.
- Gruenbaum, Y., Hochstrasser, M., Mathog, D., Saumweber, H., Agard, D., & Sedat, J. (1984). Spatial organization of the *Drosophila* nucleus: a three-dimensional cytogenetic study. *J Cell Sci*, 1984(Supplement 1), 223-234.

- Gruenbaum, Y., Landesman, Y., Drees, B., Bare, J. W., Saumweber, H., Paddy, M. R., . . . Fisher, P. A. (1988). Drosophila nuclear lamin precursor Dm0 is translated from either of two developmentally regulated mRNA species apparently encoded by a single gene. *The Journal of Cell Biology*, *106*(3), 585-596.
- Guelen, L., Pagie, L., Brasset, E., Meuleman, W., Faza, M. B., Talhout, W., . . . de Laat, W. (2008). Domain organization of human chromosomes revealed by mapping of nuclear lamina interactions. *Nature*, *453*(7197), 948-951.
- Hallstrom, T. C., Mori, S., & Nevins, J. R. (2008). An E2F1-dependent gene expression program that determines the balance between proliferation and cell death. *Cancer cell*, *13*(1), 11-22.
- Haraguchi, T., Holaska, J. M., Yamane, M., Koujin, T., Hashiguchi, N., Mori, C., . . . Hiraoka, Y. (2004). Emerin binding to Btf, a death - promoting transcriptional repressor, is disrupted by a missense mutation that causes Emery–Dreifuss muscular dystrophy. *European Journal of Biochemistry*, *271*(5), 1035-1045.
- Harborth, J., Elbashir, S. M., Bechert, K., Tuschl, T., & Weber, K. (2001). Identification of essential genes in cultured mammalian cells using small interfering RNAs. *Journal of cell science*, *114*(24), 4557-4565.
- Harper, M., Tillit, J., Kress, M., & Ernoult - Lange, M. (2009). Phosphorylation - dependent binding of human transcription factor MOK2 to lamin A/C. *FEBS journal*, *276*(11), 3137-3147.
- Heessen, S., & Fornerod, M. (2007). The inner nuclear envelope as a transcription factor resting place. *EMBO reports*, *8*(10), 914-919.
- Heitlinger, E., Peter, M., Häner, M., Lustig, A., Aebi, U., & Nigg, E. (1991). Expression of chicken lamin B2 in Escherichia coli: characterization of its structure, assembly, and molecular interactions. *The Journal of Cell Biology*, *113*(3), 485-495.
- Heitzer, M., & DeFranco, D. (2006). Mechanism of action of Hic-5/androgen receptor activator 55, a LIM domain-containing nuclear receptor coactivator. *Molecular Endocrinology*, *20*(1), 56-64.
- Heitzer, M. D., & DeFranco, D. B. (2006). Hic-5, an adaptor-like nuclear receptor coactivator. *Nucl Recept Signal*, *4*, e019.
- Herrmann, H., & Aebi, U. (2004). Intermediate filaments: molecular structure, assembly mechanism, and integration into functionally distinct intracellular scaffolds. *Annual review of biochemistry*, *73*(1), 749-789.
- Hilenski, L. L., Clempus, R. E., Quinn, M. T., Lambeth, J. D., & Griendling, K. K. (2004). Distinct subcellular localizations of Nox1 and Nox4 in vascular smooth muscle cells. *Arteriosclerosis, thrombosis, and vascular biology*, *24*(4), 677-683.

- Ho, C. Y., Jaalouk, D. E., Vartiainen, M. K., & Lammerding, J. (2013). Lamin A/C and emerin regulate MKL1-SRF activity by modulating actin dynamics. *Nature*, *497*(7450), 507-511.
- Ho, C. Y., & Lammerding, J. (2012). Lamins at a glance. *J Cell Sci*, *125*(9), 2087-2093.
- Hofemeister, H., Kuhn, C., Franke, W. W., Weber, K., & Stick, R. (2002). Conservation of the gene structure and membrane-targeting signals of germ cell-specific lamin LIII in amphibians and fish. *European journal of cell biology*, *81*(2), 51-60.
- Holaska, J. M., Lee, K. K., Kowalski, A. K., & Wilson, K. L. (2003). Transcriptional repressor germ cell-less (GCL) and barrier to autointegration factor (BAF) compete for binding to emerin in vitro. *Journal of Biological Chemistry*, *278*(9), 6969-6975.
- Holaska, J. M., Rais-Bahrami, S., & Wilson, K. L. (2006). Lmo7 is an emerin-binding protein that regulates the transcription of emerin and many other muscle-relevant genes. *Human molecular genetics*, *15*(23), 3459-3472.
- Holaska, J. M., & Wilson, K. L. (2006). Multiple roles for emerin: Implications for Emery - Dreifuss muscular dystrophy. *The Anatomical Record Part A: Discoveries in Molecular, Cellular, and Evolutionary Biology*, *288*(7), 676-680.
- Holaska, J. M., & Wilson, K. L. (2007). An emerin “proteome”: purification of distinct emerin-containing complexes from HeLa cells suggests molecular basis for diverse roles including gene regulation, mRNA splicing, signaling, mechanosensing, and nuclear architecture. *Biochemistry*, *46*(30), 8897-8908.
- Holaska, J. M., Wilson, K. L., & Mansharamani, M. (2002). The nuclear envelope, lamins and nuclear assembly. *Current opinion in cell biology*, *14*(3), 357-364.
- Hu, Y., Cascone, P. J., Cheng, L., Sun, D., Nambu, J. R., & Schwartz, L. M. (1999). Lepidopteran DALP, and its mammalian ortholog HIC-5, function as negative regulators of muscle differentiation. *Proceedings of the National Academy of Sciences*, *96*(18), 10218-10223.
- Hutchison, C. J., & Worman, H. J. (2004). A-type lamins: guardians of the soma? *Nature Cell Biology*, *6*(11), 1062-1067.
- Ishino, M., Aoto, H., Sasasaki, H., Suzuki, R., & Sasaki, T. (2000). Phosphorylation of Hic - 5 at tyrosine 60 by CAK β and Fyn. *FEBS letters*, *474*(2-3), 179-183.
- Ivorra, C., Kubicek, M., González, J. M., Sanz-González, S. M., Álvarez-Barrientos, A., O'Connor, J.-E., . . . Andrés, V. (2006). A mechanism of AP-1 suppression through interaction of c-Fos with lamin A/C. *Genes & Development*, *20*(3), 307-320.

- Jahn, D., Schramm, S., Schnölzer, M., Heilmann, C. J., De Koster, C. G., Schütz, W., . . . Alsheimer, M. (2012). A truncated lamin A in the *Lmna*^{-/-} mouse line: implications for the understanding of laminopathies. *Nucleus*, 3(5), 463-474.
- Kamand, L. A. (2012). *Deregulated caveolin-1 and Hic-5 expression in mouse embryo fibroblasts lacking A-type lamin and homozygous for the N195K mutant form*.
- Kasai, M., Guerrero-Santoro, J., Friedman, R., Leman, E. S., Getzenberg, R. H., & DeFranco, D. B. (2003). The Group 3 LIM domain protein paxillin potentiates androgen receptor transactivation in prostate cancer cell lines. *Cancer research*, 63(16), 4927-4935.
- Katta, S. S., Smoyer, C. J., & Jaspersen, S. L. (2014). Destination: inner nuclear membrane. *Trends in cell biology*, 24(4), 221-229.
- Kennedy, B. K., Barbie, D. A., Classon, M., Dyson, N., & Harlow, E. (2000). Nuclear organization of DNA replication in primary mammalian cells. *Genes & Development*, 14(22), 2855-2868.
- Kim-Kaneyama, J.-r., Shibamura, M., & Nose, K. (2002). Transcriptional activation of the c-fos gene by a LIM protein, Hic-5. *Biochemical and biophysical research communications*, 299(3), 360-365.
- Kim-Kaneyama, J.-r., Suzuki, W., Ichikawa, K., Ohki, T., Kohno, Y., Sata, M., . . . Shibamura, M. (2005). Uni-axial stretching regulates intracellular localization of Hic-5 expressed in smooth-muscle cells in vivo. *J Cell Sci*, 118(5), 937-949.
- Kind, J., & van Steensel, B. (2014). Stochastic genome-nuclear lamina interactions: modulating roles of Lamin A and BAF. *Nucleus*, 5(2), 124-130.
- Klapper, M., Exner, K., Kempf, A., Gehrig, C., Stuurman, N., Fisher, P. A., & Krohne, G. (1997). Assembly of A- and B-type lamins studied in vivo with the baculovirus system. *Journal of Cell Science*, 110(20), 2519-2532.
- Koch, A. J., & Holaska, J. M. (2014). Emerin in health and disease. *Semin Cell Dev Biol*, 29, 95-106. doi:10.1016/j.semcdb.2013.12.008
- Kosako, H., Yamaguchi, N., Aranami, C., Ushiyama, M., Kose, S., Imamoto, N., . . . Hattori, S. (2009). Phosphoproteomics reveals new ERK MAP kinase targets and links ERK to nucleoporin-mediated nuclear transport. *Nature structural & molecular biology*, 16(10), 1026-1035.
- Krüger, A., Batsios, P., Baumann, O., Luckert, E., Schwarz, H., Stick, R., . . . Gräf, R. (2012). Characterization of NE81, the first lamin-like nucleoskeleton protein in a unicellular organism. *Molecular biology of the cell*, 23(2), 360-370.

- Kubben, N., Voncken, J. W., Konings, G., van Weeghel, M., van den Hoogenhof, M. M., Gijbels, M., . . . Dahlmans, V. (2011). Post-natal myogenic and adipogenic developmental: defects and metabolic impairment upon loss of A-type lamins. *Nucleus*, 2(3), 195-207.
- Kumaran, R. I., & Spector, D. L. (2008). A genetic locus targeted to the nuclear periphery in living cells maintains its transcriptional competence. *The Journal of cell biology*, 180(1), 51-65.
- Lammerding, J., Hsiao, J., Schulze, P. C., Kozlov, S., Stewart, C. L., & Lee, R. T. (2005). Abnormal nuclear shape and impaired mechanotransduction in emerin-deficient cells. *The Journal of cell biology*, 170(5), 781-791.
- Lammerding, J., Schulze, P. C., Takahashi, T., Kozlov, S., Sullivan, T., Kamm, R. D., . . . Lee, R. T. (2004). Lamin A/C deficiency causes defective nuclear mechanics and mechanotransduction. *The Journal of clinical investigation*, 113(3), 370-378.
- Lee, D. C., Welton, K. L., Smith, E. D., & Kennedy, B. K. (2009). A-type nuclear lamins act as transcriptional repressors when targeted to promoters. *Experimental cell research*, 315(6), 996-1007.
- Lee, K. K., Haraguchi, T., Lee, R. S., Koujin, T., Hiraoka, Y., & Wilson, K. L. (2001). Distinct functional domains in emerin bind lamin A and DNA-bridging protein BAF. *Journal of Cell Science*, 114(24), 4567-4573.
- Lehner, C. F., Stick, R., Eppenberger, H. M., & Nigg, E. A. (1987). Differential expression of nuclear lamin proteins during chicken development. *The Journal of cell biology*, 105(1), 577-587.
- Lewis, T. S., Hunt, J. B., Aveline, L. D., Jonscher, K. R., Louie, D. F., Yeh, J. M., . . . Ahn, N. G. (2000). Identification of novel MAP kinase pathway signaling targets by functional proteomics and mass spectrometry. *Molecular cell*, 6(6), 1343-1354.
- Li, J., Wang, J., Wang, J., Nawaz, Z., Liu, J. M., Qin, J., & Wong, J. (2000). Both corepressor proteins SMRT and N - CoR exist in large protein complexes containing HDAC3. *The EMBO journal*, 19(16), 4342-4350.
- Liu, B., Wang, J., Chan, K. M., Tjia, W. M., Deng, W., Guan, X., . . . Chen, D. J. (2005). Genomic instability in laminopathy-based premature aging. *Nature medicine*, 11(7), 780-785.
- Liu, Q., Pante, N., Misteli, T., Elsagga, M., Crisp, M., Hodzic, D., . . . Roux, K. J. (2007). Functional association of Sun1 with nuclear pore complexes. *The Journal of cell biology*, 178(5), 785-798.

- Lombardi, M. L., Jaalouk, D. E., Shanahan, C. M., Burke, B., Roux, K. J., & Lammerding, J. (2011). The interaction between nesprins and sun proteins at the nuclear envelope is critical for force transmission between the nucleus and cytoskeleton. *Journal of Biological Chemistry*, 286(30), 26743-26753.
- Lombardi, M. L., & Lammerding, J. (2011). Keeping the LINC: the importance of nucleocytoskeletal coupling in intracellular force transmission and cellular function. *Biochemical Society Transactions*, 39(6), 1729-1734.
- Lund, E., Oldenburg, A. R., Delbarre, E., Freberg, C. T., Duband-Goulet, I., Eskeland, R., . . . Collas, P. (2013). Lamin A/C-promoter interactions specify chromatin state-dependent transcription outcomes. *Genome research*, 23(10), 1580-1589.
- Lyakhovetsky, R., & Gruenbaum, Y. (2014). Studying lamins in invertebrate models *Cancer Biology and the Nuclear Envelope* (pp. 245-262): Springer.
- Lyle, A. N., Deshpande, N. N., Taniyama, Y., Seidel-Rogol, B., Pounkova, L., Du, P., . . . Griendling, K. K. (2009). Poldip2, a novel regulator of Nox4 and cytoskeletal integrity in vascular smooth muscle cells. *Circulation research*, 105(3), 249-259.
- Maeshima, K., Yahata, K., Sasaki, Y., Nakatomi, R., Tachibana, T., Hashikawa, T., . . . Imamoto, N. (2006). Cell-cycle-dependent dynamics of nuclear pores: pore-free islands and lamins. *Journal of Cell Science*, 119(21), 4442-4451.
- Maggi, L., Carboni, N., & Bernasconi, P. (2016). Skeletal Muscle Laminopathies: A Review of Clinical and Molecular Features. *Cells*, 5(3), 33.
- Malone, C. J., Fixsen, W. D., Horvitz, H. R., & Han, M. (1999). UNC-84 localizes to the nuclear envelope and is required for nuclear migration and anchoring during *C. elegans* development. *Development*, 126(14), 3171-3181.
- Manilal, S., thi Man, N., Sewry, C., & Morris, G. (1996). The Emery-Dreifuss muscular dystrophy protein, emerin, is a nuclear membrane protein. *Human molecular genetics*, 5(6), 801-808.
- Manju, K., Muralikrishna, B., & Parnaik, V. K. (2006). Expression of disease-causing lamin A mutants impairs the formation of DNA repair foci. *Journal of cell science*, 119(13), 2704-2714.
- Margalit, A., Brachner, A., Gotzmann, J., Foisner, R., & Gruenbaum, Y. (2007). Barrier-to-autointegration factor—a BAFFling little protein. *Trends in cell biology*, 17(4), 202-208.
- Markiewicz, E., Tilgner, K., Barker, N., van de Wetering, M., Clevers, H., Dorobek, M., . . . Blankesteyn, W. M. (2006). The inner nuclear membrane protein Emerin regulates β -catenin activity by restricting its accumulation in the nucleus. *The EMBO journal*, 25(14), 3275-3285.

- Maron, B. J., Towbin, J. A., Thiene, G., Antzelevitch, C., Corrado, D., Arnett, D., . . . Young, J. B. (2006). Contemporary definitions and classification of the cardiomyopathies an American heart association scientific statement from the council on clinical cardiology, heart failure and transplantation committee; quality of care and outcomes research and functional genomics and translational biology interdisciplinary working groups; and council on epidemiology and prevention. *Circulation*, *113*(14), 1807-1816.
- Mashimo, J. i., Shibamura, M., Satoh, H., Chida, K., & Nose, K. (2000). Genomic structure and chromosomal mapping of the mouse hic-5 gene that encodes a focal adhesion protein. *Gene*, *249*(1), 99-103.
- McPherson, J. P., Sarras, H., Lemmers, B., Tamblyn, L., Migon, E., Matysiak-Zablocki, E., . . . Fish, J. (2009). Essential role for Bclaf1 in lung development and immune system function. *Cell Death & Differentiation*, *16*(2), 331-339.
- Meister, P., & Taddei, A. (2013). Building silent compartments at the nuclear periphery: a recurrent theme. *Current opinion in genetics & development*, *23*(2), 96-103.
- Mekhail, K., & Moazed, D. (2010). The nuclear envelope in genome organization, expression and stability. *Nature Reviews Molecular Cell Biology*, *11*(5), 317-328.
- Melcon, G., Kozlov, S., Cutler, D. A., Sullivan, T., Hernandez, L., Zhao, P., . . . Rottman, J. N. (2006). Loss of emerin at the nuclear envelope disrupts the Rb1/E2F and MyoD pathways during muscle regeneration. *Human molecular genetics*, *15*(4), 637-651.
- Merz, C., Urlaub, H., Will, C. L., & Lührmann, R. (2007). Protein composition of human mRNPs spliced in vitro and differential requirements for mRNP protein recruitment. *Rna*, *13*(1), 116-128.
- Meuleman, W., Peric-Hupkes, D., Kind, J., Beaudry, J.-B., Pagie, L., Kellis, M., . . . van Steensel, B. (2013). Constitutive nuclear lamina-genome interactions are highly conserved and associated with A/T-rich sequence. *Genome research*, *23*(2), 270-280.
- Meune, C., Van Berlo, J. H., Anselme, F., Bonne, G., Pinto, Y. M., & Duboc, D. (2006). Primary prevention of sudden death in patients with lamin A/C gene mutations. *New England Journal of Medicine*, *354*(2), 209-210.
- Michaeloudes, C., Sukkar, M. B., Khorasani, N. M., Bhavsar, P. K., & Chung, K. F. (2011). TGF- β regulates Nox4, MnSOD and catalase expression, and IL-6 release in airway smooth muscle cells. *American Journal of Physiology-Lung Cellular and Molecular Physiology*, *300*(2), L295-L304.
- Miralles, F., Posern, G., Zaromytidou, A.-I., & Treisman, R. (2003). Actin dynamics control SRF activity by regulation of its coactivator MAL. *Cell*, *113*(3), 329-342.

- Moir, R. D., Montag-Lowy, M., & Goldman, R. D. (1994). Dynamic properties of nuclear lamins: lamin B is associated with sites of DNA replication. *The Journal of Cell Biology*, *125*(6), 1201-1212.
- Moir, R. D., Spann, T. P., Lopez-Soler, R. I., Yoon, M., Goldman, A. E., Khuon, S., & Goldman, R. D. (2000). Review: the dynamics of the nuclear lamins during the cell cycle—relationship between structure and function. *Journal of structural biology*, *129*(2), 324-334.
- Mori, K., Hamanaka, H., Oshima, Y., Araki, Y., Ishikawa, F., Nose, K., & Shibamura, M. (2012). A Hic-5-and KLF4-dependent mechanism transactivates p21Cip1 in response to anchorage loss. *Journal of Biological Chemistry*, *287*(46), 38854-38865.
- Mouilleron, S., Guettler, S., Langer, C. A., Treisman, R., & McDonald, N. Q. (2008). Molecular basis for G - actin binding to RPEL motifs from the serum response factor coactivator MAL. *The EMBO journal*, *27*(23), 3198-3208.
- Mounkes, L. C., Kozlov, S. V., Rottman, J. N., & Stewart, C. L. (2005). Expression of an LMNA-N195K variant of A-type lamins results in cardiac conduction defects and death in mice. *Human molecular genetics*, *14*(15), 2167-2180.
- Nagano, A., Koga, R., Ogawa, M., Kurano, Y., Kawada, J., Okada, R., . . . Arahata, K. (1996). Emerin deficiency at the nuclear membrane in patients with Emery-Dreifuss muscular dystrophy. *Nature genetics*, *12*(3), 254-259.
- Newport, J. W., Wilson, K. L., & Dunphy, W. G. (1990). A lamin-independent pathway for nuclear envelope assembly. *The Journal of Cell Biology*, *111*(6), 2247-2259.
- Nishiya, N., Shirai, T., Suzuki, W., & Nose, K. (2002). Hic-5 interacts with GIT1 with a different binding mode from paxillin. *Journal of biochemistry*, *132*(2), 279-289.
- Nishiya, N., Tachibana, K., Shibamura, M., Mashimo, J.-I., & Nose, K. (2001). Hic-5-reduced cell spreading on fibronectin: competitive effects between paxillin and Hic-5 through interaction with focal adhesion kinase. *Molecular and cellular biology*, *21*(16), 5332-5345.
- Olson, E. N., & Nordheim, A. (2010). Linking actin dynamics and gene transcription to drive cellular motile functions. *Nature reviews Molecular cell biology*, *11*(5), 353-365.
- Ooshio, T., Irie, K., Morimoto, K., Fukuhara, A., Imai, T., & Takai, Y. (2004). Involvement of LMO7 in the association of two cell-cell adhesion molecules, nectin and E-cadherin, through afadin and α -actinin in epithelial cells. *Journal of Biological Chemistry*, *279*(30), 31365-31373.

- Ostlund, C., Ellenberg, J., Hallberg, E., Lippincott-Schwartz, J., & Worman, H. J. (1999). Intracellular trafficking of emerin, the Emery-Dreifuss muscular dystrophy protein. *Journal of Cell Science*, *112*(11), 1709-1719.
- Östlund, C., Sullivan, T., Stewart, C. L., & Worman, H. J. (2006). Dependence of diffusional mobility of integral inner nuclear membrane proteins on A-type lamins. *Biochemistry*, *45*(5), 1374-1382.
- Otto, A., Schmidt, C., Luke, G., Allen, S., Valasek, P., Muntoni, F., . . . Patel, K. (2008). Canonical Wnt signalling induces satellite-cell proliferation during adult skeletal muscle regeneration. *Journal of cell science*, *121*(17), 2939-2950.
- Pagon, R. A., Adam, M. P., Ardinger, H. H., Bird, T. D., Dolan, C. R., Fong, C.-T., . . . Leturcq, F. (2013). Emery-Dreifuss Muscular Dystrophy.
- Pappas, G. D. (1956). The fine structure of the nuclear envelope of Amoeba proteus. *The Journal of biophysical and biochemical cytology*, *2*(4), 431-434.
- Pasotti, M., Klersy, C., Pilotto, A., Marziliano, N., Rapezzi, C., Serio, A., . . . Grasso, M. (2008). Long-term outcome and risk stratification in dilated cardiomyopathies. *Journal of the American College of Cardiology*, *52*(15), 1250-1260.
- Pekovic, V., Gibbs - Seymour, I., Markiewicz, E., Alzoghaibi, F., Benham, A. M., Edwards, R., . . . Hutchison, C. J. (2011). Conserved cysteine residues in the mammalian lamin A tail are essential for cellular responses to ROS generation. *Aging cell*, *10*(6), 1067-1079.
- Peric-Hupkes, D., Meuleman, W., Pagie, L., Bruggeman, S. W., Solovei, I., Brugman, W., . . . van Lohuizen, M. (2010). Molecular maps of the reorganization of genome-nuclear lamina interactions during differentiation. *Molecular cell*, *38*(4), 603-613.
- Peter, A., & Stick, R. (2012). Evolution of the lamin protein family: what introns can tell. *Nucleus*, *3*(1), 44-59.
- Peter, M., Nakagawa, J., Doree, M., Labbe, J., & Nigg, E. (1990). In vitro disassembly of the nuclear lamina and M phase-specific phosphorylation of lamins by cdc2 kinase. *Cell*, *61*(4), 591-602.
- Pickersgill, H., Kalverda, B., de Wit, E., Talhout, W., Fornerod, M., & van Steensel, B. (2006). Characterization of the Drosophila melanogaster genome at the nuclear lamina. *Nature genetics*, *38*(9), 1005-1014.
- Pignatelli, J., Tumbarello, D. A., Schmidt, R. P., & Turner, C. E. (2012). Hic-5 promotes invadopodia formation and invasion during TGF- β -induced epithelial-mesenchymal transition. *The Journal of cell biology*, *197*(3), 421-437.

- Pillers, D.-A. M., & Von Bergen, N. H. (2016). emery–Dreifuss muscular dystrophy: a test case for precision medicine. *The application of clinical genetics*, 9, 27.
- Puente, X. S., Quesada, V., Osorio, F. G., Cabanillas, R., Cadiñanos, J., Fraile, J. M., . . . Fanjul-Fernández, M. (2011). Exome sequencing and functional analysis identifies BANF1 mutation as the cause of a hereditary progeroid syndrome. *The American Journal of Human Genetics*, 88(5), 650-656.
- Putilina, T., Jaworski, C., Gentleman, S., McDonald, B., Kadiri, M., & Wong, P. (1998). Analysis of a human cDNA containing a tissue-specific alternatively spliced LIM domain. *Biochemical and biophysical research communications*, 252(2), 433-439.
- Ragnauth, C. D., Warren, D. T., Liu, Y., McNair, R., Tajsic, T., Figg, N., . . . Shanahan, C. M. (2010). Prelamin A acts to accelerate smooth muscle cell senescence and is a novel biomarker of human vascular aging. *Circulation*, 121(20), 2200-2210.
- Rahman-Roblick, R., Roblick, U. J., Hellman, U., Conrotto, P., Liu, T., Becker, S., . . . Wiman, K. G. (2007). p53 targets identified by protein expression profiling. *Proceedings of the National Academy of Sciences*, 104(13), 5401-5406.
- Razafsky, D., & Hodzic, D. (2015). Nuclear envelope: Positioning nuclei and organizing synapses. *Current opinion in cell biology*, 34, 84-93.
- Riemer, D., Wang, J., Zimek, A., Swalla, B. J., & Weber, K. (2000). Tunicates have unusual nuclear lamins with a large deletion in the carboxyterminal tail domain. *Gene*, 255(2), 317-325.
- Riemer, D., & Weber, K. (1994). The organization of the gene for Drosophila lamin C: limited homology with vertebrate lamin genes and lack of homology versus the Drosophila lamin Dmo gene. *European journal of cell biology*, 63(2), 299-306.
- Rober, R.-A., Weber, K., & Osborn, M. (1989). Differential timing of nuclear lamin A/C expression in the various organs of the mouse embryo and the young animal: a developmental study. *Development*, 105(2), 365-378.
- Rothballer, A., & Kutay, U. (2013). The diverse functional LINC's of the nuclear envelope to the cytoskeleton and chromatin. *Chromosoma*, 122(5), 415-429.
- Rowat, A., Lammerding, J., & Ipsen, J. H. (2006). Mechanical properties of the cell nucleus and the effect of emerin deficiency. *Biophysical journal*, 91(12), 4649-4664.
- Rowat, A. C., Jaalouk, D. E., Zwerger, M., Ung, W. L., Eydelnant, I. A., Olins, D. E., . . . Lammerding, J. (2013). Nuclear envelope composition determines the ability of neutrophil-type cells to passage through micron-scale constrictions. *Journal of Biological Chemistry*, 288(12), 8610-8618.

- Rusiñol, A. E., & Sinensky, M. S. (2006). Farnesylated lamins, progeroid syndromes and farnesyl transferase inhibitors. *Journal of cell science*, *119*(16), 3265-3272.
- Sadaie, M., Salama, R., Carroll, T., Tomimatsu, K., Chandra, T., Young, A. R., . . . Chong, H. (2013). Redistribution of the Lamin B1 genomic binding profile affects rearrangement of heterochromatic domains and SAHF formation during senescence. *Genes & development*, *27*(16), 1800-1808.
- Saitoh, N., Spahr, C. S., Patterson, S. D., Bubulya, P., Neuwald, A. F., & Spector, D. L. (2004). Proteomic analysis of interchromatin granule clusters. *Molecular biology of the cell*, *15*(8), 3876-3890.
- Scaffidi, P., & Misteli, T. (2006). Lamin A-dependent nuclear defects in human aging. *Science*, *312*(5776), 1059-1063.
- Schaller, M. D. (2001). Paxillin: a focal adhesion-associated adaptor protein. *Oncogene*, *20*(44).
- Scharner, J., Gnocchi, V. F., Ellis, J. A., & Zammit, P. S. (2010). Genotype–phenotype correlations in laminopathies: how does fate translate? *Biochemical Society Transactions*, *38*(1), 257-262.
- Schirmer, E. C., & Gerace, L. (2005). The nuclear membrane proteome: extending the envelope. *Trends in biochemical sciences*, *30*(10), 551-558.
- Schreiber, K. H., & Kennedy, B. K. (2013). When lamins go bad: nuclear structure and disease. *Cell*, *152*(6), 1365-1375.
- Segura-Totten, M., & Wilson, K. L. (2004). BAF: roles in chromatin, nuclear structure and retrovirus integration. *Trends in cell biology*, *14*(5), 261-266.
- Semenova, E., Wang, X., Jablonski, M. M., Levorse, J., & Tilghman, S. M. (2003). An engineered 800 kilobase deletion of Uchl3 and Lmo7 on mouse chromosome 14 causes defects in viability, postnatal growth and degeneration of muscle and retina. *Human molecular genetics*, *12*(11), 1301-1312.
- Shah, P., Donahue, G., Otte, G., Capell, B., Nelson, D., Cao, K., . . . McBryan, T. (2013). Lamin B1 depletion in senescent cells triggers large scale changes in gene expression and in the chromatin landscape genes and development.
- Shibanuma, M., Iwabuchi, Y., & Nose, K. (2002). Possible involvement of hic-5, a focal adhesion protein, in the differentiation of C2C12 myoblasts. *Cell structure and function*, *27*(1), 21-27.
- Shibanuma, M., Kim-Kaneyama, J.-r., Ishino, K., Sakamoto, N., Hishiki, T., Yamaguchi, K., . . . Nose, K. (2003). Hic-5 communicates between focal adhesions and the nucleus through oxidant-sensitive nuclear export signal. *Molecular biology of the cell*, *14*(3), 1158-1171.

- Shibanuma, M., Kim - Kaneyama, J. r., Sato, S., & Nose, K. (2004). A LIM protein, Hic - 5, functions as a potential coactivator for Sp1. *Journal of cellular biochemistry*, 91(3), 633-645.
- Shibanuma, M., Mashimo, J.-i., Kuroki, T., & Nose, K. (1994). Characterization of the TGF beta 1-inducible hic-5 gene that encodes a putative novel zinc finger protein and its possible involvement in cellular senescence. *Journal of Biological Chemistry*, 269(43), 26767-26774.
- Shibanuma, M., Mori, K., & Nose, K. (2011). HIC-5: A mobile molecular scaffold regulating the anchorage dependence of cell growth. *International journal of cell biology*, 2012.
- Shimi, T., Butin-Israeli, V., Adam, S. A., Hamanaka, R. B., Goldman, A. E., Lucas, C. A., . . . Goldman, R. D. (2011). The role of nuclear lamin B1 in cell proliferation and senescence. *Genes & development*, 25(24), 2579-2593.
- Shimi, T., & Goldman, R. D. (2014). Nuclear lamins and oxidative stress in cell proliferation and longevity *Cancer Biology and the Nuclear Envelope* (pp. 415-430): Springer.
- Shimi, T., Pflieger, K., Kojima, S.-i., Pack, C.-G., Solovei, I., Goldman, A. E., . . . Cremer, T. (2008). The A-and B-type nuclear lamin networks: microdomains involved in chromatin organization and transcription. *Genes & development*, 22(24), 3409-3421.
- Shumaker, D. K., Lopez-Soler, R. I., Adam, S. A., Herrmann, H., Moir, R. D., Spann, T. P., & Goldman, R. D. (2005). Functions and dysfunctions of the nuclear lamin Ig-fold domain in nuclear assembly, growth, and Emery–Dreifuss muscular dystrophy. *Proceedings of the National Academy of Sciences*, 102(43), 15494-15499.
- Shumaker, D. K., Solimando, L., Sengupta, K., Shimi, T., Adam, S. A., Grunwald, A., . . . Goldman, R. D. (2008). The highly conserved nuclear lamin Ig-fold binds to PCNA: its role in DNA replication. *The Journal of cell biology*, 181(2), 269-280.
- Simon, D. N., & Wilson, K. L. (2011). The nucleoskeleton as a genome-associated dynamic network of networks'. *Nature reviews Molecular cell biology*, 12(11), 695-708.
- Simon, D. N., & Wilson, K. L. (2013). Partners and post-translational modifications of nuclear lamins. *Chromosoma*, 122(1-2), 13-31.
- Small, E. M., Thatcher, J. E., Sutherland, L. B., Kinoshita, H., Gerard, R. D., Richardson, J. A., . . . Olson, E. N. (2010). Myocardin-related transcription factor-1 controls myofibroblast activation and fibrosis in response to myocardial infarction. *Circulation research*, 107(2), 294-304.

- Smythe, C., Jenkins, H. E., & Hutchison, C. J. (2000). Incorporation of the nuclear pore basket protein Nup153 into nuclear pore structures is dependent upon lamina assembly: evidence from cell - free extracts of *Xenopus* eggs. *The EMBO journal*, *19*(15), 3918-3931.
- Solovei, I., Wang, A. S., Thanisch, K., Schmidt, C. S., Krebs, S., Zwerger, M., . . . Peichl, L. (2013). LBR and lamin A/C sequentially tether peripheral heterochromatin and inversely regulate differentiation. *Cell*, *152*(3), 584-598.
- Spann, T. P., Goldman, A. E., Wang, C., Huang, S., & Goldman, R. D. (2002). Alteration of nuclear lamin organization inhibits RNA polymerase II-dependent transcription. *The Journal of cell biology*, *156*(4), 603-608.
- Spann, T. P., Moir, R. D., Goldman, A. E., Stick, R., & Goldman, R. D. (1997). Disruption of nuclear lamin organization alters the distribution of replication factors and inhibits DNA synthesis. *The Journal of cell biology*, *136*(6), 1201-1212.
- Starr, D. A., & Han, M. (2002). Role of ANC-1 in tethering nuclei to the actin cytoskeleton. *Science*, *298*(5592), 406-409.
- Starr, D. A., Hermann, G. J., Malone, C. J., Fixsen, W., Priess, J. R., Horvitz, H. R., & Han, M. (2001). unc-83 encodes a novel component of the nuclear envelope and is essential for proper nuclear migration. *Development*, *128*(24), 5039-5050.
- Steinert, P. M., & Roop, D. R. (1988). Molecular and cellular biology of intermediate filaments. *Annual review of biochemistry*, *57*(1), 593-625.
- Stewart, C., & Burke, B. (1987). Teratocarcinoma stem cells and early mouse embryos contain only a single major lamin polypeptide closely resembling lamin B. *Cell*, *51*(3), 383-392.
- Stewart, C. L., Roux, K. J., & Burke, B. (2007). Blurring the boundary: the nuclear envelope extends its reach. *Science*, *318*(5855), 1408-1412.
- Sullivan, T., Escalante-Alcalde, D., Bhatt, H., Anver, M., Bhat, N., Nagashima, K., . . . Burke, B. (1999). Loss of A-type lamin expression compromises nuclear envelope integrity leading to muscular dystrophy. *The Journal of cell biology*, *147*(5), 913-920.
- Swift, J., Ivanovska, I. L., Buxboim, A., Harada, T., Dingal, P. D. P., Pinter, J., . . . Tewari, M. (2013). Nuclear lamin-A scales with tissue stiffness and enhances matrix-directed differentiation. *Science*, *341*(6149), 1240104.
- Taylor, M. R., Carniel, E., & Mestroni, L. (2006). Cardiomyopathy, familial dilated. *Orphanet journal of rare diseases*, *1*(1), 1.

- Tesson, F., Saj, M., Uvaize, M. M., Nicolas, H., Płoski, R., & Bilińska, Z. (2014). Lamin A/C mutations in dilated cardiomyopathy. *Cardiol. J*, 21(4), 331-342.
- Thomas, S. M., Hagel, M., & Turner, C. E. (1999). Characterization of a focal adhesion protein, Hic-5, that shares extensive homology with paxillin. *Journal of cell science*, 112(2), 181-190.
- Tilgner, K., Wojciechowicz, K., Jahoda, C., Hutchison, C., & Markiewicz, E. (2009). Dynamic complexes of A-type lamins and emerin influence adipogenic capacity of the cell via nucleocytoplasmic distribution of β -catenin. *Journal of cell science*, 122(3), 401-413.
- Trembley, M. A., Velasquez, L. S., de Mesy Bentley, K. L., & Small, E. M. (2015). Myocardin-related transcription factors control the motility of epicardium-derived cells and the maturation of coronary vessels. *Development*, 142(1), 21-30.
- Turner, C. E. (2000). Paxillin and focal adhesion signalling. *Nature cell biology*, 2(12), E231-E236.
- Varney, S. D., Betts, C. B., Zheng, R., Wu, L., Hinz, B., Zhou, J., & Van De Water, L. (2016). Hic-5 is required for myofibroblast differentiation by regulating mechanically dependent MRTF-A nuclear accumulation. *J Cell Sci*, 129(4), 774-787.
- Vartiainen, M. K., Guettler, S., Larijani, B., & Treisman, R. (2007). Nuclear actin regulates dynamic subcellular localization and activity of the SRF cofactor MAL. *Science*, 316(5832), 1749-1752.
- Verstraeten, V. L., Ji, J. Y., Cummings, K. S., Lee, R. T., & Lammerding, J. (2008). Increased mechanosensitivity and nuclear stiffness in Hutchinson–Gilford progeria cells: effects of farnesyltransferase inhibitors. *Aging cell*, 7(3), 383-393.
- Walter, J., Sun, L., & Newport, J. (1998). Regulated chromosomal DNA replication in the absence of a nucleus. *Molecular cell*, 1(4), 519-529.
- Walther, T. C., Fornerod, M., Pickersgill, H., Goldberg, M., Allen, T. D., & Mattaj, I. W. (2001). The nucleoporin Nup153 is required for nuclear pore basket formation, nuclear pore complex anchoring and import of a subset of nuclear proteins. *The EMBO journal*, 20(20), 5703-5714.
- Wang, H., Song, K., Sponseller, T. L., & Danielpour, D. (2005). Novel function of androgen receptor-associated protein 55/Hic-5 as a negative regulator of Smad3 signaling. *Journal of Biological Chemistry*, 280(7), 5154-5162.
- Wente, S. R., & Rout, M. P. (2010). The nuclear pore complex and nuclear transport. *Cold Spring Harbor perspectives in biology*, 2(10), a000562.

- Worman, H., Ostlund, C., & Wang, Y. Diseases of the nuclear envelope. *Cold Spring Harb Perspect Biol* 2010; 2: a000760; PMID: 20182615.
- Yang, L., Guerrero, J., Hong, H., DeFranco, D. B., & Stallcup, M. R. (2000). Interaction of the $\tau 2$ transcriptional activation domain of glucocorticoid receptor with a novel steroid receptor coactivator, Hic-5, which localizes to both focal adhesions and the nuclear matrix. *Molecular biology of the cell*, 11(6), 2007-2018.
- Yuminamochi, T., Yatomi, Y., Osada, M., Ohmori, T., Ishii, Y., Nakazawa, K., . . . Ozaki, Y. (2003). Expression of the LIM proteins paxillin and Hic-5 in human tissues. *Journal of Histochemistry & Cytochemistry*, 51(4), 513-521.
- Yund, E. E., Hill, J. A., & Keller, R. S. (2009). Hic-5 is required for fetal gene expression and cytoskeletal organization of neonatal cardiac myocytes. *Journal of molecular and cellular cardiology*, 47(4), 520-527.
- Zhao, B., Li, L., Lei, Q., & Guan, K.-L. (2010). The Hippo–YAP pathway in organ size control and tumorigenesis: an updated version. *Genes & development*, 24(9), 862-874.
- Zimek, A., & Weber, K. (2011). Flanking genes of an essential gene give information about the evolution of metazoa. *European journal of cell biology*, 90(4), 356-364.
- Zuleger, N., Robson, M. I., & Schirmer, E. C. (2011). The nuclear envelope as a chromatin organizer. *Nucleus*, 2(5), 339-349.
- Zullo, J. M., Demarco, I. A., Piqué-Regi, R., Gaffney, D. J., Epstein, C. B., Spooner, C. J., . . . Reddy, K. L. (2012). DNA sequence-dependent compartmentalization and silencing of chromatin at the nuclear lamina. *Cell*, 149(7), 1474-1487.
- Zwergler, M., Jaalouk, D. E., Lombardi, M. L., Isermann, P., Mauermann, M., Dialynas, G., . . . Lammerding, J. (2013). Myopathic lamin mutations impair nuclear stability in cells and tissue and disrupt nucleo-cytoskeletal coupling. *Human molecular genetics*, 22(12), 2335-2349.